Kinetic studies of the silver-silver chloride electrode near ITS equilibrium potential.

Ladjouzi, M. A

KINETIC STUDIES OF THE SILVER-SILVER CHLORIDE ELECTRODE NEAR ITS EQUILIBRIUM POTENTIAL

BY

M. A. LADJOUZI.

Thesis submitted for the Degree of Doctor of Philosophy in the Faculty of Science of the University of London.

Chemistry Department,
Queen Elizabeth College,
University of London.

November 1979.

A C K N O W L E D G E M E N T S

The present work has been carried out in a friendly atmosphere of the Chemistry Department of Queen Elizabeth College in the University of London.

I am deeply indebted to my supervisor, Dr. H. P. Bennetto, who has given valuable advice and guidance on all aspects of the work, including the language. His real interest in the subject, his meticulous and stimulating discussions, and his kindness and comprehension throughout the course of this work were of a great support to me.

I shall forever be grateful to my parents, whose life was very often hard to support, and who gave a constant and rigorous attention to their children's education; to my mother, for her precious help at the early stages of my academic life, and to my father who sacrificed his entire life to noble patriotic ideals so that the Algerian youth, which I am part of, could study freely. I would like also to express my sincere thanks to my wife for her moral support and patience over the last few years, and for sacrificing most of her time which rightfully belonged to her.

I wish to thank all those who helped in any way during the present studies, and particularly my parents-in-law and Mr. A. Allahoum.

Special thanks must also go to my uncles, Nourredine, Hocine and Abderahmane, who contributed greatly in many ways to my success in Academic life.

I wish to express my gratitude to all the members of the academic

and technical staff of Queen Elizabeth College for their ready assistance.

Finally, I would like to acknowledge the financial support of the Algerian Authorities who funded the present work.

A B S T R A C T

The kinetic response of the silver-silver chloride electrode near its equilibrium potential has been studied. Using a D.C. method, electrodes were polarised at 25°C in aqueous and non-aqueous hydrochloric acid solutions in the concentration range 0 - 0.2 M and with polarising currents in the microamp range. Three solvents were used : water, N-methylpropionamide and methanol. From the analysis of the potential/time and overpotential/current curves the dependences of the exchange current, the differential capacitance of the double-layer, and various rate coefficients on the concentration and the solvent were investigated. These quantities varied with the type and age of electrode. The behaviour in dilute aqueous hydrochloric acid solutions was also examined as a function of the temperature and of anodisation-time. Simple correlations between the exchange current and the differential double-layer capacitance are found in all the systems studied. The results obtained have been compared with those from studies by previous investigators, and ideas are forwarded relating to possible mechanisms for the $Ag/AgCl/Cl^-$ reaction. The evidence points to a two-stage mechanism involving charge-transfer and surface-diffusion steps.

CONTENTS.

Page

SECTION I.

I N T R O D U C T I O N.

Any electrodic process is a complex reaction involving a number of consecutive steps. To establish the number, nature and sequence of steps which constitute an electrode process is one of the main tasks of electrode kinetics[1]. When a conductor is in contact with a solution, they both constitute a system. In the absence of any current, the system is at equilibrium,but the application of a current from an external source to this system will perturb it from its equilibrium state. The electrode processes occurring characterise the non-equilibrium state, while the current passed produces a flow of charge across the interface, and measures the rate of the reaction. This rate, determined by the energy required for the ions or electrons to cross the interface, may vary enormously from one system to another, and it is convenient to consider two extreme possibilities.

When the activation energy is so high that the rate is effectively zero, the surface is said to be "ideally polarised", but when the activation energy is so small that there is effectively no barrier to the flow of charge, the surface is considered as "ideally non-polarised". The electrical behaviour of an electrode-solution interface can be compared to that of a capacitor and resistor connected in parallel, where the capacitor is considered as the double-layer of the interface, and the resistor as the resistance of the interface to charge-transfer. The difference

between a polarisable and a non-polarisable interface is in the magnitude of the resistance : if the resistance is very high ($R \to \infty$), then the capacitor charges up to the value of the potential change produced. This is equivalent to a polarisable interface. If, now, the resistance is low ($R \to 0$), then 'leakage' of charge occurs via the low-resistance path. This is the behaviour of a non-polarisable interface. These two ideal cases of interfaces are extreme, and the different systems, traditionally studied, lie in between these extremes.

The mercury electrode in contact with aqueous solutions is a good example of a polarisable interface over a wide range of applied potential.[2] The mercury electrode has been extensively studied, being convenient for use, and having the advantage that the interfacial tension can be easily measured. As there is relatively no charge 'leakage' possible in this system in the absence of mercurous ions, the electron-transfer across the interface is poor, and therefore the structure of the double-layer associated with the capacitor is perturbed to a great extent from equilibrium. In contrast, systems where ions or electrons pass across the interface, i.e. non-polarised electrodes, might in some respects be more suitable for study, since they represent "reversible" systems which are in electrochemical equilibrium with the solution. In this case, there is continuous 'leakage' of the species between the electrode and the solution in both directions. These systems are no less worthy of study than mercury, but have hitherto been rather neglected by electrode kineticists.

Of the many experimental methods which have been applied to the study of interfaces under reversible conditions, the coulostatic impulse technique has recently received much attention, but it also requires, for reasonable accuracy of the measurements, currents of a few milliamps. Under these conditions, the departure from equilibrium is rather large and may lead to a lack of reproducibility in the results. The constant current method, in which currents even as low as 0.1 microamps can be applied to the electrode, was preferred in the present work. The method, which provides the specific features of polarisation curves and permits direct assessment of both the exchange current density and the differential capacitance of the double-layer, has the great advantage of being simple. The kinetics of the electrode processes such as the rate constants, the transfer coefficients, the charge-transfer and surface-diffusion parameters are also accessible, whilst the measurements can be obtained with reasonable accuracy and are fairly reproducible.

Although most of the previous work on reversible systems has concentrated on metal deposition[3,4], attention has been turned recently on the silver-silver halide electrodes, particularly in the work of Gu and Bennion[5], of van Leeuwen and Peverelli[6], and of Slusarek[7]. These electrodes exhibit some complex features, and have disadvantages arising from the fact that data varies from one worker to the other; the results depend on the type of preparation, the surface-treatment and the percentage of coverage of the electrode. Consequently, there are limitations on the interpretations given.

However, in the present work, the silver-silver chloride system was studied for a number of reasons. (i) It is known[8,9] as a well-behaved "reversible" electrode, much used for thermodynamic measurements; (ii) it has hitherto received little attention from the mechanistic view point, but it seemed likely that electrodes prepared by the standard procedures of reversible electrochemistry should show reproducible kinetics; (iii) it constitutes an important practical electrode which is valuable in the study of colloid stability[10], and which can be used in solid electrolyte batteries[11,12].

The aim of the work was to investigate the dependence of the exchange current and differential capacitance of the $Ag/AgCl/Cl^-$ electrode on the concentration of hydrochloric acid solutions in water, N-methylpropionamide and methanol. From an analysis of the time dependence of overpotentials, information has been extracted on the kinetic parameters of the reaction occurring at the interface. The kinetic data have been used to determine which step controls the overall reaction, and this leads to an examination of models for the interface under study.

Section II contains basic theoretical aspects, gives an account of the models of Helmholtz, Gouy and Chapman, and Stern for the double-layer, and outlines the main kinetic equations which serve later on in calculations. In Section III an account is given of the various experimental procedures used in the work. This includes the procedure for manipulating the cell and for preparing the various electrodes, the preparation and purification of the materials

used, and the preparation of the electrolyte solutions of various concentrations. This section also includes the procedures for experiments on variable temperatures and times of anodisation. A brief survey of the most relevant work on electrodic studies of silver-silver halide and other electrodes is given in section IV. It also contains a preliminary consideration of mechanistic aspects for the charge-transfer reaction occuring between the electrode and the solution. Using the polarisation curves obtained, some representative plots of potential/time and overpotential/current are presented, for aqueous and non-aqueous solutions, in section V. This section lists the values of the exchange current and the differential capacitance obtained as functions of concentration, electrode-type, time of anodisation, aging and temperature. The results are discussed in section VI. In this chapter, the values of the exchange current and the differential capacitance are compared with those obtained by previous workers. The concentration dependence of these quantities is treated in detail, and there follows an examination of the "one-step" and"two-step" models. The temperature dependence of exchange currents and differential capacitances have been examined in the light of the proposed mechanisms, although detailed analysis of the results from the standpoint of double-layer theories is considered to be beyond the scope of the thesis. This discussion is followed by the main conclusions, including some suggestions for future work. References are listed at the end of each section.

REFERENCES.

1. P. Delahay, "Kinetics of Electrode Processes Involving more than One Step", in Double Layer and Electrode Kinetics, chap. 8, Interscience, N.Y.,(1965).
2. R. Aveyard and D. A. Haydon, "An Introduction to the Principles of Surface Chemistry", University Press, Cambridge, (1973).
3. M. Fleischmann and H. R. Thirsk, "Metal Deposition and Electrocrystallization", in : P. Delahay and C. Tobias, eds., Advances in Electrochemistry and Electrochemical Engineering, vol. 3, 123, (1963).
4. W. Mehl and J. O'M. Bockris, Can.J.Chem., 37, 190, (1959).
5. H. Gu and D. N. Bennion, J. Electrochem.Soc., 124, 1364, (1977).
6. K. J. Peverelli and H. P. Van Leeuwen, J. Electroanal.Chem., 99, 157, (1979).
7. L. Slusarek, Ph.D. Thesis, Columbia University, (1977).
8. D. J. G. Ives and G. J. Janz, "Reference Electrodes, Theory and Practice", Academic Press, N.Y., (1961).
9. G. J. Janz and H. Taniguchi, Chem.Rev., 53, 297, (1953).
10. B. H. Bijsterbosch and J. Lyklema, Adv.Colloid Interface Sci., 9, 147, (1978).
11. R. T. Foley, "Solid Electrolyte Galvanic Cells", J. Electrochem. Soc., 116, 161, (1969).
12. J. N. Mrgudich, "Solid Electrolyte Batteries", Encyclopedia of Electrochemistry, Reinhold, N. Y., p. 84, (1964).

SECTION II.

THEORETICAL ASPECTS

A. THE ELECTRODE-SOLUTION INTERFACE.

1. Interfacial structure. When an electrode is immersed in an electrolytic solution, and a current applied from an external source, thermodynamics indicates that an electron-transfer reaction, i.e. of the type (1), occurs spontaneously.

$$A^+ + e^- \longrightarrow D \qquad (1)$$

There is a tendency for the positive charges in the solution to be reduced, probably following a re-arrangement of solvent molecules and ions into some required orientation[1]. (A similar scheme can be drawn up for oxidation of an anion). At the same time, the electrode feels the electric field developed by the excess charge in the electrolytic side, and liberates electrons towards the electron acceptor A^+. The electrode has acquired a net charge, and this is opposite to the diffuse charge formed, which accrues in the solution. Thus both sides of the metal-solution interface have become charged. An electrical electrode-solution interface is created whose structure consists of positive ions and mobile electrons on one side, solvent molecules, solvated and unsolvated ions on the other. Several models have been proposed in order to build up realistic conceptions of this double layer structure, and a brief summary is presented below.

2. Double-layer models. The first model was suggested by Helmholtz in 1853[2,3]. It is equivalent to an electrical parallel-plate condenser or capacitor. A capacitor is characterised by two plates of charges of opposite sign and of equal density, separated by a distance d. The potential difference V across the plates is given, for a unit area of surface, by

$$V = \frac{d\,q}{\varepsilon_o \varepsilon_r} \qquad (2)$$

where d is the distance between the plates, ε_o the permittivity of a vacuum, ε_r the dielectric constant of the material between the plates, and q the surface charge. As the capacitance of a capacitor is the total charge Q required to raise the potential difference V across the plates by 1 volt, it follows that

$$C = \frac{Q}{V} = \frac{\varepsilon_o \varepsilon_r}{d} \qquad (3)$$

An electrode-solution interface can be regarded in a similar fashion : a fixed plate corresponding to the electrode, and a mobile plate coinciding with the plane connecting the centres of the ions attracted to the metal surface by electrostatic forces in the solution, and where d is the thickness of the double layer.

It was Gouy (1910) and Chapman (1913) who freed the charges from their rigidity by introducing the diffuse-layer model[2,3]. Apart from the electrostatic forces arising between the metal and the ions, the latter are also under the influence of thermal molecular forces, and therefore under their

combined effect, are distributed diffusely relative to the metal surface. This model is very similar to the Debye and Hückel[4] ionic-cloud model where an ion is arbitrarily sp otlighted as the "central ion" (or reference sphere of charge), and develops an "ionic atmosphere" as a result of the ion-ion interactions. Here the charged electrode is like an infinite plane, replacing the central ion of the Debye and Hückel theory, and displaying a planar instead of a spherical field. In accordance with the law of electroneutrality, the net charge density, q_M, on the electrode is equal in magnitude and opposite in sign to the total excess charge density, q_L, on the solution side which forms the ionic cloud. The net charge density decreases with increasing distances from the electrode into the solution. The potential, too, decays asymptotically with distance up to a constant value taken as zero in the bulk of the solution.

In the model of Stern (1924)[2,3] some of the ions in the solution side of the double layer are adsorbed on the electrode, and the remaining ions are diffusely spread out as in the Gouy and Chapman model. Ions adsorbed in the so-called "inner Helmholtz region" were not only under the influence of electrostatic forces, but also forces of specific adsorption of a noncoulombic nature. According to Stern, there are double layers containing specifically adsorbed ions, where the number of ions in the Helmholtz region may exceed the charge

on the electrode surface by a certain amount depending on the properties of the ions and on the charge of the metal, and the total charge density, q_L, is the sum of the charge density in the Helmholtz layer, q_H, and the charge density in the diffuse layer, q_d. Hence

$$q_L = q_H + q_d = -q_M \tag{4}$$

3. Potential difference across the interface. The potential difference between two points, situated in two different phases, is defined as the electrical work required to transport a test charge from one point to the other, plus the chemical work for that transfer of charge (since the chemical potentials of the charged species are not equal in the different phases)[5]. This statement can be expressed by the equation

$$\overline{\mu_i} = \mu_i + Z_i F \phi \tag{5}$$

where: $\overline{\mu_i}$ is the electrochemical potential (total work per mole of charges), ϕ is the electrical work for a test charge, $ZF\phi$ is the electrical work for one mole of particles and μ_i, the chemical work due to other sorts of interactions. If the work done to bring a unit test charge from infinity to a point just outside the electrode (outside a charged but dipole-free phase) is the outer potential ψ, and if the work done to carry a test charge across the dipole layer at

the surface of an uncharged solution is the surface potential χ, then the inner or Galvani potential ϕ arises from the work done to bring the test charge from infinity up to and across the dipole layer at a charged phase, and is therefore the sum of the outer and surface potentials. It follows that

$$\phi = \psi + \chi \tag{6}$$

Replacing ϕ by its components in eq. (5) gives

$$\overline{\mu_i} = \mu_i + Z_i F (\psi + \chi) \tag{7}$$

Considering changes in these potentials for the electrode-solution interface, eq. (7) becomes

$$\overline{\Delta\mu_i} = \Delta\mu_i + Z_i F (\Delta\psi + \Delta\chi) \tag{8}$$

As the present work is more concerned with electrodes near equilibrium, eq. (8) is next simplified under the following conditions : the electron-transfer process near the equilibrium potential should probably not be affected by structural changes in the surface layers. Since the changes in surface potentials, $\Delta\chi$, related to the structure of the interface, will become negligible, it follows that

$$(\Delta\chi) \sim 0,$$

and eq (6) reduces to

$$\phi = \psi (\text{or } \Delta\phi = \Delta\psi) \tag{9}$$

Also, near equilibrium, the change in the electrochemical potential of a species i must be nearly the same on both sides

of the interface, that is to say that the free energy of a system is a minimum, i.e.

$$\overline{\Delta\mu_i} \sim 0,$$

then eq. (8) reduces to

$$\overline{\Delta\mu_i} = \Delta\mu_i + Z_i F\Delta\psi = 0 \qquad (10)$$

or

$$\Delta\phi = \Delta\psi = -\frac{\Delta\mu_i}{Z_i F} \qquad (11)$$

Eq. (11) can be re-written

$$\Delta\mu_i = -Z_i F\Delta\phi \qquad (12)$$

According to the thermodynamic expression:

$$\Delta G = -Z_i FE \qquad (13)$$

where ΔG is the free energy of a system, and is proportional to the e.m.f. E of the system studied, it can be seen that the Galvani potential difference $\Delta\phi$ is directly related to changes in the e.m.f. E, i.e. $\Delta\phi = E$, or $d\Delta\phi = dE$, since ΔG is related to $\Delta\mu_i$ by the relation

$$\Delta G = \Sigma\mu_i \nu_i \qquad (14)$$

where ν_i is the stoichiometric number for the component possessing the chemical potential μ_i.

4. Electrode reactions. The silver-silver chloride electrode investigated in the present work is an electrode of the second kind : it is a half-cell consisting of a metal (Ag) covered by one of its sparingly-soluble salts (AgCl), immersed in a solution containing the same anion (Cl^-) as the salt. The

reactions occurring at the electrode-solution interface are as follows. When applying current from an external source, electrons are donated to silver atoms, and the half reaction is

$$Ag \rightleftharpoons Ag^+ + e^- \qquad (15)$$

The charged silver Ag^+ reacts with Cl^- ions from the solution or the silver chloride lattice to form silver chloride. The reaction is

$$Ag^+ + Cl^- \rightleftharpoons AgCl \qquad (16)$$

The overall reaction is the sum of eq.(15) and (16) :

$$AgCl + e^- \rightleftharpoons Ag + Cl^- \qquad (17)$$

The process of electron-transfer requires that a certain activation energy must be reached to surmount the potential barrier at the interface. According to the transition state theory[1], the frequency with which the ion successfully jumps the energy barrier for diffusion is

$$\vec{r} = \frac{kT}{h} e^{-\Delta G^{o*}/RT} \qquad (18)$$

where k = Boltzmann's constant.

T = Absolute temperature.

R = Gas constant.

h = Plank's constant.

ΔG^{o*} = standard free energy of activation.

A similar expression can be used here, when the electron accomplishes the charge-transfer reaction. When this frequency

is multiplied by the concentration C^+ of the ion on the solution side of the interface, the product is the rate r of the electronation reaction

$$\vec{r} = \frac{kT}{h} C^+ e^{-\frac{\vec{\Delta G}^{o*}}{RT}} \quad (19)$$

The total free energy of activation $\vec{\Delta G}^{o*}$ is conventionally regarded as the sum of the "chemical" free energy of activation ΔG_c^{o*} plus the electrical contribution $\beta F \Delta\phi$, where β is a transfer coefficient (also known as the symmetry factor)[6].

$$\vec{\Delta G}^{o*} = \vec{\Delta G}_c^{o*} + \beta F \Delta\phi \quad (20)$$

The rate can be finally expressed for the electronation reaction as

$$\vec{r} = \frac{kT}{h} C^+ e^{-\vec{\Delta G}_c^{o*}/RT} e^{-\beta F \Delta\phi/RT} \quad (21)$$

and for the de-electronation reaction i.e. the reverse process,

$$\overleftarrow{r} = \frac{kT}{h} C^- e^{-\overleftarrow{\Delta G}_c^{o*}/RT} e^{(1-\beta) F \Delta\phi/RT} \quad (22)$$

In these equations β is the fraction of the electrical work used during the electronation, and $(1-\beta)$ is the remainder fraction of the work. Furthermore, when these two rates are multiplied by the charge per mole (the Faraday, F), the product gives rise to the electronation and de-electronation current densities respectively :

$$\vec{i} = F \vec{r} = \frac{FkT}{h} C^+ e^{-\vec{\Delta G}_c^{o*}/RT} e^{-\beta F \Delta\phi/RT} \quad (23)$$

$$\overleftarrow{i} = F \overleftarrow{r} = \frac{FkT}{h} C^- e^{-\overleftarrow{\Delta G}_c^{o*}/RT} e^{(1-\beta) F \Delta\phi/RT} \quad (24)$$

B. THE EQUILIBRIUM STATE.

The equilibrium state is characterised by forward and backward reactions proceeding at equal rates. There is no net current, and the charge on the electrode becomes constant as does the charge on the solution side. The potential difference across the interface is therefore constant. It is a characteristic equilibrium potential difference $\Delta\phi_e$ for the system. For the electronation and de-electronation current densities we may write

$$\vec{i} = F\, k_c^{\rightarrow}\, C^{+}\, e^{\frac{-\beta F \Delta\phi e}{RT}} = \overleftarrow{i} = F\, k_c^{\leftarrow}\, C^{-}\, e^{\frac{(1-\beta) F \Delta\phi e}{RT}} \qquad (25)$$

where $k_c^{\rightarrow} = \frac{kT}{h}\, e^{-\Delta \vec{G}_c^{o*}/RT}$, and $k_c^{\leftarrow} = \frac{kT}{h}\, e^{-\Delta \overleftarrow{G}_c^{o*}/RT}$, quantities given in eqns. (23) and (24) respectively. These two currents, characterizing the rate of the electron exchange between the electrode and the solution under equilibrium conditions, are defined as "the exchange-current", i_o, and written

$$i_o = \vec{i} = \overleftarrow{i} \qquad (26)$$

As the net current flowing is the difference between the two currents, it is clear that

$$i = \vec{i} - \overleftarrow{i} = 0 \qquad (27)$$

C. THE NON-EQUILIBRIUM STATE.

If a net flow of electrons is supplied to the electrode from an external source, a net current density i will pass

across the interface which is perturbed from equilibrium :

$$i = \vec{i} - \overleftarrow{i} \; ; \neq 0 \tag{28}$$

The net current will produce a change in the potential $\Delta\phi$ from the equilibrium value $\Delta\phi_e$. The difference is named the overpotential, η,

$$\eta = \Delta\phi - \Delta\phi_e \tag{29}$$

and the electrode is said to be "polarised". During the polarisation, the mass and the nature of the electrode and the composition of the solution near the electrode are being altered, relative to the equilibrium conditions. When an electrode is polarised, its potential difference value depends also on the current density (or flow of electrons), and therefore on time. When the current is just started, the electrons or ions do not succeed in crossing the double layer[7], but give a small increase of the charge dQ on each side of the double layer, and therefore a small increase of the potential difference dV. As in the case of a capacitor [see eq.(3)], the capacity is not constant and depends on the potential value and is termed "differential capacitance", C_{dl} :

$$C_{dl} = \frac{dQ}{dV} \tag{30}$$

Following the charging process, the electrode potential difference gradually reaches a steady-state. In practice, the steady-state value of the potential shows a slight drift with time (see later in section V). Actually the overvoltage η is usually

taken as the experimentally derived value, including ohmic effects. It is important to mention, however, that the total overpotential η_t, occuring at a solution-electrode interface, may contain several contributions e.g.

$$\eta_t = \eta_c + \eta_a + \eta_{sd} \qquad (31)$$

where η_c is the concentration overpotential, η_a the activation overpotential and η_{sd} the surface diffusion overpotential. The former may be reduced to a minimum when the solution is stirred during polarisation experiments (see Section III). The present studies are more concerned with η_a and η_{sd}. Assuming there are no other contributions of the overvoltage, the transition state theory (eqns. 25 to 29) leads to the Butler-Volmer equation

$$i = i_o \left[\exp^{-\beta\, nF/RT} - \exp^{(1-\beta)nF/RT}\right] \qquad (32)$$

(Other theoretical approaches yield equations identical in form[2]).

For high currents $\vec{i}$ becomes much bigger than $\overleftarrow{i}$, and eq.(32) reduces to eq. (33)

$$i = i_o \exp^{(-\frac{\beta F \eta}{RT})} \qquad (33)$$

which, on taking logarithms and re-arranging, gives the Tafel equation

$$\eta = a + b \log i \qquad (34)$$

where a and b are constants.

The present work is more concerned with the low-current approximation of eq.(32), since the electrode is slightly

perturbed from its equilibrium potential, and expansion of eq. (32) by the Taylor series and neglecting the higher terms leads to

$$i = \frac{i_o F n}{RT} \tag{35}$$

This equation, which expresses the polarisation behaviour near equilibrium, is of the form of Ohm's law, where the term $\frac{RT}{Fi_o}$ has the dimensions of a resistance. The plot of n versus i gives a slope, S, which is equal to that resistance-term,

$$S = \frac{RT}{i_o F} \tag{36}$$

Re-arranging eq. (36) gives the expression of the exchange current

$$i_o = \frac{RT}{F} \times \frac{1}{S} \tag{37}$$

In the same manner, by substituting dQ in eq.(30) by its equivalent quantity (idt), since 1Q is the passage of 1 coulomb across the interface when 1 ampere is applied during 1 second, eq.(30) becomes

$$C_{dl} = \frac{i\ dt}{dV} \tag{38}$$

If now dV is considered as a very small change in the over-potential during a short time dt when a small current i is applied to the electrode, eq.(38) may be written

$$C_{dl} = \frac{i\ dt}{d\eta} \tag{39}$$

or, on re-arranging,

$$\frac{d\eta}{dt} = \frac{1}{C_{dl}} i \qquad (40)$$

According to eq. (40), the slope S' of the plot of $d\eta/dt$, for the first linear rise of the potential, against i gives the value of the differential double layer capacitance C_{dl}

$$C_{dl} = \frac{1}{S'} \qquad (41)$$

The study of the specific features of potential/current curves is necessary for determining the nature of electrode reactions and the rate determining steps, and hence the kinetics of electrochemical processes, or charge-transfer mechanisms[1,8].

D. CHARGE TRANSFER MECHANISMS.

According to Bockris[1,8] and Gerischer[9], who studied the mechanism of the electrodeposition of metals, two models have been proposed : a one-step charge transfer mechanism, and a two-step(charge-transfer plus surface-diffusion) mechanism which implies charge-transfer and surface-diffusion resistances in series. Using the equation[8]

$$0 = \frac{\partial C_a}{\partial t} = D_a\left(\frac{\partial^2 C_a}{\partial x^2}\right) + \frac{i_o}{ZF}\left[\exp\left(\frac{\alpha_c z F \eta_t}{RT}\right) - \frac{C_a}{C_a{}^o}\exp\left(\frac{-\alpha_a z F \eta_t}{RT}\right)\right] \qquad (42)$$

(x = distance from the growth step, C_a = adion conc., and $C_a{}^o$ = equilibrium adion conc.)

They derived the total constant current (resolved into a double-layer charging-current i_{dl} and a faradaic current arising from a charge-transfer reaction i_{ctr}) under the following form

$$i = C_{dl}\frac{d\eta_t}{dt} + i_o\left(\frac{\bar{C}_t - C_o}{C_o} + \frac{F\,\eta_t}{RT}\right) \qquad (43)$$

where

C_{dl} is the differential double-layer capacitance,

$\frac{d\eta t}{dt}$, the change in the overpotential during a time dt,

i_o, the exchange current,

$\bar{C}_t$, the average adion concentration at a time t

C_o, the equilibrium adion concentration

The remaining terms are defined as usual .

Now whether the average adion concentration at the time t, $\bar{C}_t$, is assumed to be virtually equal to the equilibrium adion concentration, C_o, or not, two cases arise.

1. Time dependence of overvoltages in a one-step mechanism model.

When the charge-transfer step is assumed to be rate-determining, $\bar{C}_t \sim C_o$ (the surface diffusion of adions from crystal planes to "steps" is near equilibrium, and does not control the deposition rate), and therefore $\frac{\bar{C}_t - C_o}{C_o} \sim 0$

Under these conditions, eq(43) reduces to

$$i = C_{dl} \frac{d\eta_t}{dt} + i_o \frac{F \eta_t}{RT} \qquad (44)$$

When the steady state is reached, at $t \to \infty$, the overvoltage is η_∞. Recalling eq.(35), we may write at low overpotentials

$$i = \frac{i_o F \eta_\infty}{RT} \qquad (45)$$

Substituting this value of i in eq (44) will give

$$\frac{d\eta t}{dt} = \frac{F\ i_o}{RT\ C_{dl}}(\eta_\infty - \eta_t) \qquad (46)$$

On defining the quantity $\frac{RTC_{dl}}{Fi_o}$ "the relaxation time", τ_{ct}, of the charge transfer process, and integrating eq. (46), the equation (47) is obtained:

$$\log(\eta_\infty - \eta_t) = -\frac{t}{2.3\tau_{ct}} + \text{constant} \qquad (47)$$

The plot of $\log(\eta_\infty - \eta_t)$ against time leads to the value of τ_{ct}. At this particular value of the time, η_t is 63% of the steady-state overpotential. This statement will be briefly examined in Section VI in terms of the results obtained. However, it is assumed[1] that the observed build up of the overpotential is slower than that expected on the basis of a rate-determining charge-transfer step.

2. The two-step mechanism. In this model, the surface diffusion of adsorbed ions is no more in equilibrium, and therefore takes part in the overall deposition rate. Here, it can be stated that $\bar{C}_t - C_o$ is different from zero. Furthermore, Bockris and Gerischer have assumed that the first term of eq. (43), the double-layer charging current, is virtually equal to zero, because the double-layer charging current must be considered only in the initial stages of the potential-time curves, and not in the region where times are longer. Under these conditions, eq (43) reduces to

$$i = i_o \left(\frac{\bar{C}_t - C_o}{C_o} + \frac{Fnt}{RT}\right) \qquad (48)$$

and the time dependence can be derived in the form of eq.(49)

$$\log(\eta_t - \eta_\infty) = -\log(\frac{RT}{F^2}\frac{i}{kC_o}) - \frac{kt}{2.3} \qquad (49)$$

The plot of $\log(\eta_t - \eta_\infty)$ against time, t, gives the rate constant k, and the extrapolation of the linear graph to zero time gives the intercept I, which is the quantity $-\log(\frac{RT}{F^2}\frac{i}{kC_o})$ in eq. (49). We may write

$$I = -\log(\frac{RT}{F^2}\frac{i}{kC_o}) \qquad (50)$$

On re-arranging eq.(50), the equilibrium adion concentration, C_o, can be obtained,

$$C_o = \frac{RTi}{F^2k}\frac{1}{e^{2.3x}-I} \qquad (51)$$

The total process, being the sum of a charge-transfer plus a surface-diffusion contributions, it can be deduced that

$$\eta_{\infty total} = \frac{RT}{F}\left[\frac{1}{i_o} + \frac{1}{FkC_o}\right] i \qquad (52)$$

Eq. (52), where $\frac{\eta_{\infty total}}{i}$ has the dimensions of a resistance, and if FkC_o is termed the surface-diffusion exchange current, i_{SD}, can be expressed

$$R_{total} = R_{C.T.} + R_{S.D.} \qquad (53)$$

where $R_{C.T.} = \frac{RT}{Fi_o}$ and $R_{S.D.} = \frac{RT}{F^2kC_o}$.

Eq.(52), on re-arranging, leads to eq. (54)

$$\frac{1}{i'_o} = \frac{1}{i_o} + \frac{1}{i_{SD}} \qquad (54)$$

where i'_o is the apparent exchange current obtained from the Butler-Volmer plots, and i_o the calculated exchange current controlled by activation polarisation.

These mechanisms, as applied to the silver-silver chloride electrode, will be examined further in the discussion section.

REFERENCES

1. J. O'M. Bockris and A. K. N. Reddy, "Modern Electrochemistry", vol. 2, chap. 7 (p. 687), chap. 10 (p. 1194), (1976).
2. L. I. Antropov, "Theoretical Electrochemistry", Mir Publishers, 2nd edition, chap. 11 (p. 296), Moscow, (1977).
3. M. J. Sparnaay, "The International Encyclopaedia of Physical Chemistry and Chemical Physics", Vol. 4, "The Electrical Double Layer", Pergamon Press, Glasgow, (1972).
4. P. Debye and E. Hückel, Physik. Z., 24, 185, (1923).
5. W. J. Moore, "Physical Chemistry", 4th Edition, chap. 12, (1963).
6. J. P. Brenet and K. Traore, "Transfer Coefficients in Electro-chemical Kinetics", Academic Press, London, N.Y., (1971).
7. J. A. V. Butler, "Electrocapillarity", Chap. 4, 57 and 72, Methuen, (1940)
8. A. Damjanovic in "Modern Aspects of Electrochemistry - The Mechanism of the Electrodeposition of Metals", ed. J. O'M. Bockris and B. E. Conway, Vol. III, London, (1964).
9. H. Gerischer and R. P. Tischer, Z. Elektrochem., 61, 1159, (1957).

SECTION III

E X P E R I M E N T A L

A. THE CELL ASSEMBLY.

1. Design of the cell. The cell, which had been successfully used in preliminary work in this laboratory[1], was of all-glass construction, consisting of two parts, a "main-cell" section and a reference electrode section. The main features are illustrated in figs. 1(a) and 1(b). The test electrode and counter electrode compartments were connected by a central tap (T_1) of wide bore (3 mm), such as to provide a good conducting path between the test and counter electrodes. The main cell and reference electrode sections were joined by an adjustable Luggin capillary tube, which passed through a plastic screw-fitting and was sealed in place with a neoprene gasket (fig. 2). To minimise the "ohmic drop", the capillary tube was positioned very close to the test electrode (< 1 mm). (To avoid the possibility of screening effects which could be produced by the non-conducting capillary tube adjacent to the test electrode, however, the capillary tube was narrowed to 1 mm diameter, and was thin-walled at the tip[2]).

The cell required only a small amount of solution, less than 35 cc, so that solvents were used economically.

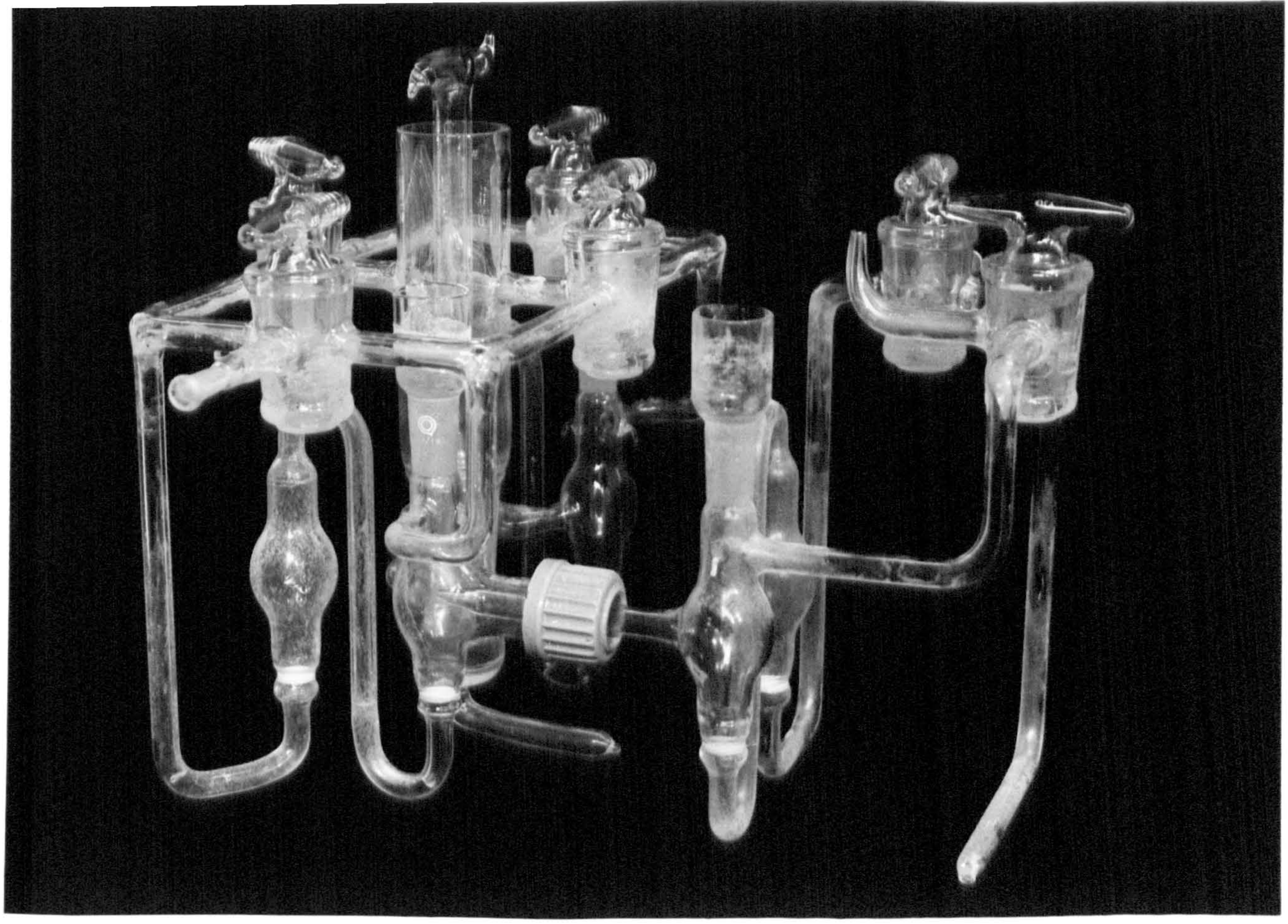

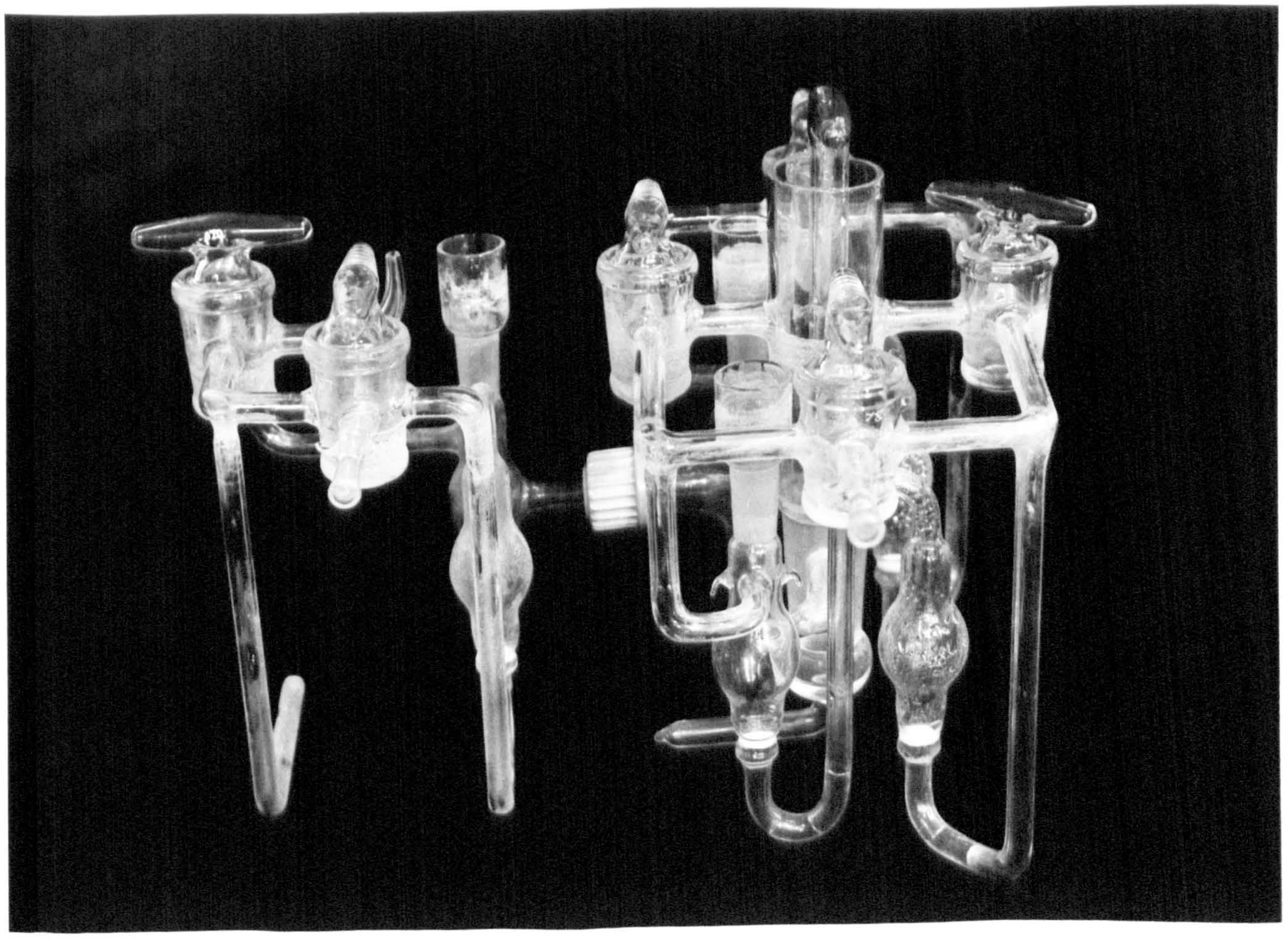

FIG. 1. THE CELL.

(a) Main Section.

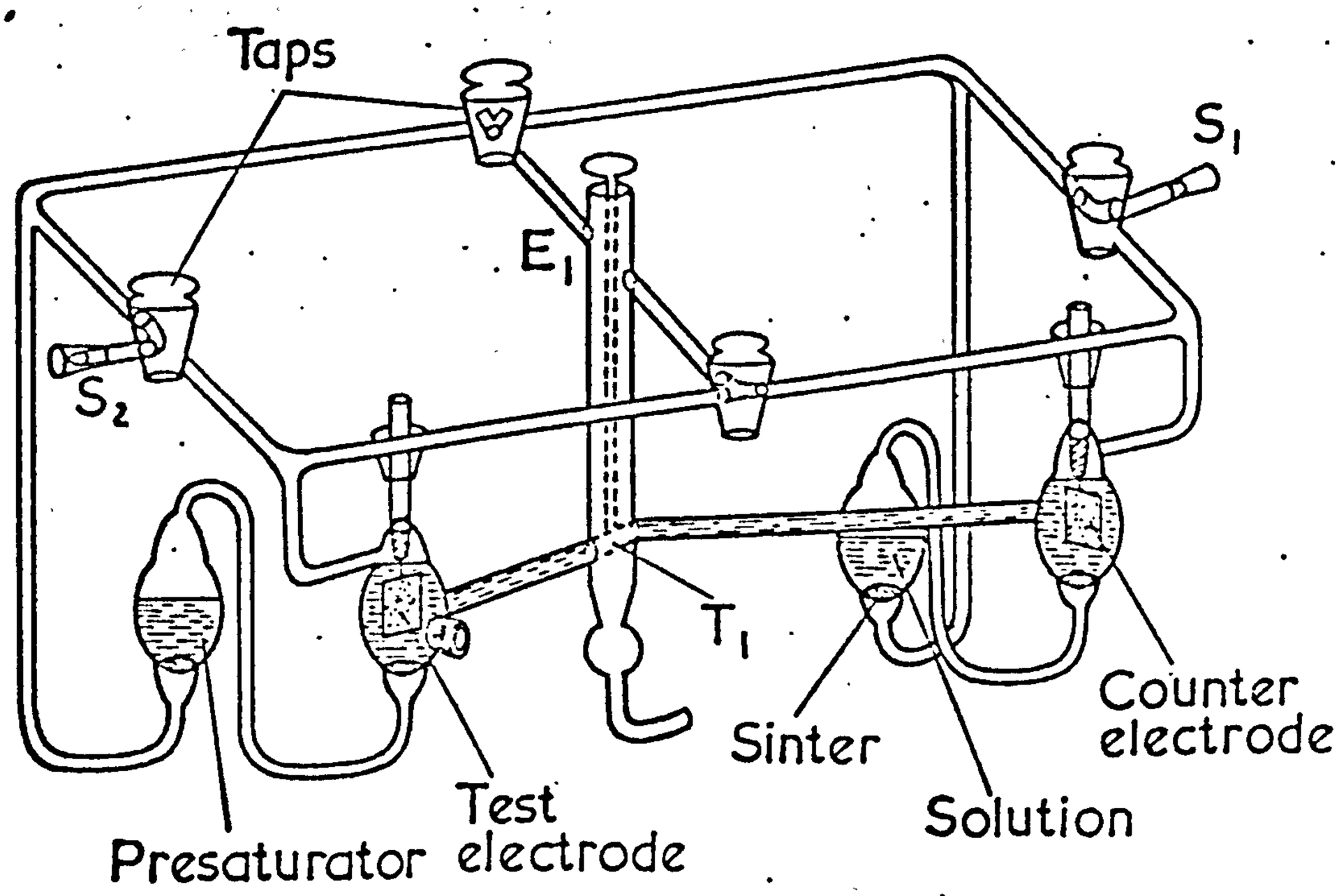

(b) Reference electrode section.

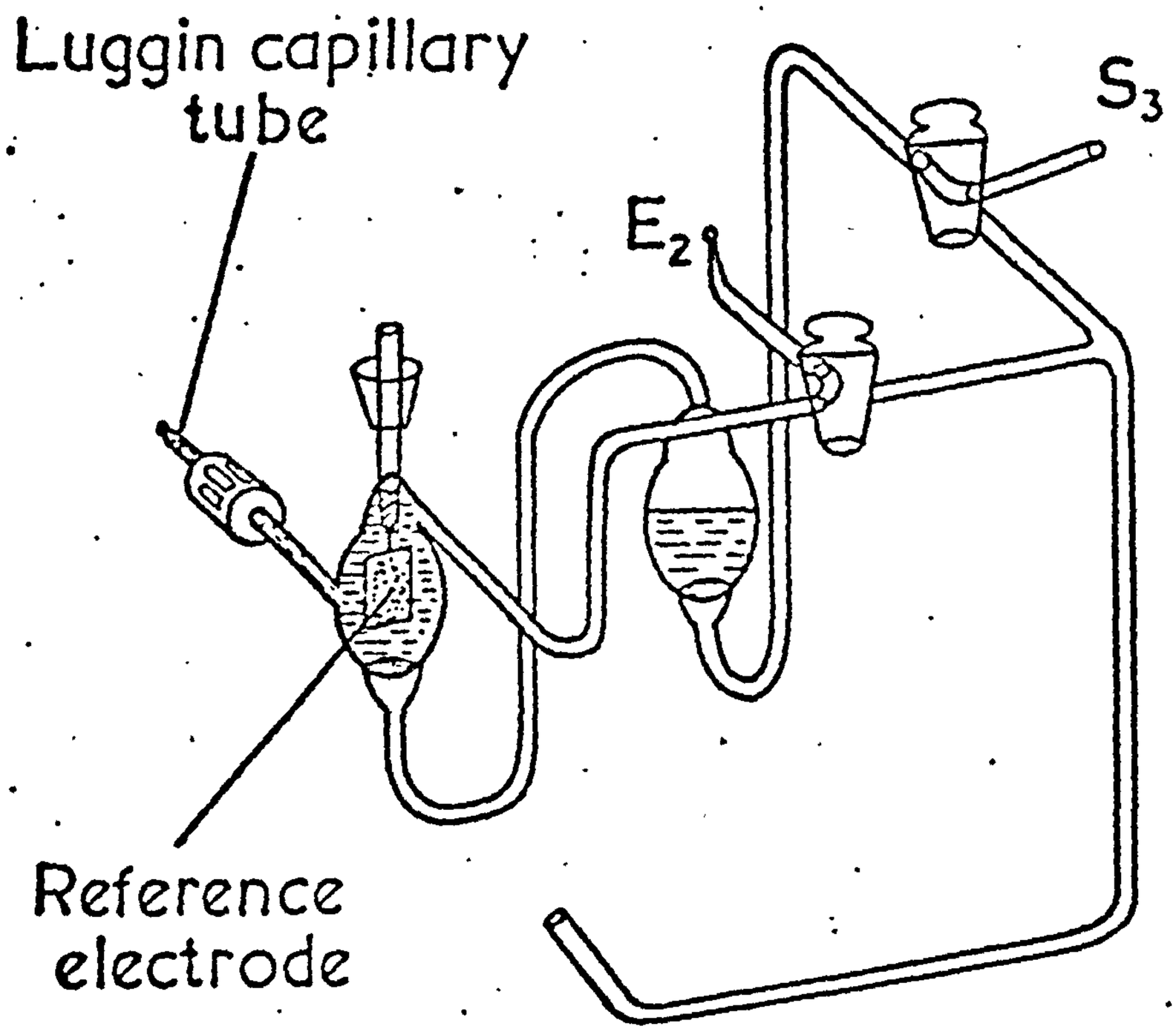

FIG. 2. LUGGIN CAPILLARY CONNECTION.

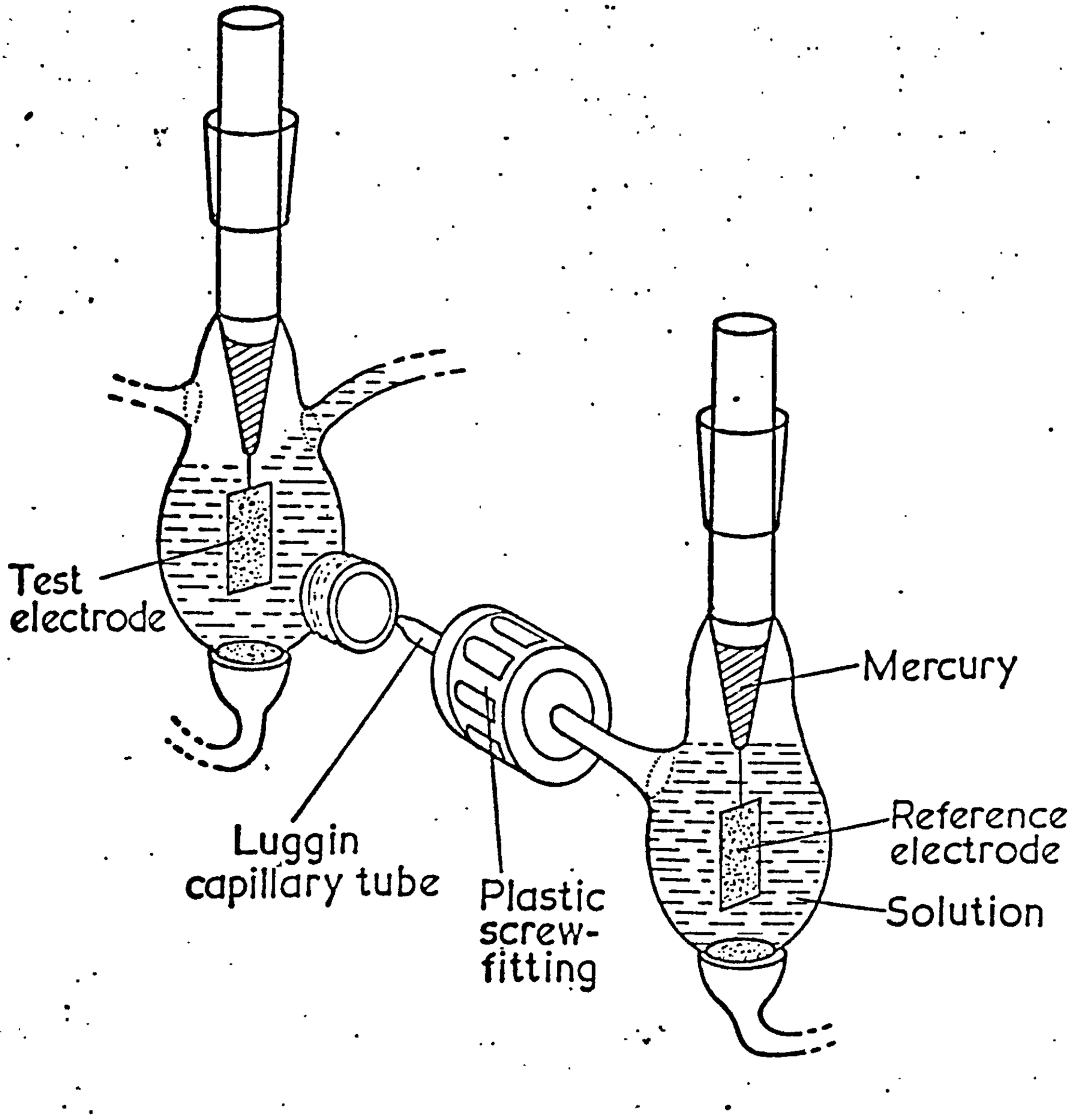

Another important advantage of the small size was that equilibrium conditions were rapidly attained when a steady stream of nitrogen was passed through the solutions. For this purpose, the taps were delicately manipulated in nearly closed positions. One problem occasionally encountered was that the contact between the reference and the test compartments could be sometimes interrupted by small bubbles of air inside the capillary tube. It was possible to eject these bubbles, however, by applying a slight pressure on the outlet E_2 of the cell.

2. Manipulation of the cell. The cell, which had been previously cleaned in fuming nitric acid, washed several times with distilled water and oven-dried, was clamped in position in the tank with the aid of an adjustable "lab-jack" stand as a base, and was connected, using the B_5 sockets (S_1, S_2, S_3), to an all-glass gas line. The procedure for filling and operating the cell was as follows. Oxygen-free nitrogen purified by passage through columns of silica gel and potassium hydroxide to remove water and carbon dioxide respectively, was passed through all the lines and the cell to flush out residual air. Solution was placed in the main compartments, and by operating the appropriate taps of gas lines and of the cell, it was directed through the presaturators, before being released

via the exit tubes. With the electrodes in place, the main compartments and the electrodes were washed twice with the solution to be studied, and the main compartments were then filled to a level so as to cover the electrodes entirely. The presaturators were half-filled in a similar manner. The cell could be emptied by passing solution through the presaturators. Flexible glass coils incorporated into the delivery lines facilitated removal and re-assembly of all parts of the apparatus.

B. ELECTRODES.

1. General considerations. One requirement for polarisation experiments is that there should be uniformity of potential over the entire area of a test electrode. Silver-silver chloride electrodes match up to this requirement since they can be made with a homogeneous structure. For convenience a silver-silver chloride electrode was also used as the reference electrode.

2. Preparation. The silver-silver chloride electrodes were of the thermal-electrolytic[3,4,5] type, which have been found the most reliable. Those of the electrolytic type[3,4] have previously shown large bias potentials (up to 1 mv), and were not used. Attempts to prepare circular foil "silver-mirror" electrodes[3] in this study were less than satisfactory. These electrodes gave bias potentials of 1 - 8 mv. Many

sets of thermal electrolytic electrodes of different shape and of different surface area were prepared (Fig.3), using (a) flat platinum foil of 2 x 0.5 cm, (b) curved platinum foil of 1.2 x .5 cm, and (c) platinum spiral of 0.5 cm diameter. These foils and spirals were sealed into B10 pyrex cones. (For the purpose of contact with the outside circuit, a small drop of mercury was added to the inside of the glass cone before the electrodes were used in an experiment). The exterior ends of the platinum wires were covered with a freshly prepared silver oxide paste (see paragraph C), which was decomposed to white silver by heating gradually in a muffle furnace (Cromartie Kilns Ltd.) from 100^{o}C to 500^{o}C. The electrodes were allowed to cool within the oven to avoid thermal shock. The whole process was repeated until a relatively smooth and unbroken deposit was obtained. Electrodes of type (a) were anodised in a 1 molar solution of high purity "Aristar" hydrochloric acid using a current density of 9 mA per electrode for five hours. For type (b) electrodes, a current density of 0.9 mA per electrode was passed for one day. The type (c) electrodes were anodised in 0.1 molar solution of hydrochloric acid, using a current of 2 mA per electrode for 45 min. All electrodes were thoroughly washed with double-distilled water after anodisation, and stored in 0.01 molar solution of hydrochloric acid under a slow stream of nitrogen gas. They

FIG. 3. DIFFERENT TYPES OF ELECTRODES.

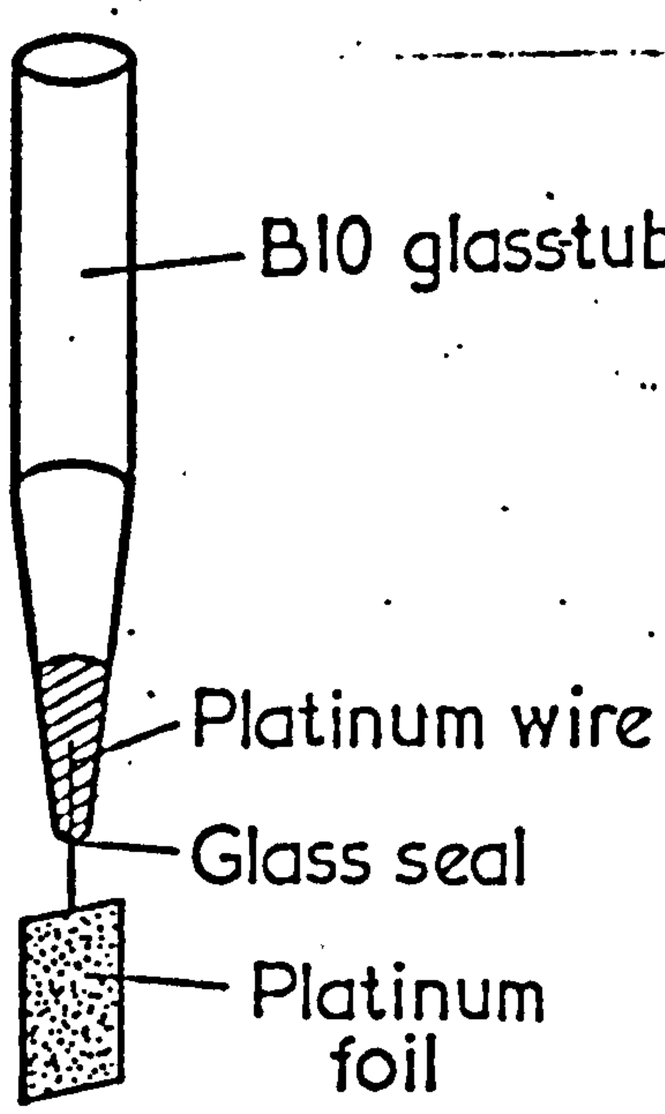

(a) Flat platinum foil electrode

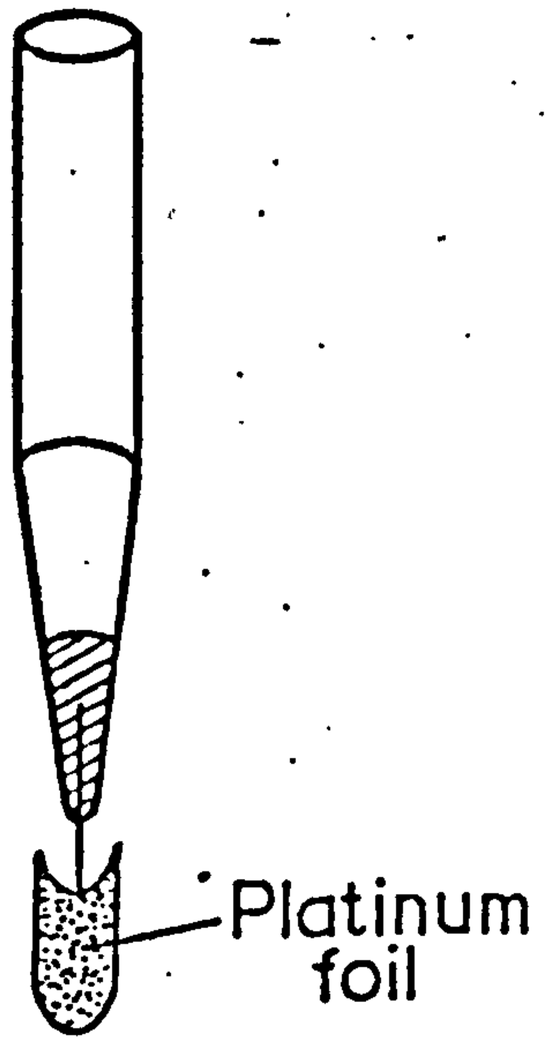

(b) Curved platinum foil electrode

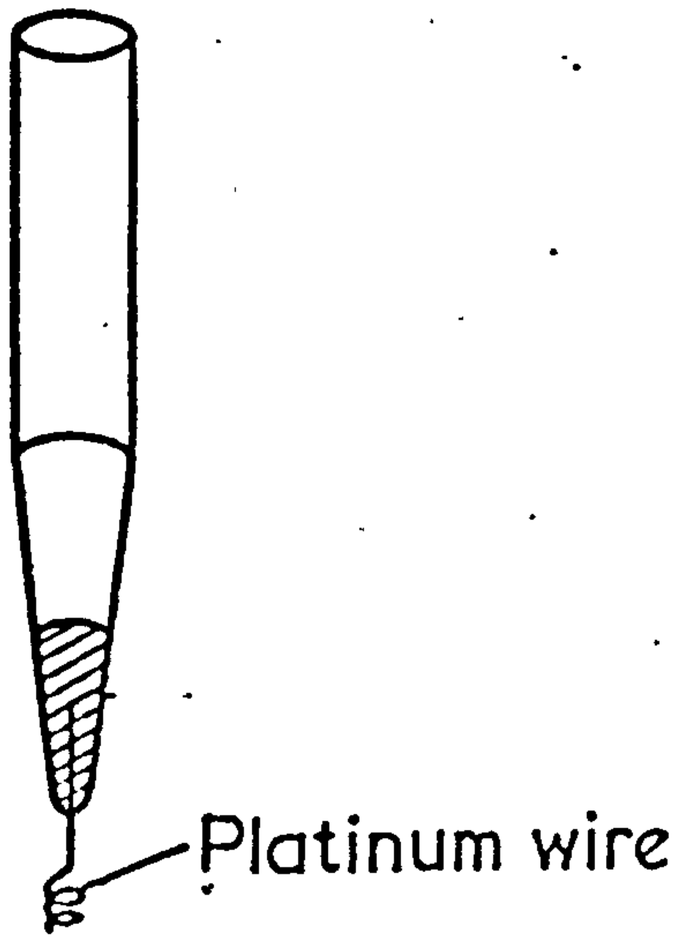

(c) Platinum spiral electrode

were kept under such conditions for at least ten days to allow for the aging process[3,4]. The bias potentials were then measured with reference to electrodes already prepared in the same manner and aged for several months. Electrodes showing bias potential greater than ±0.05 mv in aqueous medium were rejected. Typical values of bias potentials were ±0.02 mv (type (a)); ±0.04 mv (type (b)), and ±0.01 mv (type (c)). However, it was noted that the bias potentials sometimes increased when the electrodes were transferred into the cell solutions to reach values of the order of 0.1 mv in aqueous medium, and 0.3 mv in non-aqueous solvents. This was not regarded as serious deficiency for the purposes of the polarisation experiments. Before an experiment, electrodes were inserted in B10 sockets of storage test tubes containing a 0.01 molar hydrochloric solution diluted in the appropriate solvent, and were kept in there several hours before the experiment. To avoid the possible risks of contamination with impurities, the test tubes were stored in a desiccator over silica gel.

3. Procedure for electrodes having variable times of anodisation.

One important part of the project was to investigate the electrodic characteristics as a function of anodisation time. The procedure was as follows : Silver electrodes of type (b) were anodised for 15 min during which time a certain amount of silver was converted to silver chloride

The electrodes were then left to age until the bias potentials had become stable. This normally took 48 hours. The first polarisation experiment was then performed. The same electrode was then anodised once more, thus increasing the thickness of the silver chloride layer. After a second equilibration period, the electrode was again polarized. The whole process was repeated several times to determine the electrode characteristics as a function of anodisation time. These results are presented later in Section V.

C. PREPARATION AND PURIFICATION OF MATERIALS.

1. Silver oxide paste. A slight excess of 1 M potassium hydroxide solution was added to 1 M silver nitrate solution to give a dark brown and spongy precipitate. The mixture was then vigorously stirred, and the precipitate allowed to settle. The supernatant liquid was then decanted, and the silver oxide washed about forty times by decantation with double distilled water, to ensure the removal of all electrolytic impurities[3]. The specific conductance of water rejected from the final washings, and measured with a Doran conductivity bridge and a Mullard conductivity cell (type E7591/A, cell constant = 1.57), was $\sim 5 \times 10^{-5}\ \Omega^{-1}\ cm^{-1}$, indicating that the paste was free of alkaline impurities.

A less dense khaki precipitate, obtained from mixing dilute solutions, i.e. 0.1 M $AgNO_3$ and 0.1 M KOH, either

with or without stirring, proved unsatisfactory for electrode preparation.

2. Solvents.

(a) Water. Double distilled water was used throughout the experiments. The specific conductance was $\sim 10^{-6}\ \Omega^{-1}\ cm^{-1}$.

(b) N-methylpropionamide. This was prepared by the method described by Leader and Gormley[7] and Kamboj[8]. Anhydrous methylamine gas was passed through a vigorously stirred solution of propionic acid until the mixture had acquired a brown colour. The mixture was then distilled above 100°C to remove water at atmospheric pressure, using a simple distilling head. Water and propionic acid were removed from the distillate by shaking it with calcium oxide. The liquid was then purified by repeated fractional distillation under vacuum (0.01 mm Hg). To minimise fluctuations of the distilling temperature (about 65°C), the flask containing the liquid was entirely covered with aluminium foil. "Head" and "tail" fractions of ca.50 cc were rejected each time. The NMP obtained after about 10 distillations had no smell, and the specific conductance was $\sim(0.3 - 2.5) \times 10^{-6}\ \Omega^{-1}\ cm^{-1}$ at 25°C. [The literature[7] $= 1 \times 10^{-6}\ \Omega^{-1}\ cm^{-1}$]. The solvent was stored in a stoppered flask and kept in a desiccator over silica gel until needed.

(c) Methanol. "Analar" grade methanol was purified by the method

of Leighton, Crary and Schripp[9]. Aldehydic impurities were first removed by heating the solution in the presence of 10 gms of silver nitrate and 20 gms of potassium hydroxide per litre of methanol. After the mixture had been refluxed under nitrogen for 3 hours, using a condenser opened to the atmosphere, the solvent was distilled at 65°C directly into a flask containing granular anhydrous calcium sulphate in proportions of 20 gms/litre of methanol to remove water. The flask was left stoppered for a few hours and shaken occasionally. Methanol was then decanted and distilled three times through a 4 ft. column of glass helices. The "head" and "tail" fractions were rejected each time (about 250 ml). The specific conductance was $\sim 2 \times 10^{-6}\ \Omega^{-1}\ cm^{-1}$; [Lit[5]. $= 1.5 \times 10^{-7}\ \Omega^{-1}\ cm^{-1}$]. The purified solvent was stored in a desiccator over silica gel.

3. Preparation of hydrochloric acid solutions. "Analar" grade hydrochloric acid was used to prepare HCl solutions of different concentrations in doubly distilled water. Solutions were made up by volume. The concentration of each solution was determined by potentiometric titration with sodium hydroxide solutions (0.001 - 1M), using a glass electrode and a digital pH meter (Radiometer pHM 64).

Solutions of HCl in NMP were prepared in a specially constructed apparatus according to a procedure described

by Kamboj[8], and Taniguchi and Janz[10]. Gaseous hydrochloric acid,formed by dropwise addition of concentrated hydrochloric acid onto concentrated sulphuric acid, was carried in a stream of dry nitrogen through a column of silica gel and thence onto NMP. The concentration of the stock solution thus prepared (pH titration) was 0.409 molar. This solution was kept in a desiccator over silica gel to prevent ingress of moisture, and checks showed that the concentration remained unchanged during the time the experiments were performed (few weeks). The stock solution was diluted by volume with NMP as required to prepare solutions of different concentrations. 50 cc from each diluted solution was titrated (pH titration) to determine concentrations.

For the preparation of hydrochloric acid solutions in methanol, the same procedure as above was adopted, with one restriction, however. Methanolic hydrochloric acid at concentrations greater than 0.05 mole Kg^{-1} slowly decomposes into chloroform and water[11,12], causing a change in the concentration. To minimise such decomposition, a less concentrated stock solution (C = 0.0278 molar) was prepared. This concentration was checked from time to time, and no changes in concentration were detected during the period of the experiments. (Later analysis, however, showed a 45% fall in concentration over a period of one year).

D. ANCILLARY EQUIPMENT.

1. Temperature control. A glass tank, insulated and filled with distilled water, was used as a thermostat bath. For polarisation experiments performed at 25°C, the water was maintained at 25 ±0.01°C by a 50 W electric heater controlled by a contact thermometer and relay, and was circulated by an electric pump. At higher temperatures (30 - 40°C), a 500 W heater was used with an additional booster heater of 50 W. When experiments were carried out at lower temperatures (10 - 20°C), a small fridge probe was necessary to maintain the bath temperature below the room temperature (22 - 25°C), and control was provided with the 500 W heater and the on/off relay. Temperature control, over the whole range of 10 - 40°C, was within ±0.015°C. Temperatures were read with the aid of a digital quartz thermometer (Hewlett Packard 2801 A), reading up to 0.0001°C.

2. Measurement of overvoltages and currents. Cell voltages were read with a digital voltmeter (Hewlett Packard 3450 A) reading to ±1 μV. It was standardized periodically against a standard cell (Weston type 1268). The digital voltmeter was connected to a digital recorder (Hewlett Packard 5055A) which had a variable recording time, and could be used to record the cell voltage automatically, at a rate as fast as 1 reading per second. The main advantage of using such instrumentation

was that the operator was free to make adjustments to the apparatus, and to make other observations while the e.m.f. reading was in progress.

A constant current generator contructed by the electronics unit at Queen Elizabeth College, used to select current values in the range of 0 - 100 μA, was connected to a digital multimeter (Keithley Model 160), used as a microammeter to note values read to ±1 ηA (± 0.1% of current value).

E. POLARISATION EXPERIMENTS.

1. Circuitry. The circuit diagram is depicted in fig. 4 below.

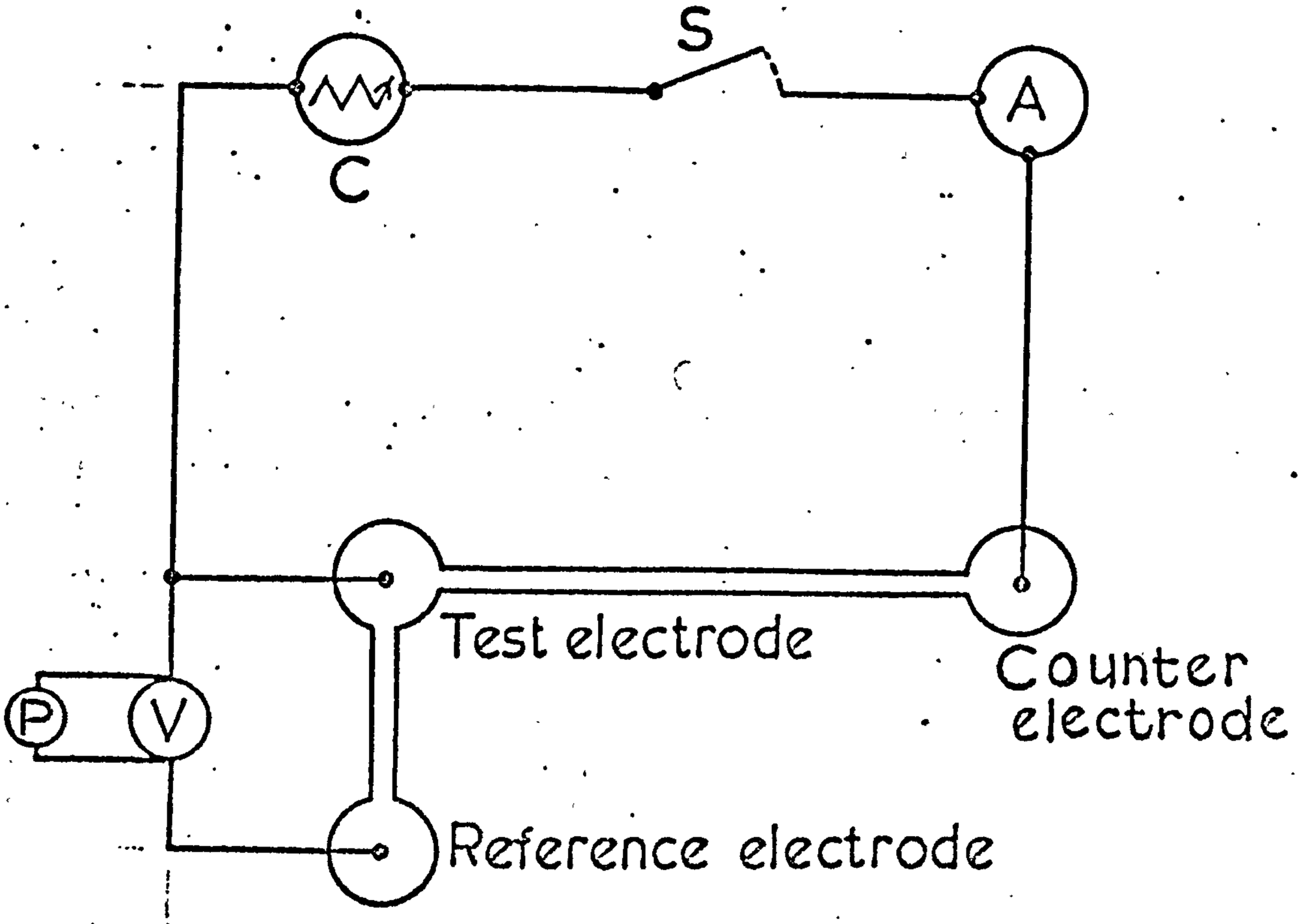

The polarizing current was produced by the constant current generator (C) connected to the ammeter (A). Once switched on, using a fast switch (S), the current passed through the counter electrode and the test electrode. The cell e.m.f., measured across the test and reference electrodes, was read on the voltmeter (V) and printed correspondingly on the printer (P).

2. Preparation of the cell for polarisation experiments.

Once the cell had been filled with the solution to be studied, the capillary tube was adjusted to its nearest position to the test electrode (< 1 mm). A slow steady flow of nitrogen was passed through the presaturators and main compartments, and was maintained during the run. The electrodes were then allowed to reach equilibrium, i.e. a very stable difference of potential between the test and reference electrodes. The equilibration time was 3 - 24 hours, and the equilibrium bias 1 - 100μV.

3. Procedure for polarisation experiments. A constant current value was selected on the generator dial, starting with a low value, usually 0.1 - 0.3 μA. The polarizing circuit was then switched on, and at the same moment a stop watch was started by hand. The cell potential was automatically recorded at 1 sec. intervals over the initial rise portion of the polarisation. This normally took 5 - 10 seconds,

after which time the recording speed was reduced and the potential was recorded at 15 sec. intervals, until a steady state was reached. The current was then switched off, and the test electrode was allowed to return to its initial equilibrium potential to within 10 - 40 μV. During this "relaxation time", the initial change of the cell voltage was again recorded in the same manner, determining a second value for the decay of the differential double layer capacitance (see Section V). The current was then reversed by exchanging the connecting wires, and the complete procedure was repeated.

The whole process is illustrated in fig. 5. At A, at t = 0, the polarizing current is switched on and the cell potential starts changing from its equilibrium value. Part B shows the initial rise portion of the potential change, while Part C indicates a slower variation of the potential, where the recording speed was reduced. Part D marks the steady state of near-constant potential. At E, the current was switched off and the depolarisation profile was recorded. The rapid drop in potential arises from the collapse of the double layer, the inverse of part B. When the electrode had nearly reached its initial equilibrium value at G, the current was reversed, and the test electrode was polarized in the reverse way ("negative potential"), then depolarized, as shown from H to I.

FIG. 5. PROFILE OF POLARISATION EXPERIMENTS.

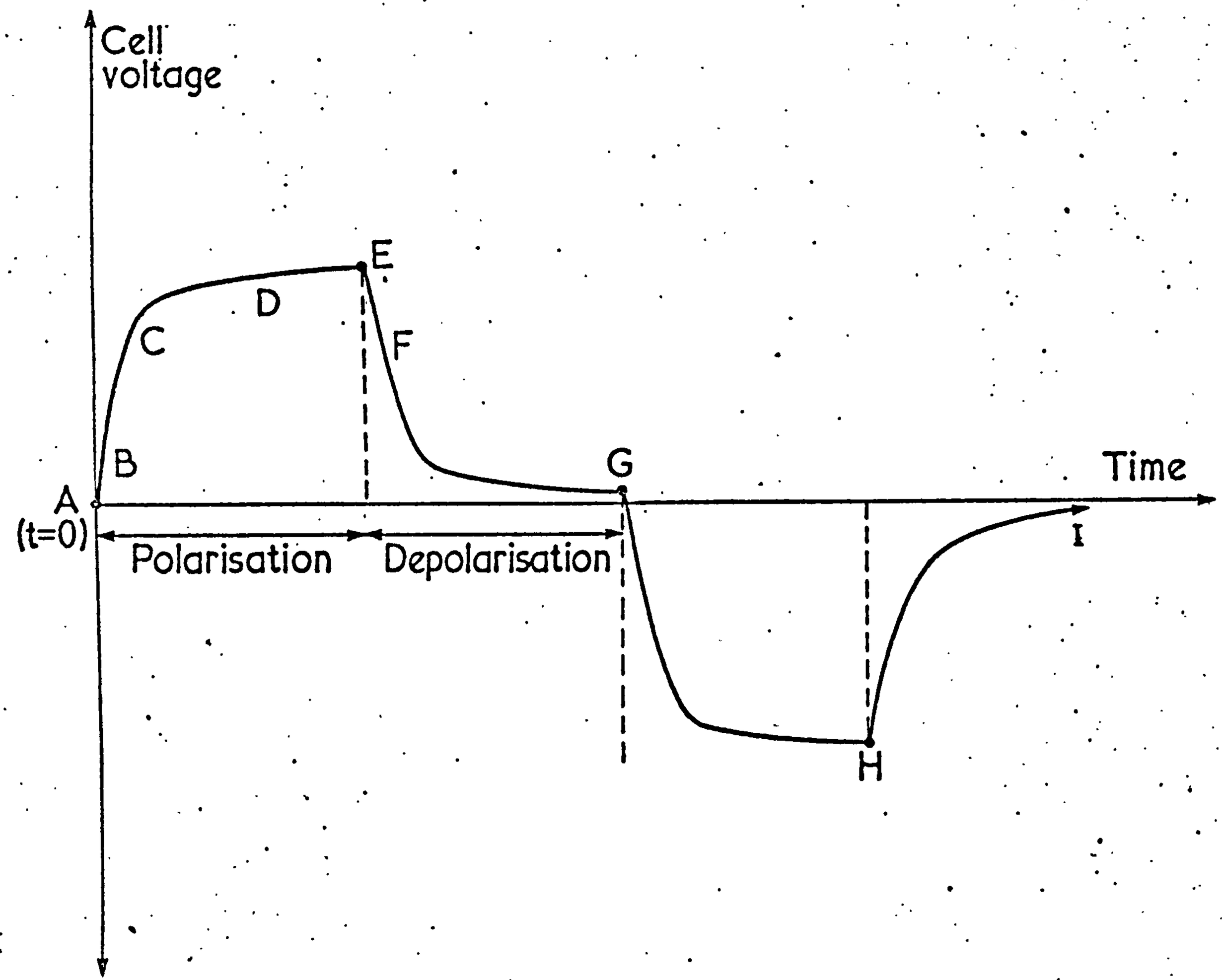

The current was then increased, i.e. from 0.1 - 0.3 to 0.5 - 0.6 μA(and gradually up to 2.7 μA in the following runs). The cell voltage was recorded for 3 or 4 different values of the current and for both directions of the current. The whole procedure was then repeated with solutions of different concentrations (0.001 - 0.2 M), representing a series of polarization experiments for each solvent. Many series of experiments were performed in the same manner to investigate electrodic characteristics as a function of solution concentration, anodisation time, and temperature.

A very few experiments gave potential profiles which were erratic and not in accordance with fig. 5. These were adjudged to be unsatisfactory (presumably because of the presence of impurities or for other unknown reasons) and were rejected.

REFERENCES.

(1). H. P. Bennetto and E. K. C. Pang, (unpublished work).

(2). G. Hills, M. Fleischmann and co.workers : "Advanced Instrumental Methods in Electrode Kinetics", Southampton (1973).

(3). D. J. G. Ives and G. J. Janz, "Reference electrodes, Theory and Practice", Academic Press, New York, (1961).

(4). G. J. Janz and H. Taniguchi, Chem.Rev., "The silver-silver halide electrodes", 53, 297, (1953).

(5). H. S. Keston, J. A. C. S., 57, 1671, (1935).

(6). P. Watson, Ph.D. Thesis, London, (1963).

(7). G. R. Leader and J. F. Gormley, J. A. C. S., 73, 5731, (1951).

(8). I. K. Kamboj, Ph.D. Thesis, London, (1978).

(9). P. A. Leighton, R. W. Crary and L. T. Schripp, J. A. C. S., 53, 3017, (1931).

(10). H. Taniguchi and J. G. Janz, Anal.Chem., 28, 287, (1956).

(11). H. P. Bennetto and J. J. Spitzer, J. C. S., Faraday, 69, 1492, (1973).

(12). G. Nonhebel and H. Hartley, Phil.Mag., 50, (6), 729, (1925).

SECTION IV

ELECTRODIC STUDIES OF SILVER-SILVER HALIDE AND OTHER ELECTRODES: A REVIEW.

A. INTRODUCTION.

The electrochemical literature reveals that very many studies have been carried out on the double-layer at mercury and other electrodes. Some information on the exchange currents of a few systems such as metal electrodes is also available, but rarely have both the exchange current and the double-layer capacitance been measured together. The reasons are connected with the techniques used in the measurements and the approach to the problem,as mentioned in the introductory section.

Following the classic work of Bowden and Rideal[1], the hydrogen electrode has been extensively studied, and the mechanism of the electrode reaction has been ruthlessly explored. This electrode is however regarded as a special case and will not be discussed here (although it may be noted that both the hydrogen electrode and the electrodes studied in the present work involve extensive adsorption of reactants). More recent work has centred on the important electrode reactions relating to metal deposition, such as the silver or the copper electrode. A brief survey will be outlined next for the metal electrodes, since models for the

electrodeposition have been applied to results for the Ag-AgCl electrodes.

B. METAL ELECTRODES.

1. Electrocapillary and related studies. Numerous investigators have examined capacitance/potential curves for metal electrodes. The recent work of Minc[2] and co-workers may be cited as fairly typical. In a study of several electrodes, they measured the differential capacitance of a silver electrode, deriving the values 11 $\mu F\ cm^{-2}$ and 17 $\mu F\ cm^{-2}$ at the minimum of the electrocapillary curve in potassium fluoride solution at 0.005 M and 0.03 M respectively. The apparatus used was rather complicated, the information obtained comparatively little. In a similar study Devanathan[3] reported that the data given by different authors do not agree for silver, perhaps because of the surface pretreatment and the effects of impurities in the solutions. They found a capacitance of about 55 $\mu F\ cm^{-2}$ for the silver electrode in solutions of high concentration (1 M KCl).

2. Electrodeposition. Schleinitz et al.[4] studied the concentration dependence of the exchange current density in the system of the type $(Fe/(CN)_5X)^{3-}$ and $(Fe/(CN)_5X)^{2-}$ with X = NH_3, H_2O, $BuNH_2$ ... These workers used a platinum rotating disk electrode.

The plots of i_o vs. concentration represented are all of different shape depending on X, but in all cases i_o increases with concentration. The values of i_o were between 3×10^{-4} and 3×10^{-2} A cm^{-2} in the concentration range (Fe(II) or Fe(III)) $10^{-2} - 10^{-4}$ mol dm^{-3}.

In an investigation of the Cu/Cu^{2+} system, Lorenz et al.[5] examined the exchange current density and the differential capacitance as a function of Cu^{2+} concentration, using the galvanostatic double pulse method. They found the values 3 - 8 x 10^{-3} A cm^{-2} and 20 - 35μF cm^{-2} respectively, over the concentration range of 0.05 - 0.5 mol l^{-1}. A plot of log i_o versus log $C_{(Cu^{++})}$ is also presented and is linear. Tests were also carried out to determine the effects of various surface treatments at a constant concentration (concentration of Cu^{2+} = 0.1 mol l^{-1}). The values of the exchange current varried from 1.6 to 8 x 10^{-3} A cm^{-2}, and those of the capacitance from 20 to 60μF cm^{-2}. These workers also indicated that the observed overpotential contains charge transfer and surface diffusion components. Further, they reported that the overall reaction is controlled by a charge transfer step rather than by a surface diffusion process at high voltages (n > ±5 mV).

Weir and Enke[6] used the current-impulse relaxation technique to study the kinetics of rapid electrochemical reduction of mercury. The system investigated was a mercury drop in solutions of $Hg_2(ClO_4)_2$ in 1 M perchloric acid, over the concentration range 2 x 10^{-5} - 5 x 10^{-3} M. The exchange currents and the differential capacitances were in the range 0.02 - 2.74 A cm^{-2} and 30 - 464 μF cm^{-2} respectively, for the charging process. The values for the relaxation process do not agree very well with those for the charging process at high concentrations (> 1 x 10^{-3} M). A plot of i_o versus $C_{[Hg_2(ClO_4)_2]}$ is represented. This plot is linear at low concentrations, but departs smoothy from linearity at

higher ones. These investigators also studied the temperature dependence of the exchange current density in solutions of $Hg_2(ClO_4)_2$ of 1×10^{-3} M. In the temperature range 5 - 45°C i_o varies from 0.212 to 0.351 A cm^{-2}. The activation energy ΔH is 9.2 ± 0.8 KJ mol^{-1}. They concluded that the reduction is a two-electron process split into 2 single-electron steps : the first step is a discharge of solvated reactant from the outer Helmholtz plane followed by adsorption of the intermediate, and the second step is a discharge of the desolvated intermediate from the inner plane of closest approach. One of them is slow relative to the other. No rate-limiting diffusion to growth sites could be observed in this system.

A key study in the field of electrodeposition was published by Mehl and Bockris[7], who investigated the mechanism of electrolytic deposition and dissolution of silver. The rate of silver crystal growth was followed as a function of potential. The exchange currents were between 0.03 and 0.1 A cm^{-2}, and the capacitances between 20 μF cm^{-2} and 5×10^{-3} μF cm^{-2} over the concentration range 0.01 - 0.2 M. These investigators used current densities of 3 mA cm^{-2}, which they considered as "low". They found that the build-up of the overpotential was more than 10 times larger than predicted for the case of a one-step model. They argued that a slow reaction in the solution cannot be responsible for this behaviour, and that slow rise-times may be explained in terms of a slow surface diffusion of adions. As the overvoltage due to the charge transfer was found to be only 10% of the total value, the major contribution arises from surface-diffusion. They deduced that up to concentrations

of Ag^+ of 10^{-4} - 10^{-5} M and at low potentials, the surface diffusion of adions is rate-determining. In more concentrated solutions, the charge transfer step becomes rate-controlling at all current densities. In their scheme, the ions transfer from the solution to the electrode surface where they carry a "partial charge". The consecutive step is surface-diffusion of adions followed by incorporation into the lattice. Later on, Bockris et al.[8-11] reported similar findings with a rate-determining step which may be due either to a charge-transfer or a surface-diffusion step, and which was found to depend on current densities and types of surface preparation of the electrode. They concluded that the overall reaction is controlled by a surface-diffusion process at low currents, and by a charge transfer step at high currents.

In most studies it has, for practical reasons, been customary to use high currents, high voltages and high concentrations. A consequence of these rather drastic conditions may in some cases be that the interfacial structure of the electrode is appreciably changed, and certainly the reversibility of the system becomes questionable.

C. SILVER-SILVER HALIDE ELECTRODES.

1. Electrodic studies. Few workers appear to have studied the electrodic characteristics of the Ag-AgX system (where X is a halide). Meyer et al.[12] applied the chronopotentiometric method to the silver-silver chloride electrode in NaCl solutions and found the exchange current to be around 5×10^{-4} A cm^{-2} for a concentration of 0.005 M. The silver-silver chloride electrode was also studied by Slusarek[13]

who used suspensions of 5 mM AgCl in 0.1 M KCl. The methods employed were oscillographic polarography and cyclic voltammetry. The evidence of this work shows that suspended AgCl particles are electrochemically active only in the presence of an excess of chloride ions, and that the chloride ions are required for the reduction process of Ag^+ ions.

Following many years of careful study of silver iodide sols by the Lyklema school[14], van Leeuwen and Peverelli[15] evaluated the exchange current densities and the differential capacitances of a thin film silver-silver iodide electrode. The electrodes were prepared in the following manner : a silver layer is deposited (vacuum deposition) at the bottom of a soft glass tube. Then the silver electrode reacts with iodine vapour under reduced pressure (1 min). The AgI thickness was 3.8×10^2 nm. These workers used aqueous AgI solution (suspensions) and an "inert" supporting electrolyte (0.1 M KNO_3). Using the coulostatic pulse method, the relaxation of the electrode potential was measured as a function of time after applying a small charge to the system, and the potential/time curves were then analyzed to determine the exchange current and the differential capacitance. These curves were followed for two time-ranges - the μ sec. range (fast relaxation) and the milli-sec. range (slow relaxation). The plots of log i_o vs. pI showed that the exchange current was independent of concentration in the case of the fast process (the electron exchange at the Ag/AgI interface), but it increased with increasing concentration of iodide or

silver ions for the slower reaction at the AgI/I^- interface. The transfer coefficients for iodide and silver ions were 0.68(±0.04) and 0.61(±0.06) respectively. The plots of the differential capacitance against pI show no variation of C_{dl} with the concentration in the case of the fast process, but C_{dl} increases with concentration above $C_{(I^-)} = 10^{-5}$ M in the case of the slow reaction. The plots of C_{dl} vs. pAg also reveal the same findings : constancy of C_{dl} with pAg (fast process) and variation of C_{dl} with pAg (slow process).

From the dependence of potentials, Watson and Yee[16] studied the rate of the exchange of chloride and iodide ions for the Ag/AgCl electrodes in solutions containing both chloride and iodide ions :

$$AgCl \rightleftharpoons Ag^+ + Cl^-$$

They found that the I-Cl exchange takes place in the solution phase rather than in the solid phase since AgI appears as a fine crystalline precipitate on the electrode surface. It appears that the electron transfer is not involved in this process, and the rate-determining step was the one below involving the iodide ions.

$$Ag^+ + I^- \longrightarrow AgI$$

2. Mechanism of the $Ag/AgX/X^-$ electrode reaction. The silver-silver halide electrode was selected for study in the present work partly because it is known as a well-behaved reversible system which gives stable potentials and reproducible equilibrium measurements. It is surprising, however, that the reactions occuring between this kind of electrode and a solution of a soluble halide have not often

been investigated from a mechanistic view point.

Let us consider the $Ag/AgCl/Cl^-$ system and attempt to analyse the net reaction represented by

$$Ag(s) + Cl^-(sln) \rightleftharpoons AgCl(s) + e \qquad (1)$$

This overall reaction can be broken down into an electron-transfer at the Ag/AgCl interface, and an electron-exchange at the $AgCl/Cl^-$ interface, leading to several possibilities for the mechanism of the reactions. If we let phase boundaries be represented by a line, then a schematic model for the electrode may be written :

$$Ag \,|\, Cl \quad Ag \quad Cl \quad Ag \quad Cl \quad Ag \,|\, Cl^-$$

We know that the AgCl layer has a cubic structure, but that the lattice has "covalent character", and contains positive and negative "holes"[17] (charge defects). These confer high conductivity, particularly on electrolytically deposited siler chloride. Let us now suppose that oxidation of a silver atom occurs at the Ag/AgCl interface. The reaction is

$$Ag \rightleftharpoons Ag^+ + e \qquad (2)$$

Elsewhere in the system a chloride ion loses its charge and becomes incorporated in the silver chloride lattice. In the absence of mechanistic information we cannot immediately be sure where in the system this process occurs, but if the access of chloride ions to the Ag/AgCl interface is considered to be restricted by a silver chloride layer of appreciable thickness, direct combination of

Cl^- with Ag^+ formed there (eqn. 2) must be ruled out. Rather we may suppose that the incorporation of Cl^- follows or accompanies charge transfer to a silver ion or positive hole at or near the AgCl/solution interface :

$$\begin{array}{cccccc|c} Cl & Ag & Cl & Ag & Cl & Ag^+ & Cl^- \\ & & & \downarrow & & & \\ Cl & Ag & Cl & Ag & Cl & Ag & \boxed{Cl} \end{array} \qquad (3)$$

Clearly de-solvation of the Cl^- ion is necessary at this stage. To complete this exploratory picture, it is necessary for the charge to be transferred through the silver chloride layer. Since there is evidence[18] that conduction in AgCl occurs predominantly via movement of silver ions, and assuming Ag^+ ions do not escape into solution, it is reasonable to suppose that the Ag^+ ion (or a positive hole) migrates from the Ag/AgCl boundary towards the $AgCl/Cl^-$ boundary :

$$\begin{array}{c|cccccc|c} Ag^+ & Cl & Ag & Cl & Ag & Cl & Ag & Cl^- \\ & & & \downarrow & & & & \\ Ag & Cl & Ag & Cl & Ag & Cl & Ag^+ & Cl^- \end{array} \qquad (4)$$

This reaction might be represented by

$$Ag^+ + Ag^*Cl \rightleftharpoons AgCl + Ag^{+*} \qquad (5)$$

where the asterisk signifies "in lattice". (Clearly a comparable scheme might be written in which a negative charge is transferred through the lattice, and a chloride ion appears at the Ag/AgCl interface). Thus the complete reaction (eqn. 1) is made up of the processes (2), (3) and (4) [or (5)]; one electron is transferred,

and a silver chloride molecule is incorporated into the lattice :

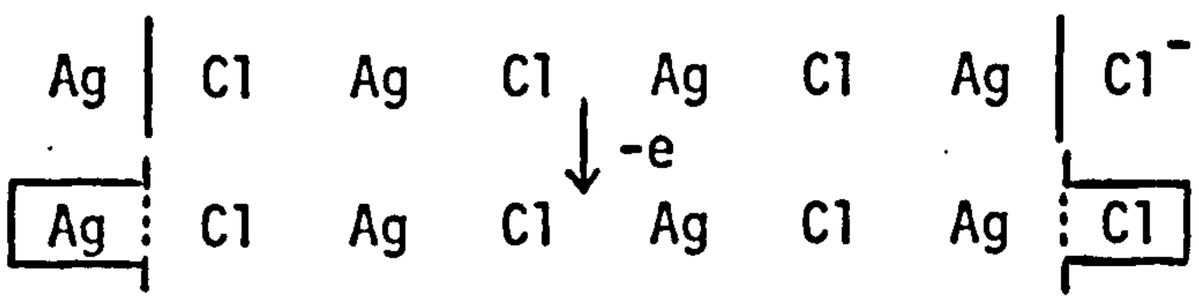

The scheme outlined above can be examined in the light of available evidence, and, later, the evidence of the present work.

Much information for the similar $Ag/AgI/I^-$ system has been obtained by Peverelli[15], who reported that the transfer processes occuring at the Ag/AgI interface are fast (conduction in AgI being regarded as very fast), and those occuring at the AgI/ solution interface are slower. The fast process was not influenced by the activity (or concentration) of electroactive ions in solution, so it seems safe to assume that silver ions (eq. 2) are indeed retained in the lattice. For the slow relaxation observed, however, the exchange current depends on the ionic concentrations. Peverelli[15] deduced from his studies the following scheme :

$$e^- + AgI \rightleftharpoons I^- + Ag \qquad \text{[Fast]}$$

(from vacancy) (soln)

and $$AgI \rightleftharpoons Ag^+ + e^- \qquad \text{[slow]}$$

(soln) (vacancy)

He reported that, as the slow process proceeds, a concentration gradient develops on the solution side, and on the AgI side. This can be considered as a gradient in silver ion vacancies which changes due to the motion of interstitial silver ions, the polarisation process involving migration of the charges (or holes). Peverelli argued that the only species able to move in the lattice are the

interstitial silver ions and that this conduction is the rate-determining step and takes place very close to or just at the electrode surface. The work of Slusarek[13] on the $Ag/AgCl/Cl^-$ system provides confirmation of Peverelli's suggestions in some respects, even though the experimental methods are entirely different. She concluded that the combination of free Ag^+ and Cl^- ions could not be rate-determining, nor could the electron exchange at the Ag/AgCl be so. Neither of these two workers considers the possibility of a surface-diffusion process as the rate-determining step.

3. Structure and aging effects. Guidance on these matters is provided by Ives and Janz[19], who made general comments on the thickness, light sensitivity, and aging of the silver-silver halide electrodes. More recently Gu and Bennion[20] studied the galvanostatic formation and the potentiostatic reduction of the silver chloride on silver in a more detailed fashion. They reported that exchange current densities on a freshly polished silver and a silver surface aged by potential "cycling" are different, a finding which is in substantial agreement with Peverelli's work. However, Gu and Bennion argued that additional "cycling" was found not to have any further effect on the electrode roughness, which is in contrast with Peverelli's conclusions(see later in Section VI). They found that the growth of silver chloride on the freshly polished and cycled surfaces is also different. The explanation given is that on a freshly prepared electrode there are a large number of silver chloride nucleation centers, but as charge is passed, the porous silver chloride film thickens, with a slow decrease in porosity. They concluded that

the true silver surface area is larger in the "cycled" case. Engel[21] used electron micrographs to estimate the surface roughness of silver chloride films grown on polished silver plates. He observed small hummocks on the aged crystals, and suggested that they were due to slow recrystallization during the aging process, since these hummocks would not be present at the non-aged surface. For these particular electrodes Engel concluded that the roughness factor would increase upon aging. Peverelli[15] used electron microscopy to examine the surfaces of the silver layer and of the AgI film. When comparing a non-aged surface to an aged one, it is possible to observe the more crystalline character of the aged surface. Thus he found that the non-aged surface shows rounded structures with ill-defined contours of crystals, but that the small crystals of a "fresh" surface have expanded to larger ones with aging. During aging, argued Peverelli, mass transfer takes place from "hummocks" to the underlying crystalline surface. The crystals grow to give a more pronounced shape, while the hummocks decrease. He defined the roughness factor of the AgI film as the ratio between the total surface area, and the geometric surface area. Then, on this basis, he estimated a roughness factor for the AgI film (by counting and estimating a measure for the irregularities observed in the two surfaces, and taking their ratio). He gives a value of 1.5 with an uncertainty of at least 10%. An important finding was that the differential capacitance of his electrodes decreased considerably with aging, which he attributed to a decrease in the roughness factor. These results will be compared with the results of the present work in the discussion section.

REFERENCES.

1. F. P. Bowden and E. K. Rideal, Proc.Roy.Soc., A, 120, 53, (1928).
2. M. Brzostowska, M. Milkowska, A. Kalinowski and S. Minc, J. Electroanal.Chem., 89, 389, (1978).
3. M. A. V. Devanathan and K. Ramakrishnaiah, Electrochim.Acta, 18, 259, (1973).
4. K. D. Schleinitz, R. Landsberg and G. V. Lowis of Menar, J.Electroanal.Chem. 28, 287, (1970).
5. Q. J. M. Slaiman and W. J. Lorenz, Electrochim.Acta,19, 791, (1974).
6. W. D. Weir and C. G. Enke, J.Phys.Chem., 71, 275, (1967).
7. W. Mehl and J. O'M. Bockris, Can.J.Chem., 37, 190, (1959).
8. J. O'M. Bockris and U. Enyo, J.Electrochem.Soc., 109, 48, (1962).
9. J. O'M. Bockris and H. Kita, J.Electrochem.Soc., 109, 928, (1962).
10. J. O'M. Bockris and E. Mattson, Trans.Faraday Soc., 55, 1586, (1959).
11. J. O'M. Bockris and A. R. Despic, J.Chem.Phys., 32, 389, (1960).
12. R. E. Meyer, F. A. Posey, P. M. Lantz, J. Electroanal. Chem. ..., 19, 99, (1968).
13. L. Slusarek, Ph.D. Thesis, Columbia University, (1977).
14. B. H. Bijsterbosch and J. Lyklema, Adv.Colloid Interface Sci.,9,147,(1978).
15. K. J. Peverelli, Ph. D. Thesis, Netherlands, (1979).
16. D. E. Watson and D. M. Yee, Electrochim.Acta, 16, 549, (1971).
17. J. O'M. Bockris and A. K. N. Reddy, "Modern Electrochemistry", Vol. 2, chap. 7, (1976).
18. H. Hoshino and M. Shimoji, J.Phys.Chem.Solids, 35, 321, (1974).
19. D. J. G. Ives and G. J. Janz, "Reference Electrode, Theory and Practice", Academic Press, New York, (1961).
20. H. Gu and D. N. Bennion, J.Electrochem.Soc., 124, 1364, (1977).
21. D. J. C. Engel, Ph. D. Thesis, Utrecht, (1968).

SECTION V.

RESULTS AND CALCULATIONS

A. CHARACTERISTICS OF THE POLARISED SILVER-SILVER CHLORIDE ELECTRODE AS A FUNCTION OF SOLUTION CONCENTRATION.

1. Determination of overpotentials and exchange current densities from the analysis of polarisation curves. As described in section III, the polarisation of silver-silver chloride electrodes was investigated in water, NMP and methanol, using hydrochloric acid solutions in the concentration range 0 - 0.2 molar. For each concentration, 6 to 8 polarisation curves were determined for as many values of the current (0.1 - 2.7 μA). The general form of these results is illustrated by the following detailed analyses for two polarisation experiments in each solvent for the same value of the current, but in forward and reverse directions. (Results presented are for a "rough" electrode of type (a)).

Table 1 gives values of the potential (V_t) of a polarised silver-silver chloride electrode (relative to a silver-silver chloride reference electrode) in aqueous hydrochloric acid(0.01 M) as a function of time. Values for both "positive" and "negative" currents are tabulated in tables 1(a) and 1(b) respectively. The corresponding graphs of V_t against time are shown in figures 1(a)

TABLE 1. Polarisation of a silver-silver chloride electrode in aqueous hydrochloric acid (0.01 M) - (a) Positive current (0.810 μA).

Time/s	$V_t/\mu V$	Time/s	$V_t/\mu V$	Time/s	$V_t/\mu V$
0	289(Vo)	300	398	735	436
2.5	292	315	400	750	437
5	304	330	402	765	438
7.5	304	345	404	780	439
10	311	360	406	795	440
12.5	316	375	408	810	441
15	319	390	409	825	442
17.5	321	405	411	840	442
20	324	420	413	855	444
22.5	324	435	414	870	444
25	324	450	416	885	445
27.5	328	465	417	900	445
30	330	480	418	915	446
45	338	495	420	930	446
60	344	510	421	945	447
75	350	525	422	960	448
90	355	540	423	975	448
105	360	555	425	990	448
120	364	570	426	1005	448
135	369	585	427	1020	449
150	372	600	428	1035	450
165	375	615	429	1050	450
180	379	630	430	1065	451
195	383	645	431	1080	451
210	384	660	432	1110	452
225	388	675	433	1140	453
240	390	690	434	1170	454
255	393	705	435	1200	455
270	394	720	436	1230	456
285	396			1260	457

TABLE 1 (contd.) (b) Negative current (-0.810 μA)

Time/s	$-V_t/\mu V$	Time/s	$-V_t/\mu V$	Time/s	$-V_t/\mu V$
0	292(V_o)	300	398	735	436
2.5	292	315	400	750	436
5	304	330	400	765	438
7.5	304	345	403	780	438
10	304	360	405	795	439
12.5	317	375	407	.810	440
15	320	390	408	825	440
17.5	322	405	410	840	441
20	325	420	412	855	442
22.5	325	435	414	870	442
25	325	450	415	885	444
27.5	329	465	416	900	444
30	330	480	418	915	444
45	338	495	419	930	445
60	345	510	420	945	445
75	350	525	422	960	446
90	354	540	423	975	447
105	360	555	424	990	447
120	364	570	425	1005	448
135	368	585	426	1020	448
150	372	600	427	1035	449
165	375	615	429	1050	449
180	378	630	429	1065	449
195	382	645	430	1080	450
210	384	660	431	1110	452
225	387	675	431	1140	452
240	388	690	432	1170	454
255	391	705	434	1200	455
270	394	720	435	1230	456
285	395			1260	456

FIG. 1.

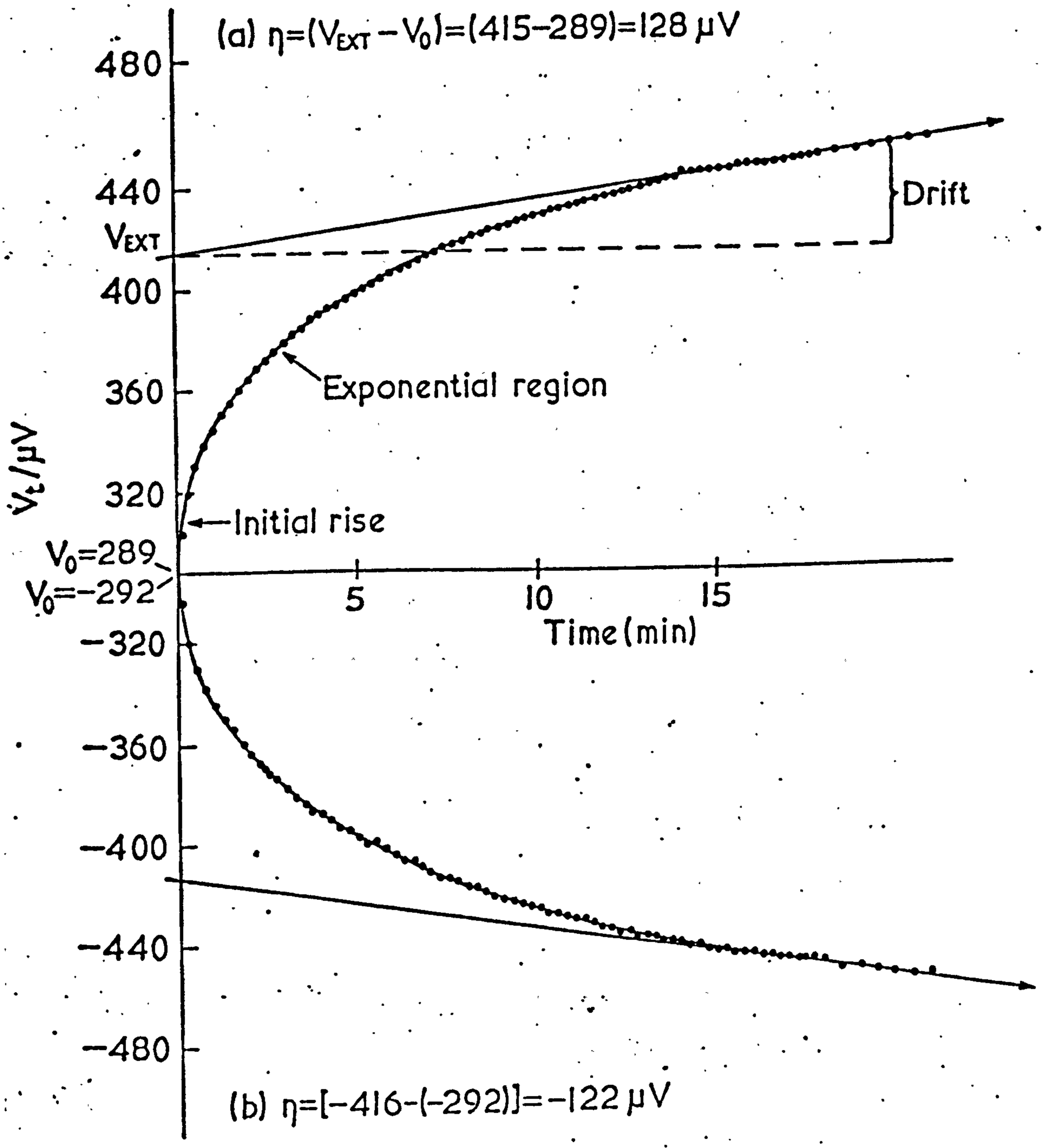

FIG. 1. Polarisation of a silver-silver chloride electrode in aqueous hydrochloric acid (0.01 M).
(a) Positive current (0.81 μA) - (b) Negative current(-0.81 μA).

and 1(b). In tables 2 and 3, and figs. 2(a), 2(b), 3(a) and 3(b), the corresponding experimental data for an NMP solution (0.016 M) and a methanol solution (0.005 M) are also presented.

The graphs show the initial linear rise of potential, used to calculate the apparent differential double layer capacitance C_{dl}, the exponential region from which kinetic data relating to surface diffusion at the electrode surface are extracted, and finally the linear portion marking a nearly constant value of the cell potential. This final linear portion, when extrapolated to zero time, gave a value for the potential called the extrapolated potential (V_{ext}). The total overpotential η was taken as the difference ($V_{ext} - V_o$), where Vo is the initial potential at equilibrium.

The final linear portion of the polarisation plot is not quite horizontal, and reflects some slowly increasing contribution to the total overpotential. This probably results from the onset of concentration polarisation, or a gradual change in the nature of the surface of the electrode resulting from surface diffusion processes. No detailed analysis of the e.m.f. "drift" has been carried out, though it is perhaps relevant that the drift is smaller for solutions of high concentration, for smooth electrodes and for higher currents. An equation for the change of potential with time at a polarised electrode which requires a dependence of η on the square root of polarisation time, has been given[1]. However, this dependence is probably only applicable to polarographic conditions in which the electrode is far from equilibrium,

TABLE 2. Polarisation of a silver-silver chloride electrode.
HCl in NMP (0.016M) (a) Positive current (1.70 μA)

Time/s	V_t/μV	Time/s	V_t/μV	Time/s	V_t/μV
0	240(Vo)	180	1055	930	1280
1	270	210	1079	960	1284
2	302	240	1097	990	1288
3	335	270	1116	1020	1289
4	367	300	1131	1050	1293
5	397	330	1144	1080	1297
6	425	360	1158	1110	1300
7	451	390	1168	1140	1302
8	475	420	1183	1170	1305
9	498	450	1192	1200	1307
10	519	480	1203	1230	1309
11	539	510	1208	1260	1317
12	557	540	1218	1290	1313
13	574	570	1225	1320	1314
14	591	600	1229	1350	1317
15	606	630	1239	1380	1320
30	756	660	1243	1410	1319
45	822	690	1248	1440	1324
60	875	720	1254	1470	1327
75	910	750	1259	1500	1327
90	943	780	1264	1530	1333
105	967	810	1270	1560	1334
120	988	840	1273	1590	1335
150	1021	870	1275	1620	1337
		900	1275		

TABLE 2 (contd.) (b) Negative current (-1.71 μA)

Time/s	$-V_t$/μV	Time/s	$-V_t$/μV	Time/s	$-V_t$/μV
0	294(Vo)	180	1096	930	1318
1	336	210	1119	960	1320
2	370	240	1138	990	1327
3	402	270	1163	1020	1327
4	434	300	1173	1050	1329
5	462	330	1192	1080	1338
6	489	360	1203	1110	1335
7	515	390	1212	1140	1336
8	538	420	1219	1170	1339
9	560	450	1228	1200	1342
10	579	480	1238	1230	1344
11	598	510	1248	1260	1345
12	616	540	1250	1290	1349
13	632	570	1260	1320	1350
14	648	600	1269	1350	1349
15	662	630	1277	1380	1352
30	796	660	1278	1410	1354
45	867	690	1284	1440	1353
60	914	720	1288	1470	1354
75	952	750	1295	1500	1357
90	989	780	1301	1530	1359
105	1018	810	1306	1560	1363
120	1031	840	1308	1590	1362
150	1066	870	1312	1620	1363
		900	1316		

FIG. 2.

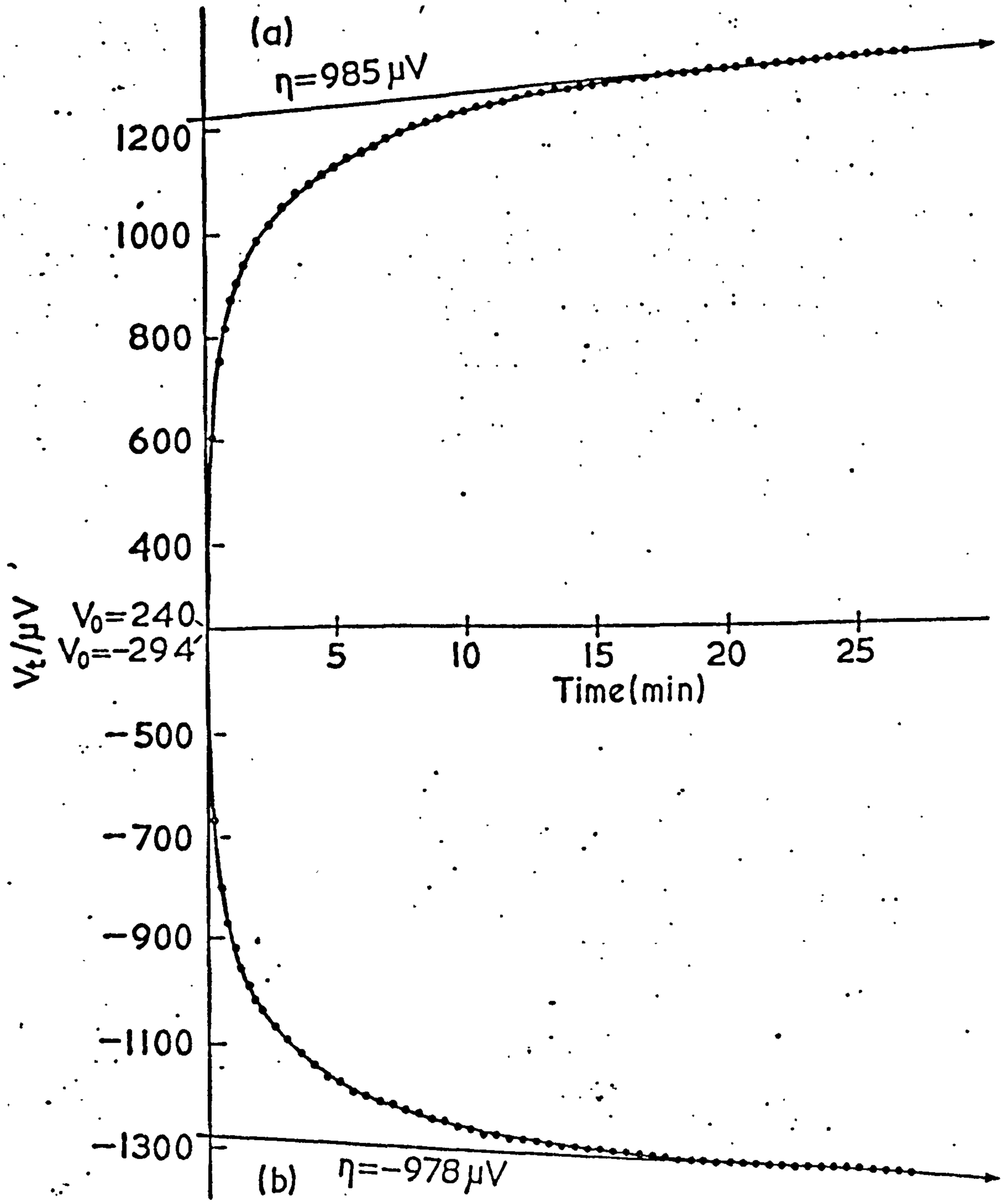

FIG. 2. Polarisation of a silver-silver chloride electrode - HCl in NMP (0.016 M)
(a) Positive current (1.7 μA) - (b) Negative current (-1.71 μA)

TABLE 3. Polarisation of a silver-silver chloride electrode; HCl in methanol (0.005 M) - (a) Positive current (1.40 μA)

Time/s	V_t/μV	Time/s	V_t/μV	Time/s	V_t/μV
0	734(V_o)	300	1489	1560	1810
1	749	360	1535	1620	1814
2	763	420	1574	1680	1814
3	777	480	1606	1740	1818
4	791	540	1633	1800	1820
5	805	600	1658	1860	1821
6	819	660	1679	1920	1820
7	832	720	1694	1980	1821
8	845	780	1711	2040	1827
9	857	840	1724	2100	1828
10	869	900	1738	2160	1831
11	880	960	1749	2220	1833
12	891	1020	1760	2280	1836
13	901	1080	1768	2340	1839
14	911	1140	1779	2400	1840
15	920	1200	1782	2460	1842
60	1149	1260	1788	2520	1849
120	1276	1320	1794	2580	1851
180	1365	1380	1799	2640	1850
240	1434	1440	1803	2700	1851
		1500	1806		

TABLE 3.(contd.) (b) Negative current (-1.41 μA)

Time/s	$-V_t$/μV	Time/s	$-V_t$/μV	Time/s	$-V_t$/μV
0	698(Vo)	300	1424	1500	1735
1	712	360	1468	1560	1736
2	727	420	1505	1620	1736
3	741	480	1535	1680	1739
4	754	540	1560	1740	1737
5	767	600	1583	1800	1738
6	780	660	1602	1860	1737
7	793	720	1621	1920	1740
8	804	780	1635	1980	1738
9	815	840	1648	2040	1741
10	826	900	1663	2100	1740
11	836	960	1680	2160	1744
12	847	1020	1693	2220	1743
13	856	1080	1698	2280	1746
14	865	1140	1704	2340	1746
15	874	1200	1711	2400	1745
60	1085	1260	1716	2460	1742
120	1214	1320	1723	2520	1742
180	1304	1380	1725	2580	1743
240	1368	1440	1731	2640	1749

FIG. 3.

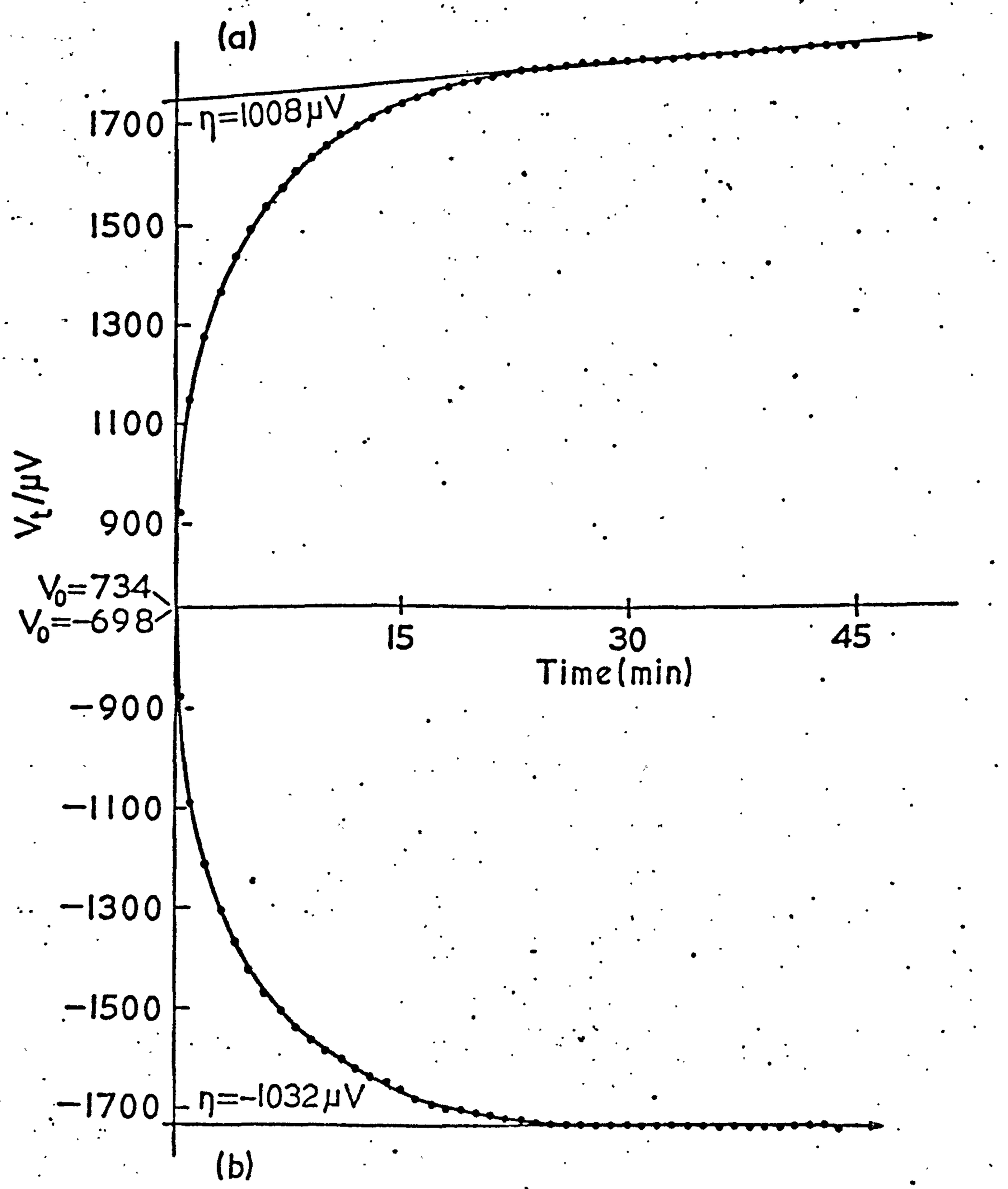

FIG. 3. Polarisation of a silver-silver chloride electrode - HCl in methanol (0.005 M)
(a) Positive current(1.40 μA) - (b) Negative current(-1.41μA).

and is likely to be inapplicable to the present study. In all cases the effective ohmic resistance corresponding to the linear drift of n was small relative to the charge transfer resistance.

As the results show, values of η obtained for positive and negative currents generally agree to ca. 1 - 5%. (The agreement is closer at higher concentrations, probably because the electrode behaviour is less sensitive to impurities or for other unknown reasons, as indicated in tables 5 - 6 - 7).

The depolarisation of the polarised silver-silver chloride electrode was also studied for a few solutions. Typical plots for the depolarisation of the silver-silver chloride electrode in aqueous hydrochloric acid for both positive and negative currents are illustrated in figs. 4(a) and 4(b). These plots use the data given in table 4, and they are the decay plots corresponding to the polarisation curves shown in figs. 1(a) and 1(b). Values of the overpotential (η = 128 and -122 μV) and for the depolarisation (η = 125 and -120 μV) agree satisfactorily. There appeared to be no great advantage in studying the decay for all cases, especially considering the large amount of time involved, and experiments were therefore restricted mainly to polarisations. Values of the overpotential, η, were determined for each solution concentration at all values of the current, forward and reverse. The values of η are given in tables 5, 6 and 7 for hydrochloric solutions in water, NMP

TABLE 4. Depolarisation of a silver-silver chloride electrode in aqueous hydrochloric acid (0.01 M) - (a) positive current (0.810 μA).

Time/s	V_t/μV	Time/s	V_t/μV	Time/s	V_t/μV
∞	457 (V_∞)	315	358	765	328
2.5	457	330	357	780	327
5	447	345	354	795	327
7.5	439	360	353	810	327
10	439	375	352	825	325
12.5	439	390	350	840	325
15	430	405	350	855	324
17.5	428	420	348	870	324
20	426	435	346	885	324
22.5	423	450	346	900	324
25	423	465	344	915	322
27.5	423	480	343	930	322
30	419	495	342	945	321
45	412	510	341	960	322
60	406	525	340	975	321
75	402	540	339	990	321
90	397	555	338	1005	320
105	392	570	338	1020	319
120	389	585	337	1035	319
135	384	600	336	1050	319
150	382	615	335	1065	318
165	378	630	335	1080	318
180	375	645	334	1140	316
195	373	660	333	1200	315
210	371	675	333	1260	313
225	368	690	331	1320	313
240	367	705	331	1380	312
255	365	720	330	1440	310
270	363	735	330	1500	309
285	361	750	329	1560	308
300	359			1620	307

TABLE 4 (contd.) - (b) Negative current (-0.810 μA)

Time/s	$V_t/\mu V$	Time/s	$V_t/\mu V$	Time/s	$V_t/\mu V$
∞	456(V_∞)	375	351	885	323
2.5	456	390	350	900	323
5	446	405	349	915	322
7.5	438	420	348	930	322
10	438	435	347	945	320
12.5	433	450	345	960	320
15	430	465	344	975	319
17.5	427	480	343	990	319
20	425	495	342	1005	318
22.5	422	510	341	1020	318
25	422	525	340	1035	318
27.5	420	540	339	1050	317
30	419	555	338	1065	316
45	412	570	337	1080	316
60	405	585	337	1095	315
75	400	600	335	1110	315
90	396	615	334	1125	315
105	391	630	334	1140	314
120	389	645	333	1155	314
135	385	660	332	1170	314
150	382	675	331	1185	314
165	378	690	331	1200	313
180	376	705	330	1215	313
195	373	720	330	1230	313
210	369	735	328	1245	312
225	368	750	328	1260	312
240	366	765	328	1275	312
255	364	780	327	1290	311
270	363	795	326	1305	311
285	360	810	326	1320	310
300	359	825	325	1380	308
315	357	840	324	1440	308
330	355	855	324	1500	307
345	354	870	323	1560	306
360	352			1620	305

FIG. 4.

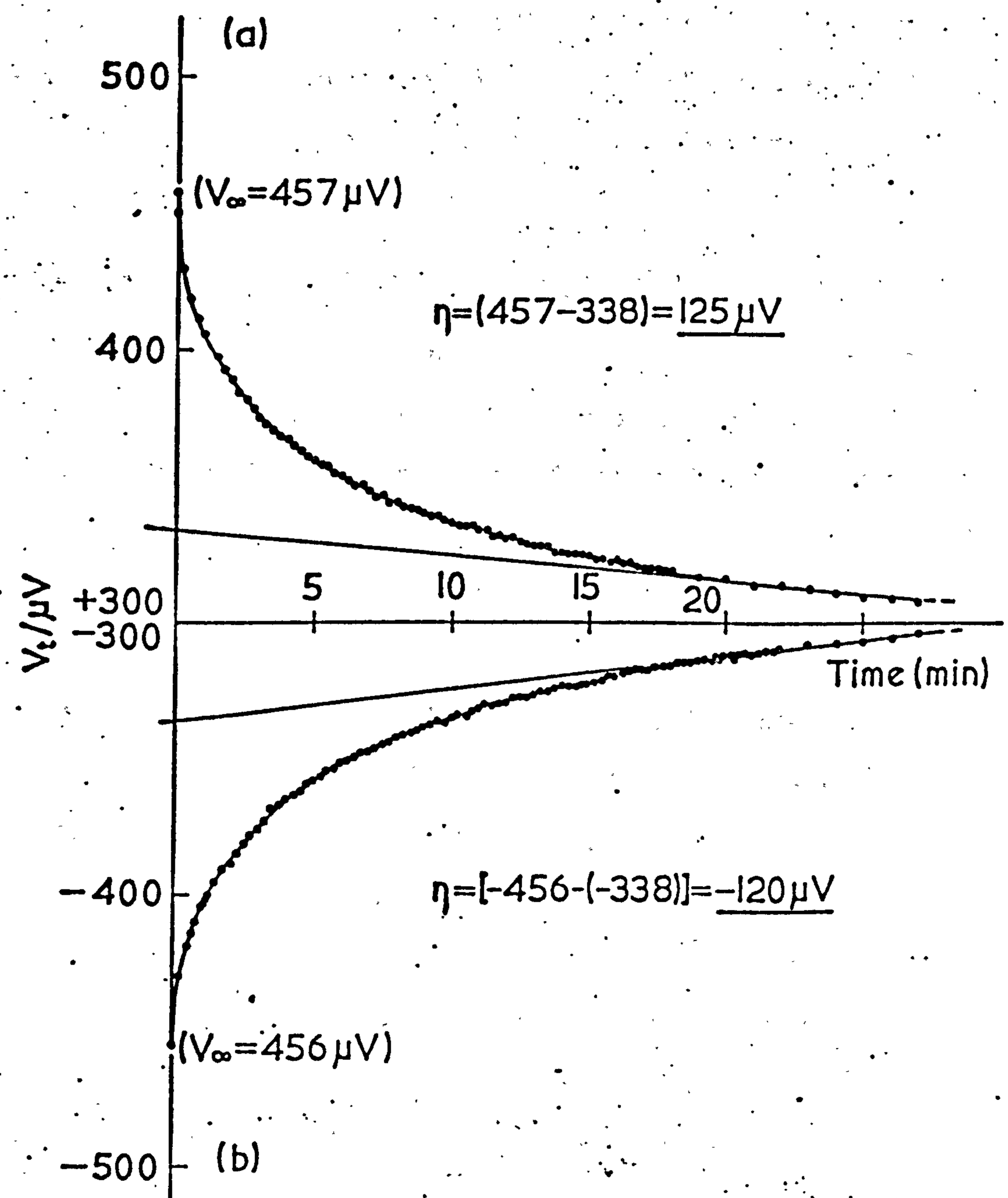

FIG. 4. Depolarisation of a silver-silver chloride electrode in aqueous hydrochloric acid (0.01 M)
(a) Following the polarisation of fig. 1(a) -
(b) Following the polarisation of fig. 1(b).

and methanol respectively. Representative plots of η versus i, in these solvents are illustrated in figs. 5, 6 and 7. The apparent exchange current density, i_o, was computed from the inverse slope of the η versus i plots, according to equation (37) section II. A linear least-squares computer programme was used for these calculations which also gave the standard error in i_o.*

2. Variation of exchange current densities with solution concentration.

Values of the exchange current density, i_o, solution concentration and square root of concentration for hydrochloric solutions in water, NMP and methanol are listed in table 8. Plots of i_o against concentration, and i_o versus square root of concentration are represented in figs. 8(a), 8(b), and 8(c), and 9(a), 9(b) and 9(c) respectively. The pictures appear to confirm previous findings in this laboratory for several Ag-AgCl electrodes of a limiting linear relationship between i_o and $\sqrt{c}$. (The same relationship was also found in the present work for several electrodes of types (a), (b) and (c).)

It can be seen that the plot for methanol (fig. 9c) shows a definite intercept on the i_o axis which must arise from some residual effect of the electrode (and is not connected with the concentration dependence) or from unknown experimental causes. Similar small intercepts may exist for H_2O and NMP solutions, but the $\sqrt{c}$ plots may be drawn through the origin within the experimental error. The limiting slopes(10^3 slope/A $mol^{-\frac{1}{2}}$ $dm^{\frac{3}{2}}$ $electrode^{-1}$). drawn in fig. 9 have the values 1.82, 0.60 and 0.31.

---

* For this section we use the nomenclature i_o=apparent exchange current (corresponding to the total measured charge-transfer resistance). In the discussion section, where the exchange current is resolved into two components, we adapt the symbolism apparent exchange current = i'_o.

TABLE 5. Values of overpotential, η, for polarisation of silver-silver chloride electrode; aqueous HCl solutions (0.001 - 0.2 M).

	i/μA	η/μV		i/μA	η/μV
C=0.001 / mol dm^{-3}	0.100	44	C=0.0034 / mol dm^{-3}	0.120	26
	-0.095	-64		-0.120	-31
	0.195	93		0.215	67
	-0.180	-105		-0.205	-62
	0.380	180		0.390	118
	-0.385	-195		-0.400	-114
	0.575	262		0.620	192
	-0.565	-270		-0.617	-185
C=0.0067 / mol dm^{-3}	0.177	38	C=0.010 / mol dm^{-3}	0.195	26
	-0.182	-32		-0.190	-25
	0.372	70		0.390	61
	-0.375	-74		-0.395	-59
	0.590	114		0.620	96
	-0.590	-118		-0.615	-94
	0.790	150		0.810	128
	-0.790	-142		-0.810	-122

TABLE 5 (contd.)

	i/μA	η/μV
C=0.0157 / mol dm^{-3}	0.215	26
	-0.220	-23
	0.417	46
	-0.425	-53
	0.622	72
	-0.625	-69
	0.856	100
	-0.865	-100

	i/μA	η/μV
C=0.0224 / mol dm^{-3}	0.315	28
	-0.310	-28
	0.460	39
	-0.452	-41
	0.612	54
	-0.605	-56
	0.810	75
	-0.812	-75

	i/μA	η/μV
C=0.0448 / mol dm^{-3}	0.630	39
	-0.635	-39
	0.902	57
	-0.905	-56
	1.285	84
	-1.235	-83
	1.735	110
	-1.695	-111

	i/μA	η/μV
C=0.1008 / mol dm^{-3}	0.735	30
	-0.745	-29
	1.170	45
	-1.145	-44
	1.460	59
	-1.420	-58
	1.775	75
	-1.745	-73

	i/μA	η/μV
C=0.20 / mol dm^{-3}	0.850	21
	-0.860	-21
	1.170	26
	-1.140	-24
	1.500	37
	-1.460	-36
	1.810	42
	-1.760	-43

FIG. 5.

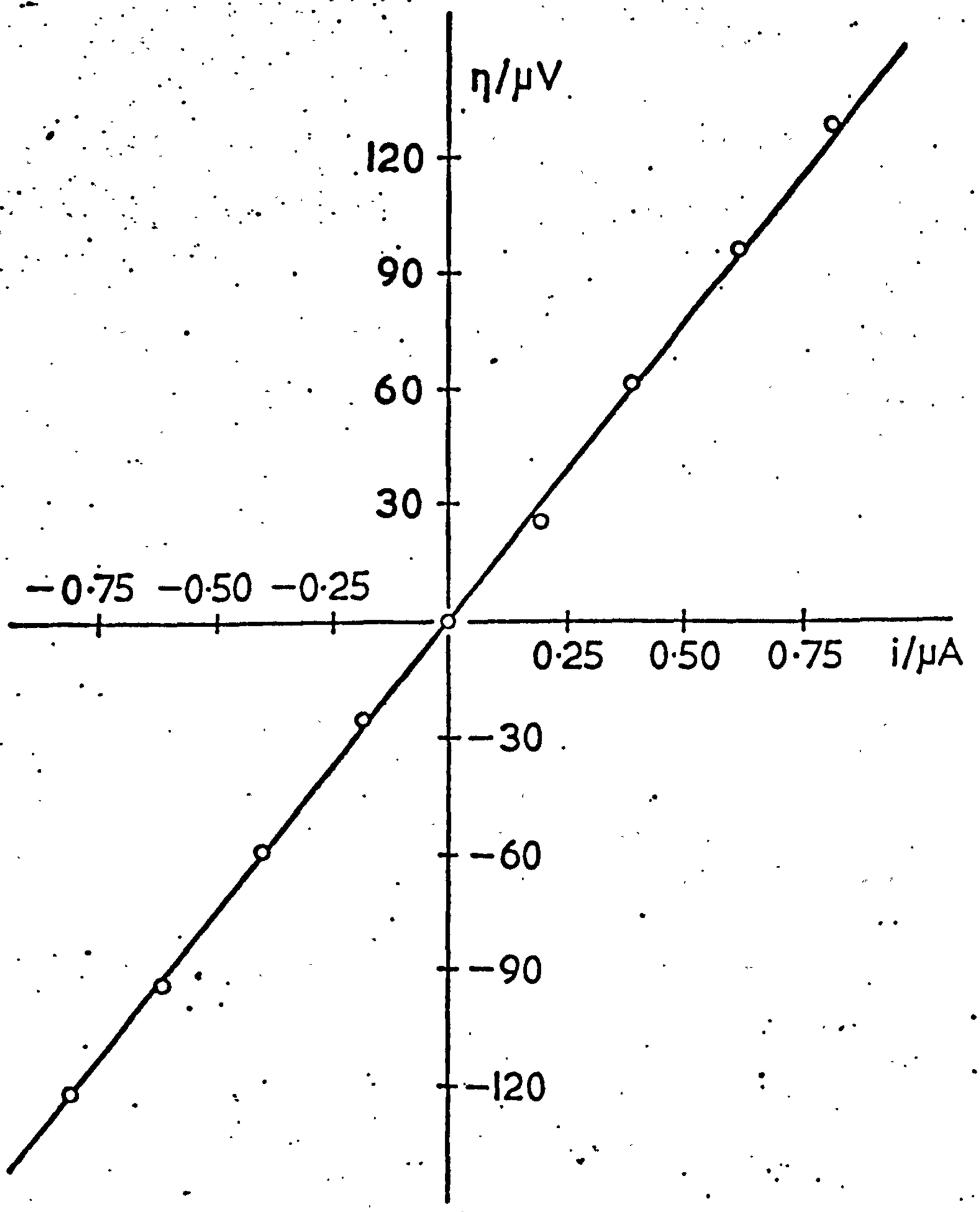

FIG. 5. Butler-Volmer plot - HCl in water (c = 0.01).

TABLE 6. Values of overpotential, η, for polarisation of silver-silver chloride electrode; HCl in NMP solutions (0.002 - 0.2 M).

	i/μA	η/μV		i/μA	η/μV
C=0.002 / mol dm^{-3}	0.155	215	C=0.005 / mol dm^{-3}	0.385	318
	-0.158	-226		-0.350	-322
	0.360	524		0.745	700
	-0.353	-512		-0.740	-700
	0.595	885		1.130	1110
	-0.600	-870		-1.140	-1085
	0.763	1065		1.690	1620

	i/μA	η/μV		i/μA	η/μV
C=0.008 / mol dm^{-3}	0.580	213	C=0.016 / mol dm^{-3}	0.530	355
	-0.560	-205		-0.566	-360
	1.330	400		0.880	540
	-1.400	-420		-0.865	-540
	1.810	591		1.70	985
	-1.735	-594		-1.71	-978

TABLE 6. (Contd.)

$C=0.032\ /\ mol\ dm^{-3}$	i/μA	η/μV	$C=0.051\ /\ mol\ dm^{-3}$	i/μA	η/μV
	0.370	75		0.920	154
	-0.380	-78		-1.050	-156
	0.935	186		1.490	248
	-0.930	-190		-1.520	-255
	1.685	333		2.490	422
	-1.695	-330		-2.520	-423

$C=0.204\ /\ mol\ dm^{-3}$	i/μA	η/μV
	1.200	84
	-1.250	-80
	1.990	151
	-2.010	-147
	2.680	184
	-2.710	-184

FIG. 6.

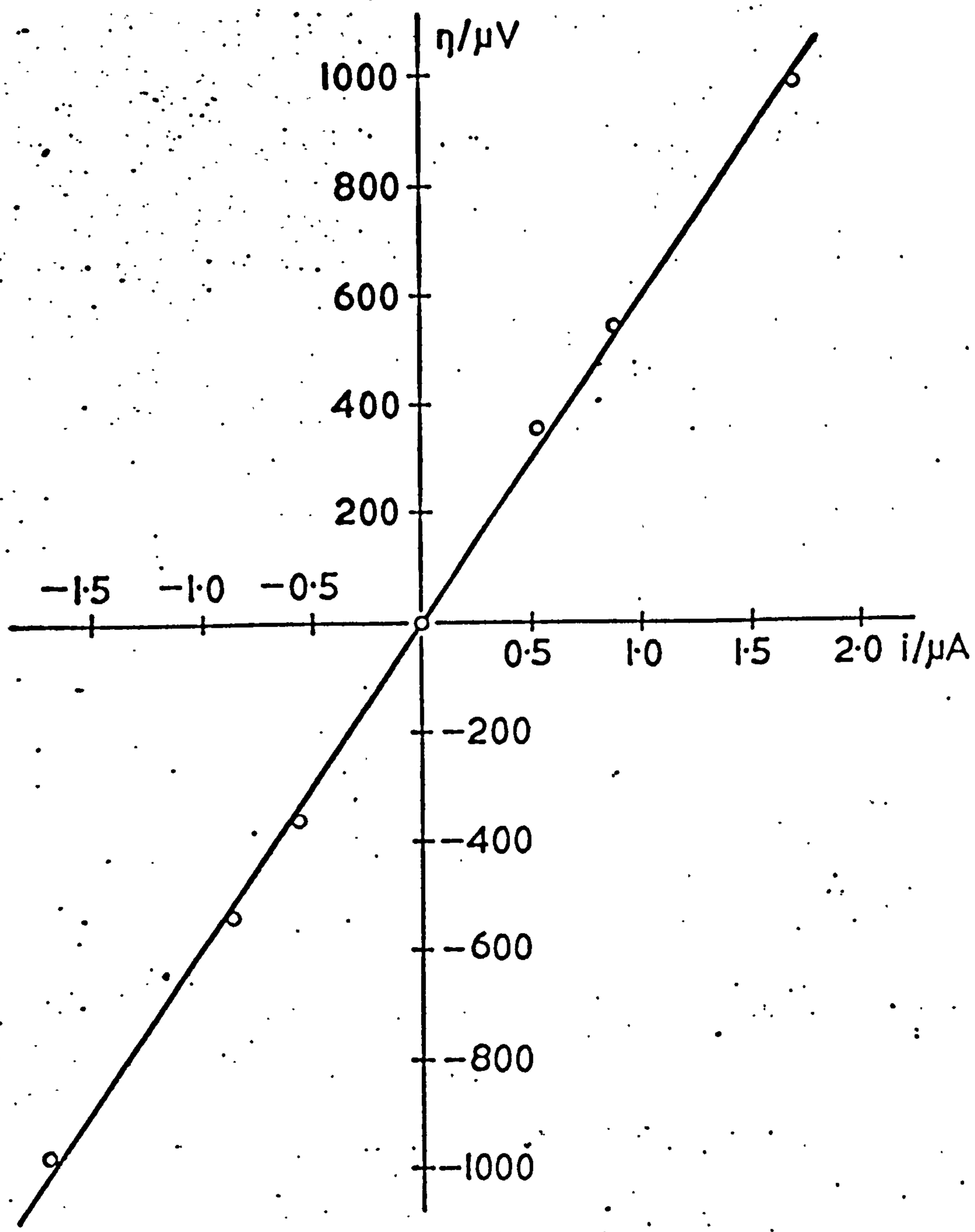

FIG. 6. Butler-Volmer plot - HCl in NMP (c = 0.016).

TABLE 7. Values of overpotential, n, for polarisation of silver-silver chloride electrode; HCl in methanol solutions (0.001 - 0.2 M).

C=0.001 mol dm^{-3}	i/μA	n/μV	C=0.0025 mol dm^{-3}	i/μA	n/μV
	0.448	510		0.458	399
	-0.449	-504		-0.462	-396
	0.839	997		0.865	800
	-0.831	-980		-0.860	-760
	1.800	2000		1.320	1120
				-1.370	-1132

C=0.005 mol dm^{-3}	i /μA	n/μV	C=0.0075 mol dm^{-3}	i/μA	n/μV
	0.530	381		0.540	304
	-0.545	-420		-0.540	-330
	0.952	704		0.942	620
	-0.967	-732		-0.955	-608
	1.400	1008		1.530	935
	-1.410	-1032		-1.500	-935

TABLE 7 (contd.)

	i/μA	η/μV		i/μA	η/μV
C=0.010 / mol dm^{-3}	0.600	338	C=0.0278 / mol dm^{-3}	0.635	225
	-0.615	-334		-0.610	-226
	1.100	620		1.240	480
	-1.100	-648		-1.200	-471
	1.720	975		1.770	664
	-1.695	-985		-1.730	-664

	i/μA	η/μV		i/μA	η/μV
C=0.067 / mol dm^{-3}	0.83	200	C=0.22 / mol dm^{-3}	1.33	354
	-0.81	-222		-1.33	-366
	1.70	504		2.60	608
	-1.69	-520		-2.65	-624

FIG. 7.

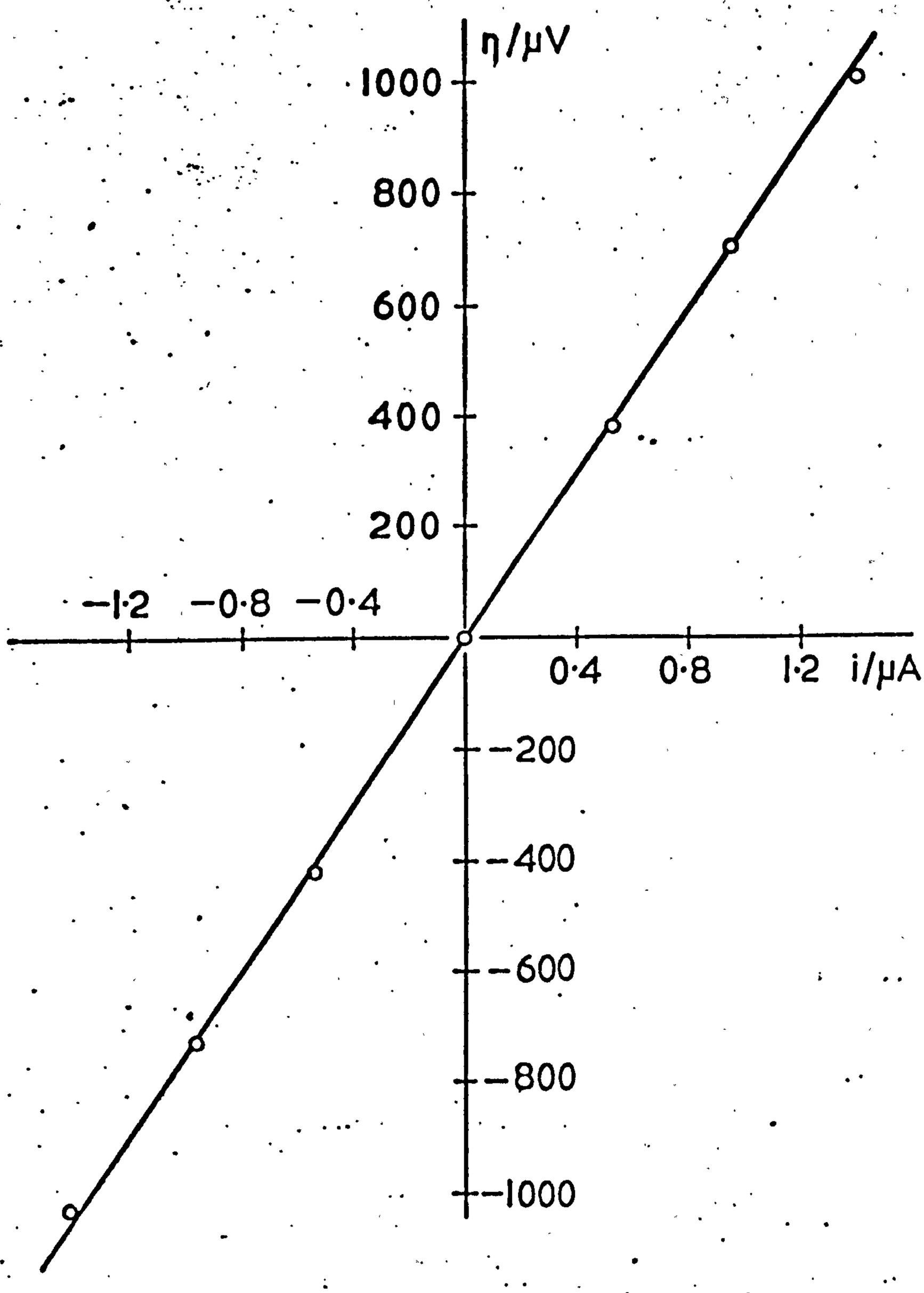

FIG. 7. Butler-Volmer plot - HCl in methanol (c = 0.005)

TABLE 8. Computed values of exchange current densities, i_o, for hydrochloric solutions in water, NMP and methanol.

SOLVENT	$10^2 c/mol\ dm^{-3}$	$\sqrt{c}/mol^{\frac{1}{2}}\ dm^{-3/2}$	$10^5\ i_o/A$	$10^5 di_o/A$
H_2O	0.112	0.033_5	5.36	0.10
	0.336	0.058	8.55	0.17
	0.672	0.082	13.55	0.16
	1.008	0.100	16.76	0.11
	1.568	0.125	22.27	0.13
	2.24	0.150	28.25	0.09
	4.48	0.212	39.85	0.10
	10.08	0.317_5	63.01	0.13
	20.16	0.45	107.68	0.19
NMP	0.204	0.045	1.78_5	0.02
	0.490	0.070	2.69	0.03
	0.801	0.089	7.92	0.24
	1.603	0.127	4.38	0.10
	3.24	0.180	12.99	0.11
	5.11	0.226	15.38	0.19
	20.44	0.452	36.41	0.60
CH_3OH	0.100	0.032	2.26	0.04
	0.250	0.050	3.00	0.05
	0.500	0.071	3.50	0.02
	0.750	0.087	4.13	0.07
	1.00	0.10	4.48_5	0.04
	2.78	0.167	6.74	0.07
	6.72	0.26	8.65	0.05
	22.0	0.47	10.80	0.07

(di_o is the computed standard error in i_o)

FIG. 8. Variation of i_o with solution concentration - (a) HCl in H_2O (b) HCl in NMP - (c) HCl in CH_3OH

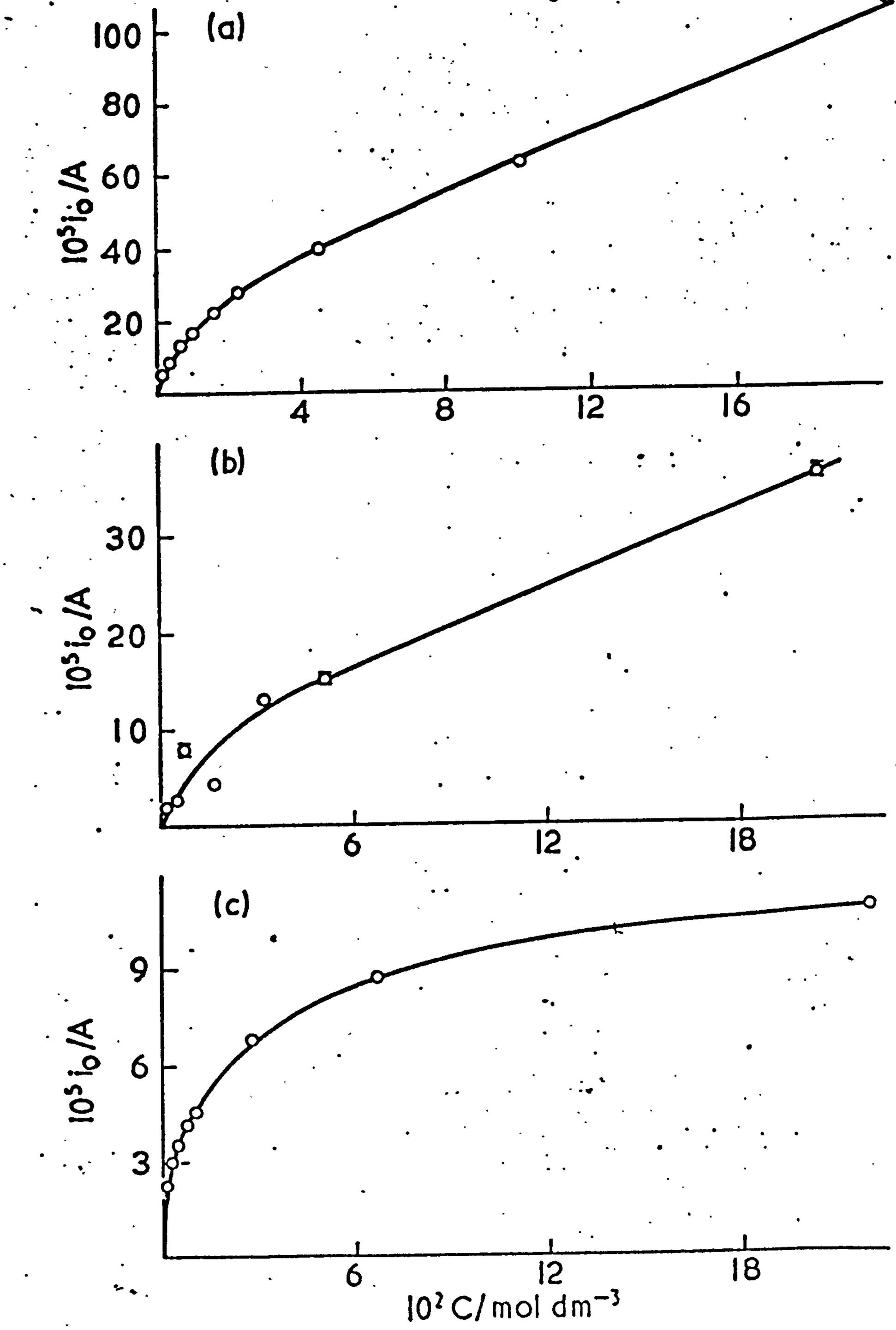

FIG. 9. Variation of i_o with square root of concentration
(a) H_2O - (b) NMP - (c). CH_3OH

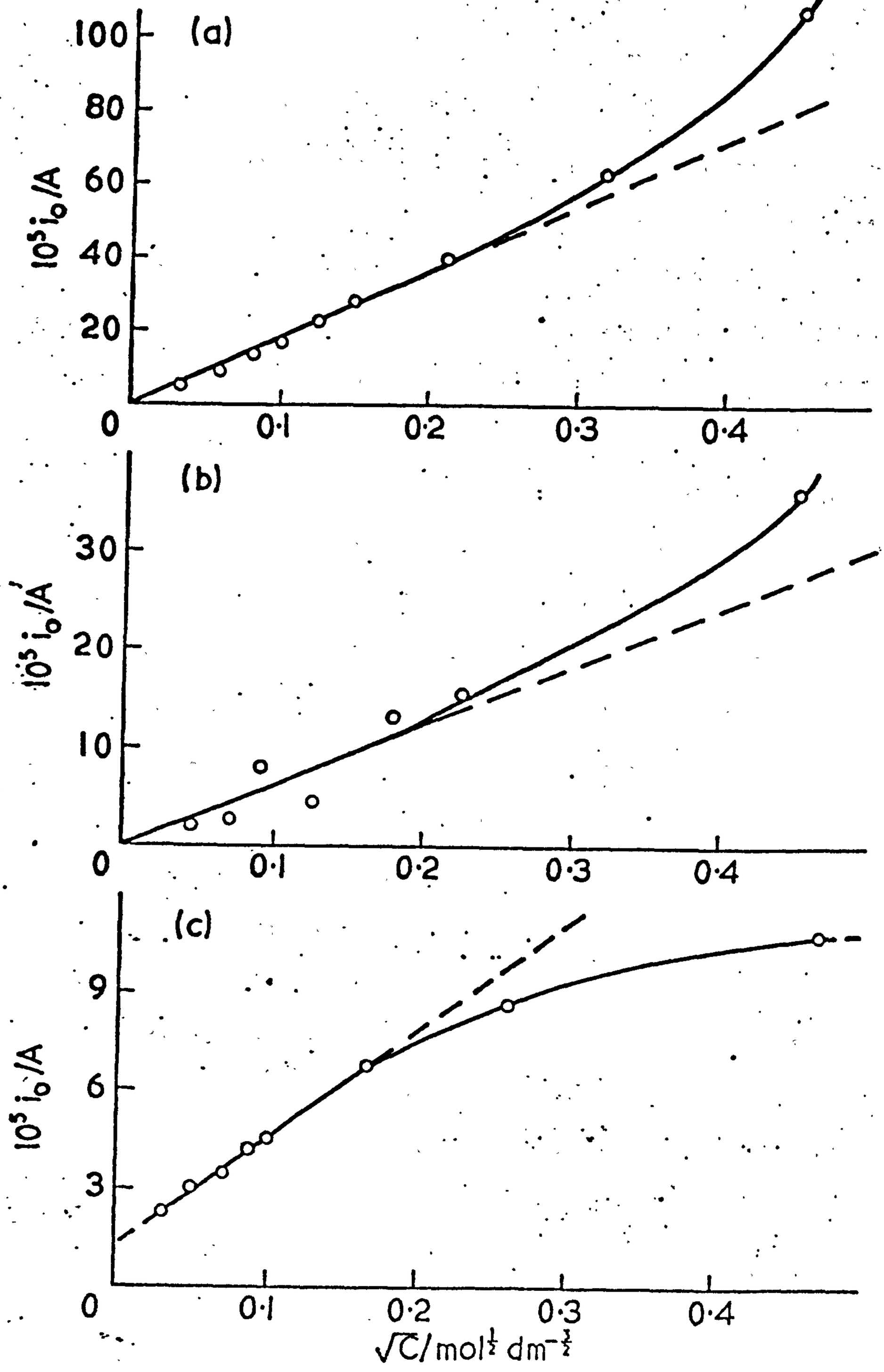

3. <u>Determination of rise-times and apparent differential double-layer capacitances from the analysis of polarisation curves</u>. The values of the potential change V_t (also called dn) for the initial linear rise of potential during polarisation and depolarisation of silver-silver chloride electrodes in water, NMP and methanol, were plotted against time. Using the first values listed in tables 1(a), 2(a) and 3(a) (polarisation for each solvent), and 4(a) (depolarisation in water), the graphs 10(a), 10(b), 10(c) and 10(d) were obtained. These figs. show initially a linearity between V_t and t, followed by a gradual deviation from the linear rise, thus introducing the exponential region (as described earlier in this section). Figs. 10(a) and 10(b) represent a nearly symmetrical picture. They illustrate the initial rise and initial decay under the same experimental conditions (same solution, same experiment). In contrast to the time-consuming determination of decay-values of the overpotential, it was here convenient and advantageous to determine values for the initial decay of the potential with time. The rise-times(dn/dt) of polarisation and depolarisation agree, in general, to ca. 5%. This agreement (5%) though goed, was less satisfactory than for the determination of overvoltages (2%).

The average value between the polarisation and depolarisation rise-times, ($\overline{dn/dt}$), was calculated. The values of current and average dn/dt for all hydrochloric solutions in water, NMP and methanol are given in tables 9, 10 and 11 respectively.

FIG. 10 (a) & (b). Determination of rise-times d_n/dt.

(a) Polarisation of Ag-AgCl electrode - Aqueous hydrochloric acid (0.01 M - i = 0.81 μA).

(b) Depolarisation of Ag-AgCl electrode - Aqueous hydrochloric acid (0.01 M).

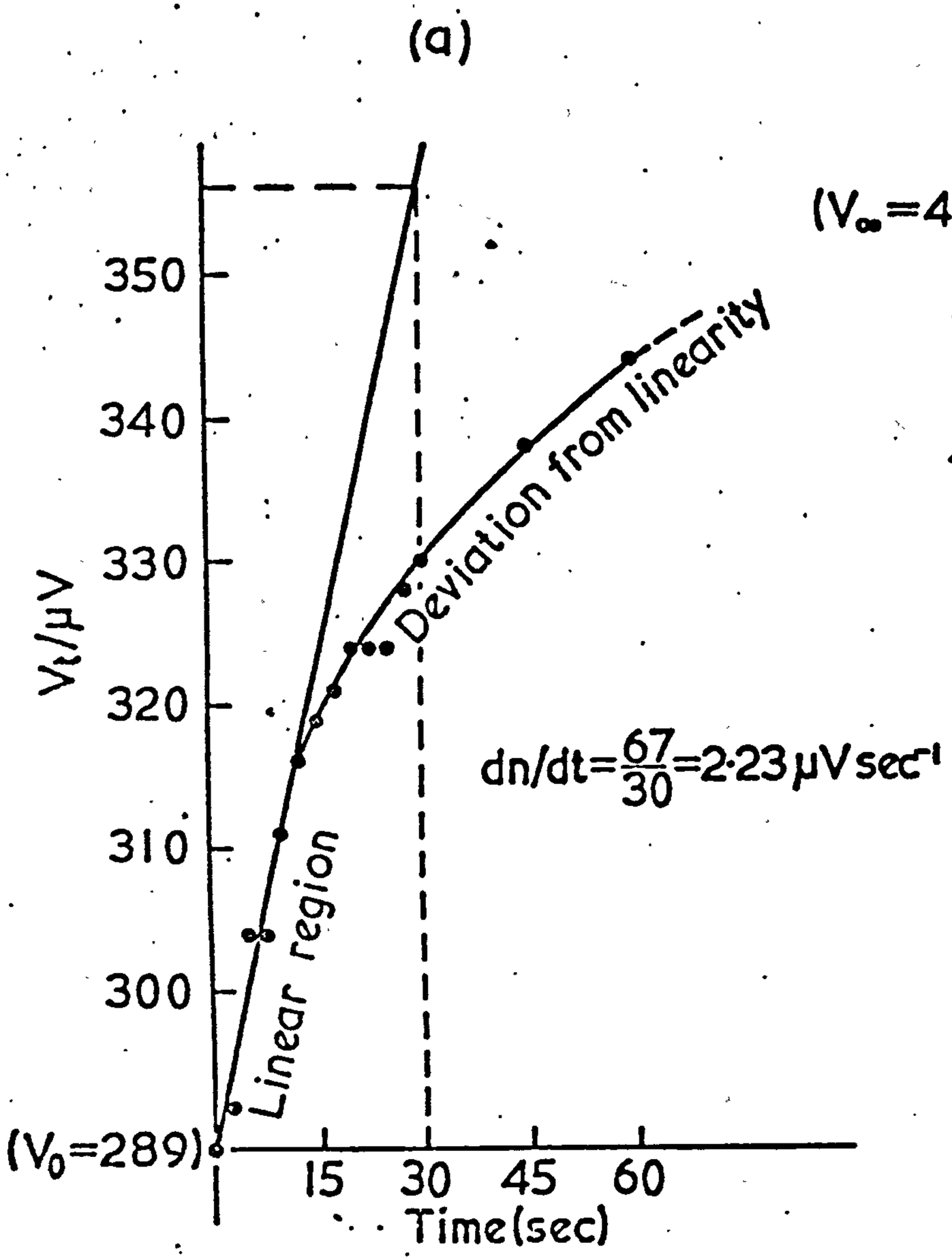

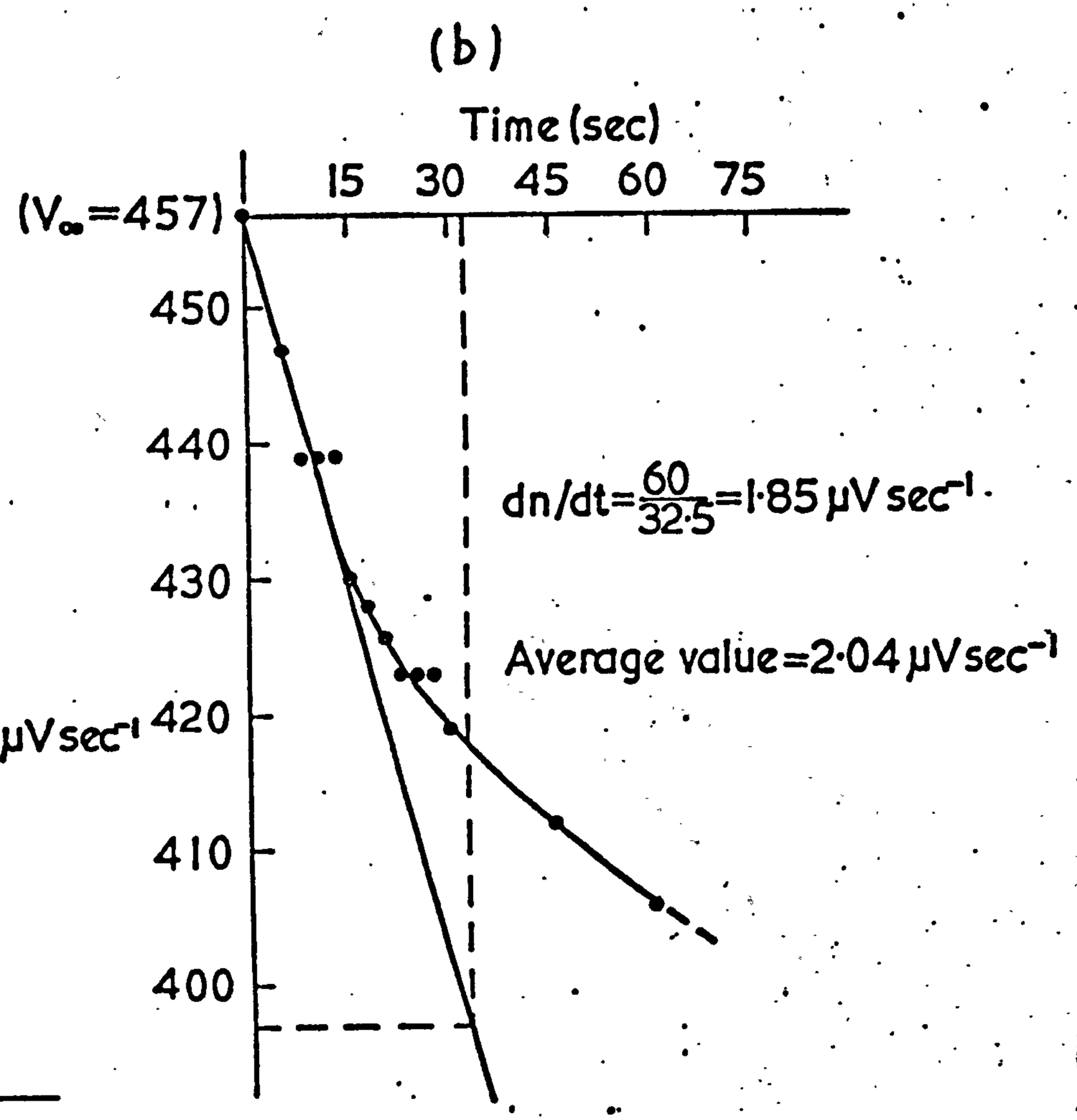

FIG. 10-(c).

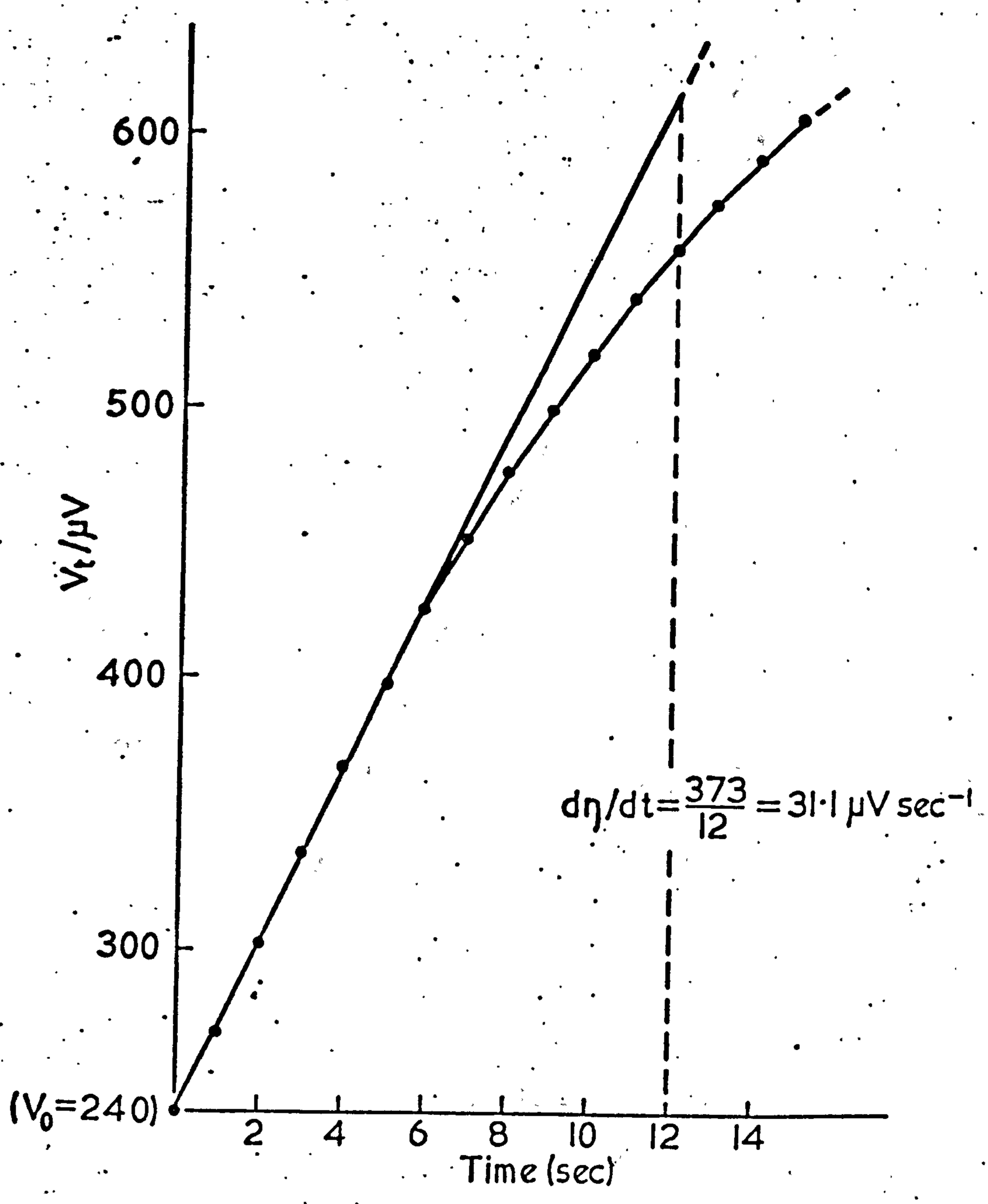

FIG. 10(c). Determination of rise-times dn/dt - Polarisation of Ag-AgCl electrode - HCl in NMP (0.016 M i = 1.70 μA)

FIG. 10 (d).

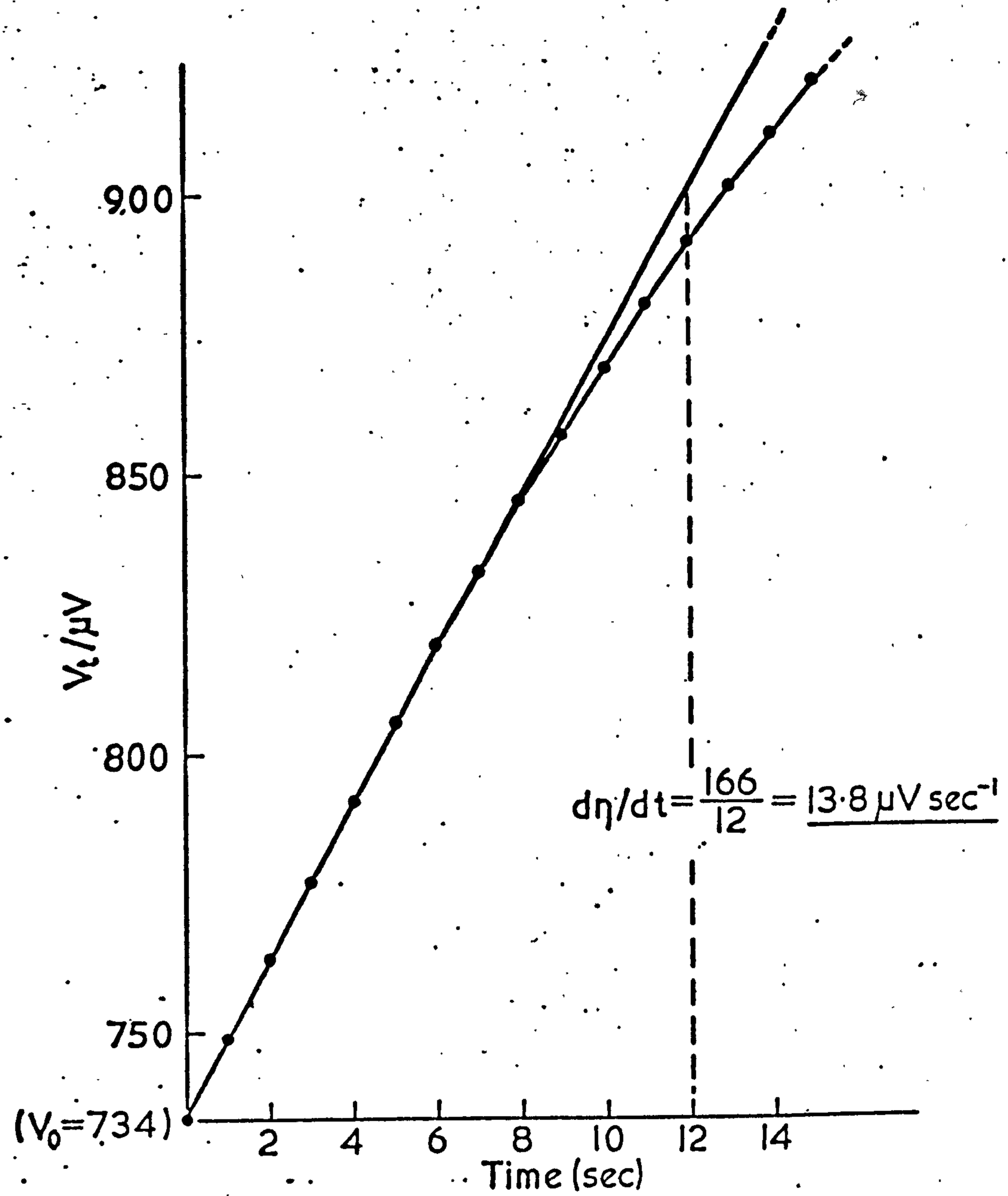

FIG. 10(d). Determination of rise-times dn/dt - Polarisation of Ag-AgCl electrode - HCl in methanol(0.005M - i = 1.40 μA).

TABLE 9. Average rise-times ($\overline{dn/dt}$) for polarisation and depolarisation of Ag-AgCl electrodes in aqueous hydrochloric acid solutions. (C=0.003 - 0.2 M).

C=0.0034 / mol dm^{-3}	i/μA	$\overline{dn/dt}$/μVs^{-1}	C=0.0067 / mol dm^{-3}	i/μA	$\overline{dn/dt}$/μVs^{-1}
	0.120	0.70		0.177	0.56
	-0.120	-0.85		-0.182	-0.60
	0.215	0.94		0.372	1.04
	-0.205	-0.90		-0.375	-0.90
	0.390	1.60		0.590	1.68
	-0.400	-		-0.590	-1.64
	0.620	2.52		0.790	2.26
	-0.617	-2.47		-0.790	-2.32

C=0.010 / mol dm^{-3}	i/μA	$\overline{dn/dt}$/μVs^{-1}	C=0.0157 / mol dm^{-3}	i/μA	$\overline{dn/dt}$/μVs^{-1}
	0.195	0.60		0.215	0.48
	-0.190	-0.54		-0.220	-0.50
	0.390	1.24		0.417	0.84
	-0.395	-1.08		-0.425	-0.86
	0.620	1.70		0.622	1.14
	-0.615	-1.60		-0.625	-1.10
	0.810	2.04		0.856	1.52
	-0.810	-2.10		-0.865	-1.50

TABLE 9 (contd.)

	i/μA	$\overline{dn/dt}/\mu Vs^{-1}$		i/μA	$\overline{dn/dt}/\mu Vs^{-1}$
$C=0.022_4$ mol dm^{-3}	0.315	0.40	$C=0.044_8$ mol dm^{-3}	0.630	0.68
	-0.310	-0.40		-0.635	-0.76
	0.460	0.60		0.902	1.02
	-0.452	-0.60		-0.905	-1.02
	0.612	0.80		1.285	1.40
	-0.605	-0.86		-1.235	-1.38
	0.810	1.10		1.735	1.88
	-0.812	-1.04		-1.695	-1.82

	i/μA	$\overline{dn/dt}/\mu Vs^{-1}$		i/μA	$\overline{dn/dt}/\mu Vs^{-1}$
$C=0.100_8$ mol dm^{-3}	0.735	0.64	$C=0.205$ mol dm^{-3}	0.850	0.63
	-0.745	-0.62		-0.860	-0.75
	1.170	0.94		1.170	0.72
	-1.145	-0.90		-1.140	-0.78
	1.460	1.06		1.500	1.00
	-1.420	-1.02		-1.460	-1.01
	1.775	1.30		1.810	1.34
	-1.745	-1.34		-1.760	-1.15

Representative plots of $\overline{dn/dt}$ versus i are illustrated in figs. 11, 12 and 13. The slopes of $\overline{dn/dt}$ versus i plots were computed, using a linear least-squares programme, and the inverse values of such slopes, giving the values of differential double layer capacitances, C_{dl}, according to eq. (41) section II, were deduced. The standard error in C_{dl} was also given.

4. Variation of the differential capacitance with solution concentration.

The different values of C_{dl} were plotted against concentration and square root of concentration for each solvent. Values of c, $\sqrt{c}$, and C_{dl} are presented in table 12. Plots of C_{dl} versus c are illustrated in graph 14, whereas values of C_{dl} vs. $\sqrt{c}$ are plotted in fig. 15. A limiting linear relationship between C_{dl} and $\sqrt{c}$ appears, as for the previous case of i_o vs. $\sqrt{c}$. The plot for methanol (fig. 15(c)) also shows a definite intercept on the C_{dl} axis, and similar small intercepts may exist for H_2O and NMP solutions. These intercepts may be attributed to some residual effect of the electrode, and are not connected with the concentration dependence. However, the Cdl vs. $\sqrt{c}$ plots may be drawn through the origin within the experimental error. The limiting slopes $(F\ mol^{-\frac{1}{2}}\ dm^{\frac{3}{2}})$ are : 4.4, 0.88, and 0.75.

B. DETERMINATION OF THE KINETIC CHARACTERISTICS FROM THE ANALYSIS OF POLARISATION CURVES.

The initial linear rise of overpotentials, yielding values of the differential double layer capacitances, was dealt with in section A. Here the exponential region is analysed to extract

FIG. 11.

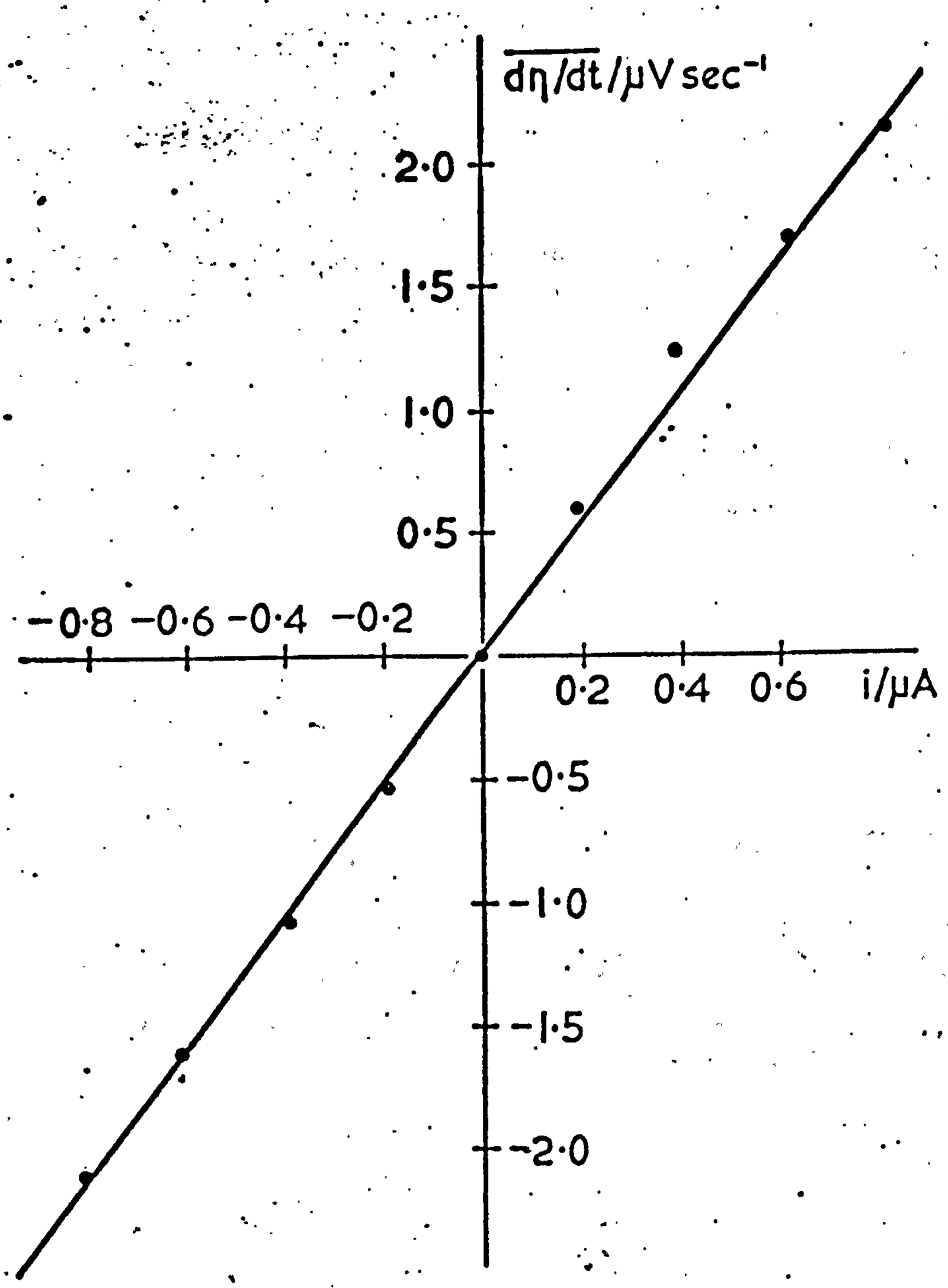

FIG. 11. Plot of $\overline{dn/dt}$ versus i.
HCl in H_2O - 0.01 M.

TABLE 10. Average rise-times ($\overline{dn/dt}$) for polarisation and depolarisation of Ag-AgCl electrodes; HCl in NMP(C=0.002-0.205 M).

$C=0.005\ /\ mol\ dm^{-3}$	i/μA	$\overline{dn/dt}/\mu Vs^{-1}$	$C=0.008\ /\ mol\ dm^{-3}$	i/μA	$\overline{dn/dt}/\mu Vs^{-1}$
	0.385	7.84		0.580	5.32
	-0.350	-8.64		-0.560	-5.20
	0.745	18.0		1.330	10.40
	-0.740	-15.60		-1.400	-9.60
	1.130	24.0		1.810	15.20
	-1.140	-24.30		-1.735	-15.10
	1.690	36.80			

$C=0.016\ /\ mol\ dm^{-3}$	i/μA	$\overline{dn/dt}/\mu Vs^{-1}$	$C=0.0324\ /\ mol\ dm^{-3}$	i/μA	$\overline{dn/dt}/\mu Vs^{-1}$
	0.530	12.20		0.370	2.04
	-0.566	-12.50		-0.380	-2.04
	0.880	17.20		0.935	5.20
	-0.865	-17.10		-0.930	-5.20
	1.700	32.40		1.685	8.80
	-1.710	-33.60		-1.695	-8.70

TABLE 10 (contd.)

	i/μA	$\overline{dη/dt}$/μVs^{-1}		i/μA	$\overline{dη/dt}$/μVs^{-1}
C=0.050 / mol dm^{-3}	0.920	4.96	C=0.205 / mol dm^{-3}	1.200	2.56
	-1.050	-4.66		-1.250	-2.40
	1.490	7.44		1.990	4.02
	-1.520	7.70		-2.010	-3.96
	2.490	12.60		2.680	5.20
	-2.520	-12.60		-2.710	-5.20

	i/μA	$\overline{dη/dt}$/μVs^{-1}
C=0.002 / mol dm^{-3}	0.155	6.67
	-0.158	-
	0.360	13.57
	-0.353	-14.77
	0.595	20.00
	-0.600	-18.58
	0.763	22.20

FIG. 12.

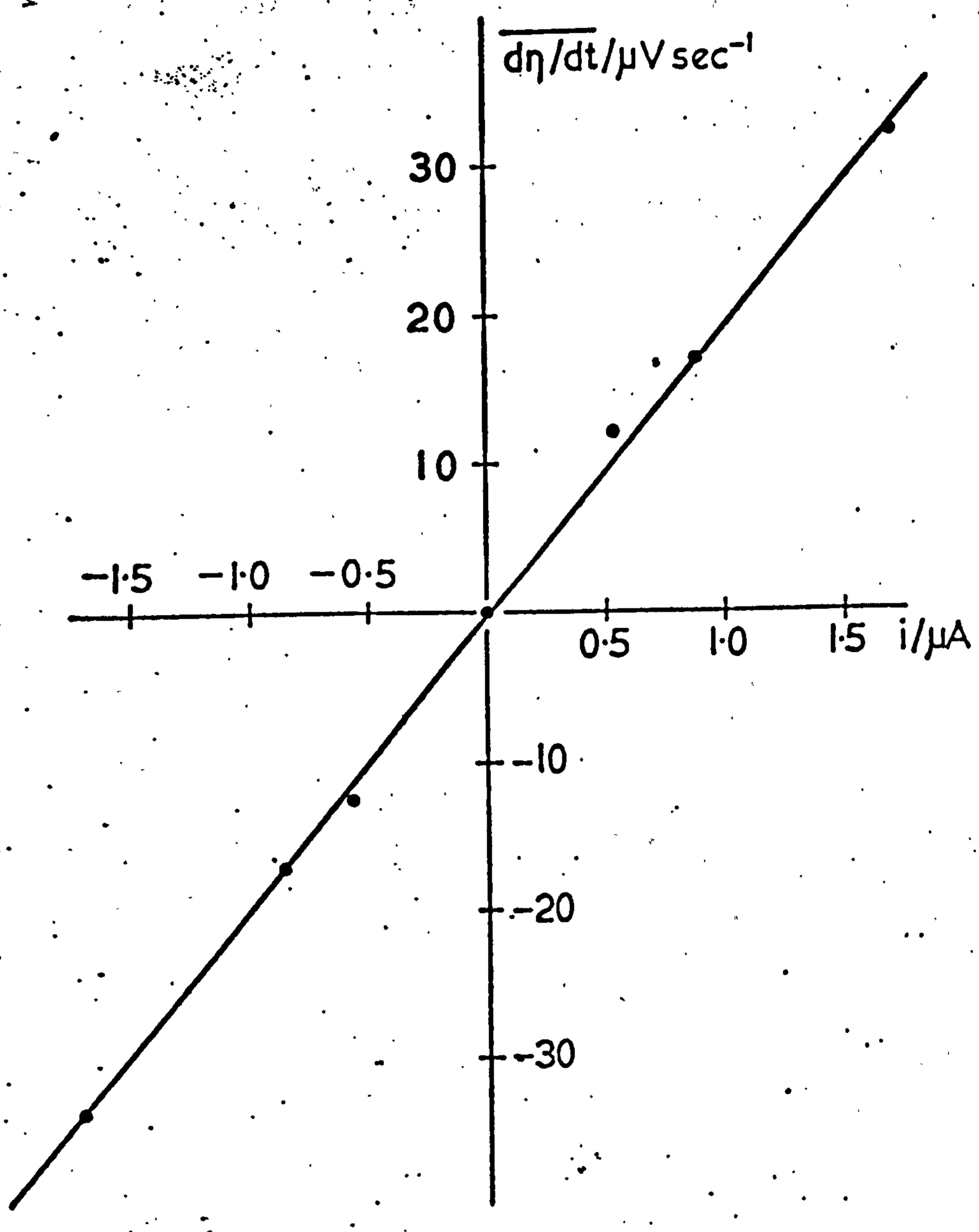

FIG. 12. Plot of $\overline{dn/dt}$ versus i,
HCl in NMP - 0.016.M.

TABLE 11. Average rise-times ($\overline{d\eta/dt}$) for polarisation and depolarisation of Ag-AgCl electrodes; HCl in methanol(C=0.001 - 0.2 M)

	i/μA	$\overline{d\eta/dt}$/μVs^{-1}		i/μA	$\overline{d\eta/dt}$/μVs^{-1}
C=0.001 / mol dm^{-3}	0.448	5.60	C=0.0025 / mol dm^{-3}	0.458	5.20
	-0.449	-5.80		-0.462	-5.00
	0.839	10.80		0.865	8.80
	-0.831	-10.60		-0.860	-8.80
	1.800	21.20		1.320	13.20
				-1.370	-13.60

	i/μA	$\overline{d\eta/dt}$/μVs^{-1}		i/μA	$\overline{d\eta/dt}$/μVs^{-1}
C=0.005 / mol dm^{-3}	0.530	5.70	C=0.0075 / mol dm^{-3}	0.540	4.80
	-0.545	-5.60		-0.540	-4.60
	0.952	9.80		0.942	7.90
	-0.967	-9.70		-0.955	-7.80
	1.400	13.80		1.530	12.20
	-1.410	-13.50		-1.500	-12.20

TABLE 11 (contd.)

	i/μA	$\overline{dη/dt}$/μVs^{-1}		i/μA	$\overline{dη/dt}$/μVs^{-1}
C=0.010/mol·dm^{-3}	0.600	5.50	C=0.028/mol dm^{-3}	0.635	3.92
	-0.615	-5.60		-0.610	-4.00
	1.100	10.20		1.240	6.86
	-1.100	-10.40		-1.200	-6.80
	1.720	15.14		1.770	9.80
	-1.695	-15.10		-1.730	-9.80

	i/μA	$\overline{dη/dt}$/μVs^{-1}		i/μA	$\overline{dη/dt}$/μVs^{-1}
C=0.067/mol dm^{-3}	0.83	3.45	C=0.22/moldm^{-3}	1.33	4.50
	-0.81	-3.45		-1.33	-4.55
	1.70	6.85		2.60	8.60
	-1.69	-6.75		-2.65	-8.70

FIG. 13.

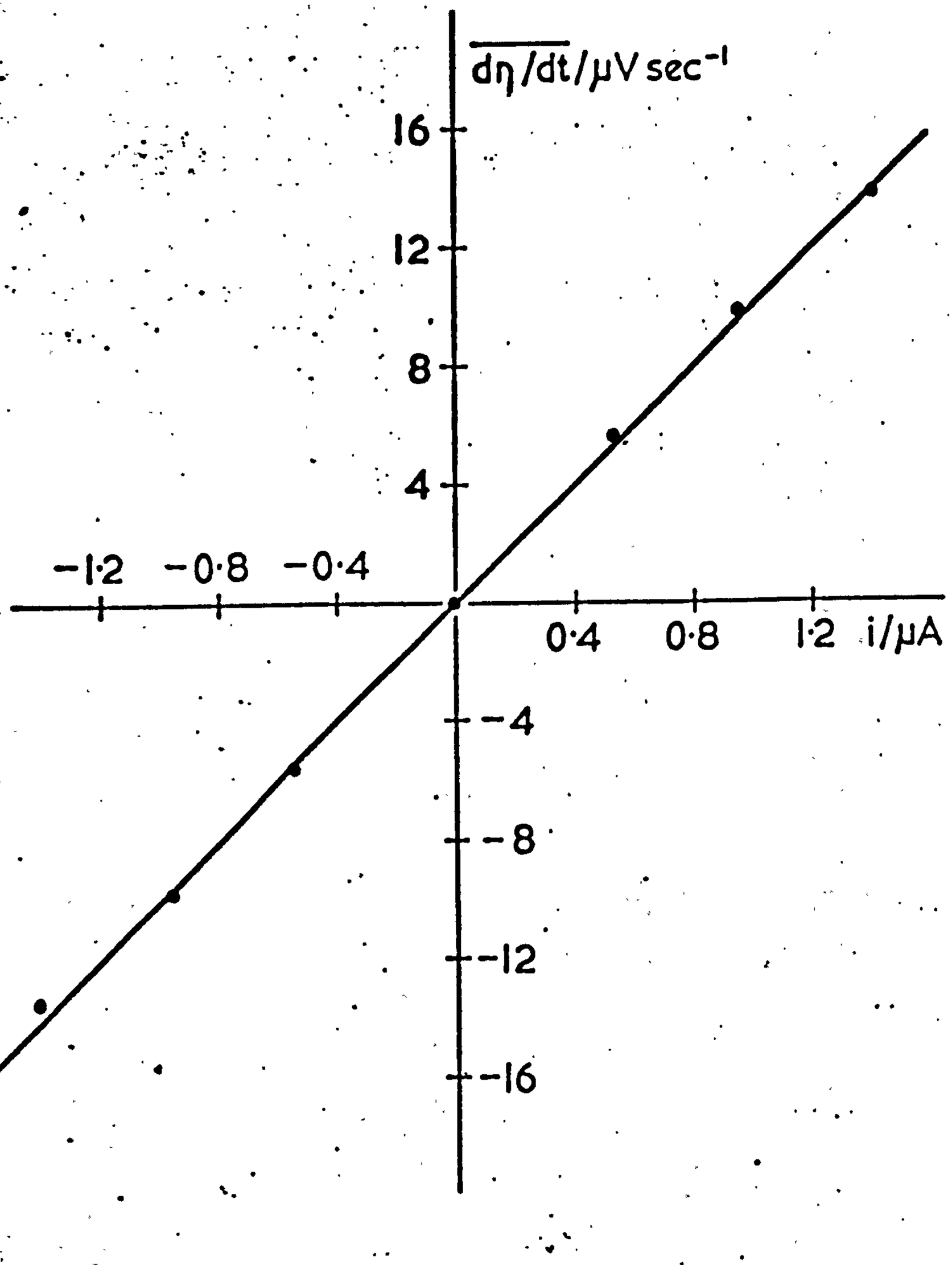

FIG. 13. Plot of $\overline{d\eta/dt}$ versus i;
HCl in methanol - 0.005 M.

TABLE 12. Computed values of differential double-layer capacitances for hydrochloric acid solutions in water, NMP and methanol.

SOLVENT	$10^2 C$/mol dm^{-3}	$\sqrt{c}$/mol$^{\frac{1}{2}}$ dm$^{-3/2}$	Cdl/F	dC_{dl}/F
	0.336	0.058	0.21_5	0.08
	0.672	0.082	0.35	0.007
	1.008	0.100	0.37	0.007
H_2O	1.568	0.125	0.55	0.01_5
	2.24	0.150	0.75	0.01
	4.48	0.212	0.90	0.008
	10.08	0.317_5	1.32	0.03
	20.16	0.45	1.45	0.05
	0.204	0.045	0.03	0.001
	0.490	0.070	0.05	0.001
	0.801	0.089_5	0.12	0.005
NMP	1.603	0.127	0.05	0.001
	3.24	0.180	0.19	0.003
	5.11	0.226	0.20	0.002
	20.44	0.452	0.52	0.007
	0.100	0.032	0.08	0.002
	0.250	0.050	0.10	0.002
	0.500	0.071	0.10	0.001
CH_3OH	0.750	0.087	0.12	0.001
	1.00	0.10	0.11	0.001
	2.78	0.167	0.17_6	0.001
	6.72	0.26	0.24_5	0.001
	22.0	0.47	0.30	0.001_5

(dC_{dl} is the computed standard error in C_{dl})

FIG. 14. Variation of C_{dl} with solution concentration - (a) HCl in H_2O - (b) HCl in NMP - (c) HCl in CH_3OH.

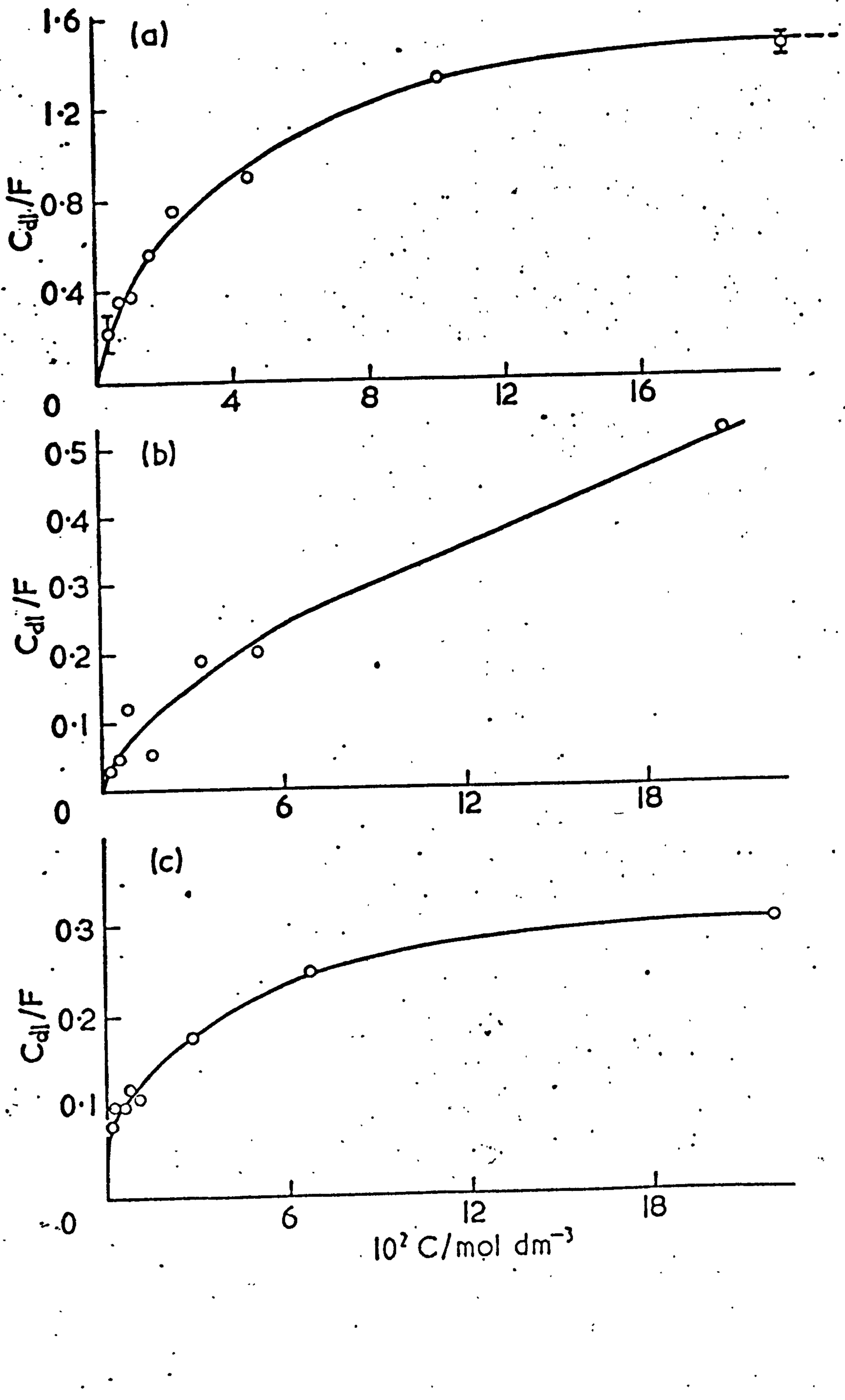

FIG. 15. C_{dl} vs. $\sqrt{c}$ plots for (a) HCl in H_2O - (b) HCl in NMP - (c) HCl in CH_3OH

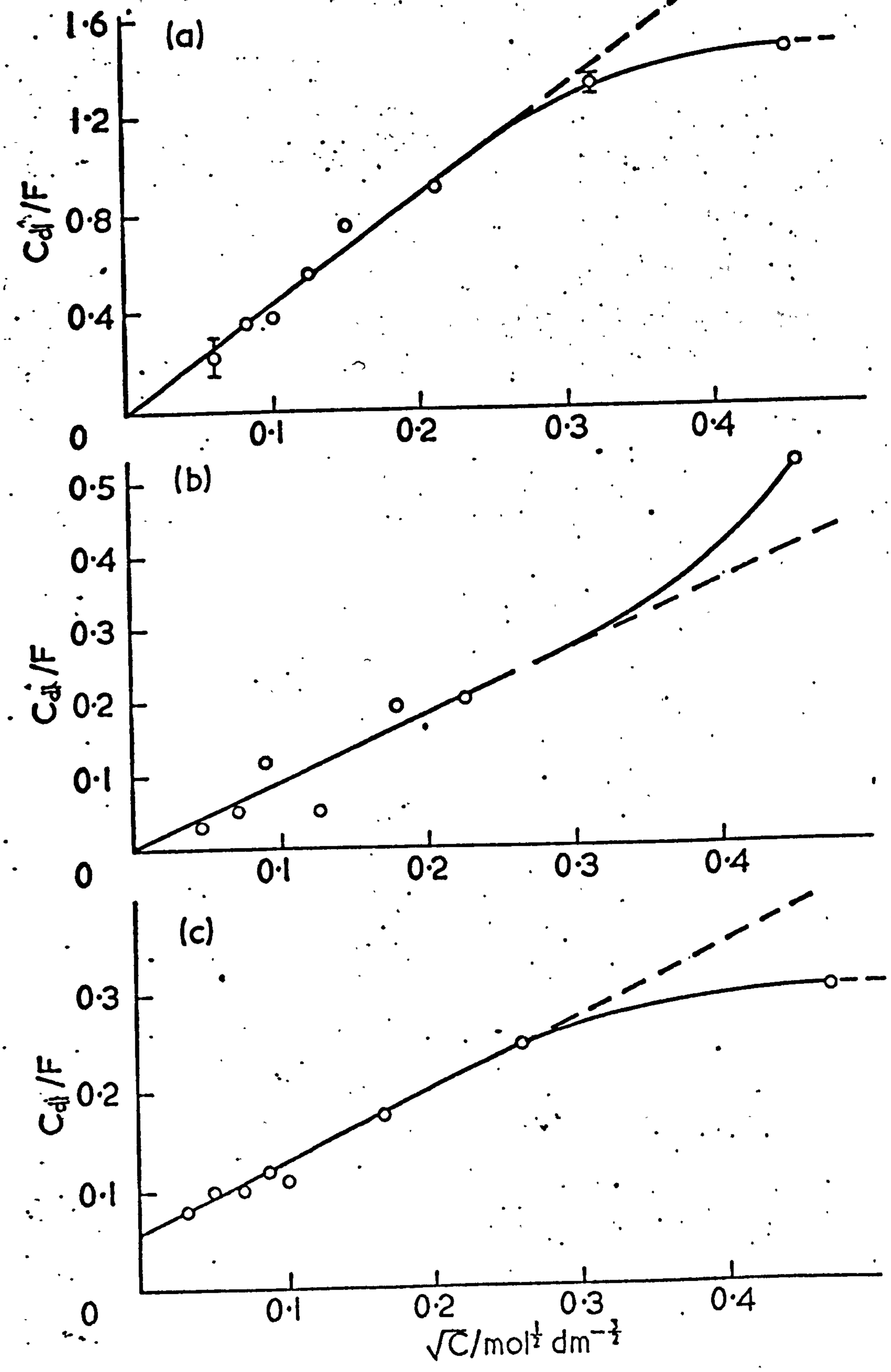

the kinetic characteristics of a slower relaxation process for the silver-silver chloride electrode. (As will be discussed later, this relates to a surface-diffusion mechanism).

According to section A of the results chapter, where it was mentioned that the final linear portion of the polarisation plot was not quite flat but, in fact, increasing slowly with time, a correction from that extra part of the potential at the steady state was made on V_t, giving a theoretical curve slightly different from the experimental one. The procedure is as follows:

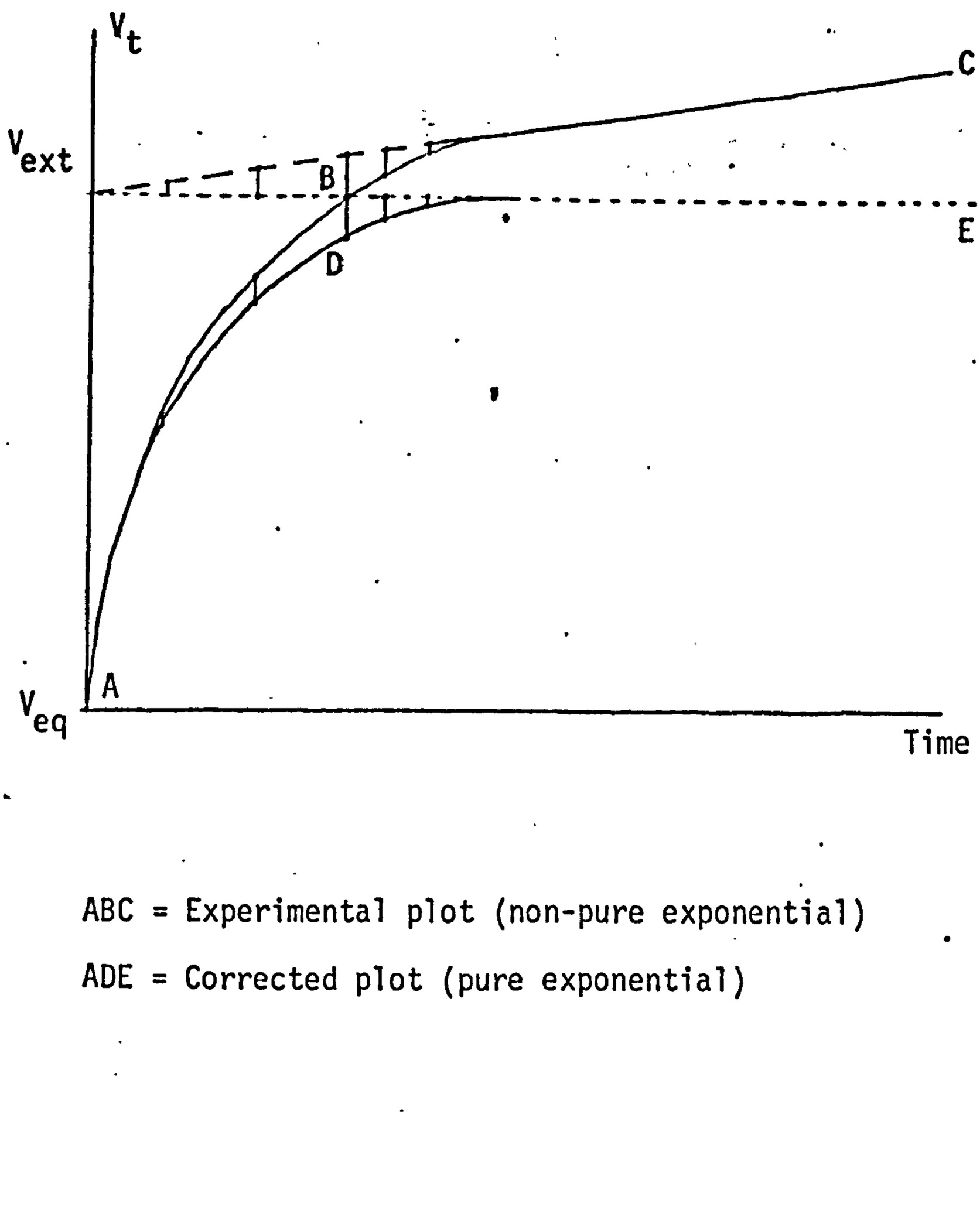

ABC = Experimental plot (non-pure exponential)

ADE = Corrected plot (pure exponential)

The values of V_t selected from the ideal polarisation curve, and termed V_t^*, were determined for different times. The values of $\eta_t(V_t^* - V_o)$ were then calculated. According to eq. (47), section II, the quantities $(\eta_\infty - \eta_t)$ and $\log(\eta_\infty - \eta_t)$ were determined for different times and for all hydrochloric acid solutions. Representative plots of $\log(\eta_\infty - \eta_t)$ against time for the polarisation of the silver-silver chloride electrode in aqueous hydrochloric acid solution (C = 0.01) are given in fig. 16. These plots use the data given in table 13. The slopes of such plots give the value of the characteristic rate constant k (k = -2.303 slope) and the intercept I. It is apparent that k is nearly independent of current, but I is not.

The values of k and I, for all hydrochloric acid solutions, are given in table 14.

C. CHARACTERISTICS OF THE POLARISED SILVER-SILVER CHLORIDE ELECTRODE AS A FUNCTION OF TEMPERATURE.

The silver-silver chloride electrode (type (c)) was polarised in aqueous hydrochloric acid (0.01 M) in the temperature range 5 - 40^{o}C as described in section III. From the analysis of the polarisation curves, the values of exchange

current densities and differential double-layer capacitances were extracted at each temperature. (The behaviour at the extremes of temperature, 5^{o} and 40^{o}, was erratic and these results were rejected.)

As described earlier (paragraph B), the characteristic rate constants (k) were extracted from the analysis of the exponential region of the polarisation curves. The values of k and the intercepts (I) obtained by plotting log $(\eta_{\infty} - \eta_{t})$ against time are presented with the i_{o} and C_{dl} values in table 15.

D. VARIATION OF THE CHARACTERISTICS OF THE POLARISED SILVER-SILVER CHLORIDE ELECTRODE WITH AGE.

The same electrode, which was polarised a few weeks after preparation (type (a)), was again,polarised one year later in solutions of HCl in water and NMP. The characteristics of the aged electrode are tabulated in table 16.

E. DEPENDENCE OF THE CHARACTERISTICS OF THE POLARISED SILVER-SILVER CHLORIDE ELECTRODE ON THE TIME OF ANODISATION.

A silver-silver chloride electrode type (b) was anodised four times in succession, thus increasing gradually

TABLE 13. Time dependence of the overpotentials for the polarisation of the silver-silver chloride electrode in aqueous hydrochloric acid (0.01M).

	TIME/S	$-\log(\eta_\infty - \eta_t)$		TIME/S	$-\log(\eta_\infty - \eta_t)$
i=0.620/μA	30	4.16_8	i=-0.615/μA	30	4.19
	45	4.21_2		45	4.23_6
	60	4.26		60	4.26_3
	75	4.29		75	4.30
	90	4.33		90	4.32_4
	105	4.34_4		105	4.35_8
	120	4.38		120	4.39_5
	135	4.40_7		135	4.42_5
	150	4.43_6		150	4.45_3
	165	4.45_3		165	4.47_4
	180	4.47_2		180	4.53_8

	TIME/S	$-\log(\eta_\infty - \eta_t)$		TIME/S	$-\log(\eta_\infty - \eta_t)$
i=0.810/μA	30	4.05_6	i=-0.810/μA	30	4.07
	45	4.1		45	4.11
	60	4.12_7		60	4.15
	75	4.16		75	4.17_6
	90	4.18_8		90	4.20
	105	4.21_6		105	4.24
	120	4.24_6		120	4.26_7
	135	4.28_2		135	4.29_6
	150	4.30_5		150	4.32_8
	165	4.32_8		165	4.37_3
	180	4.35_8		180	4.39_9

FIG. 16. Kinetic plots for a polarised silver-silver chloride electrode in aqueous HCl solution (0.01M).

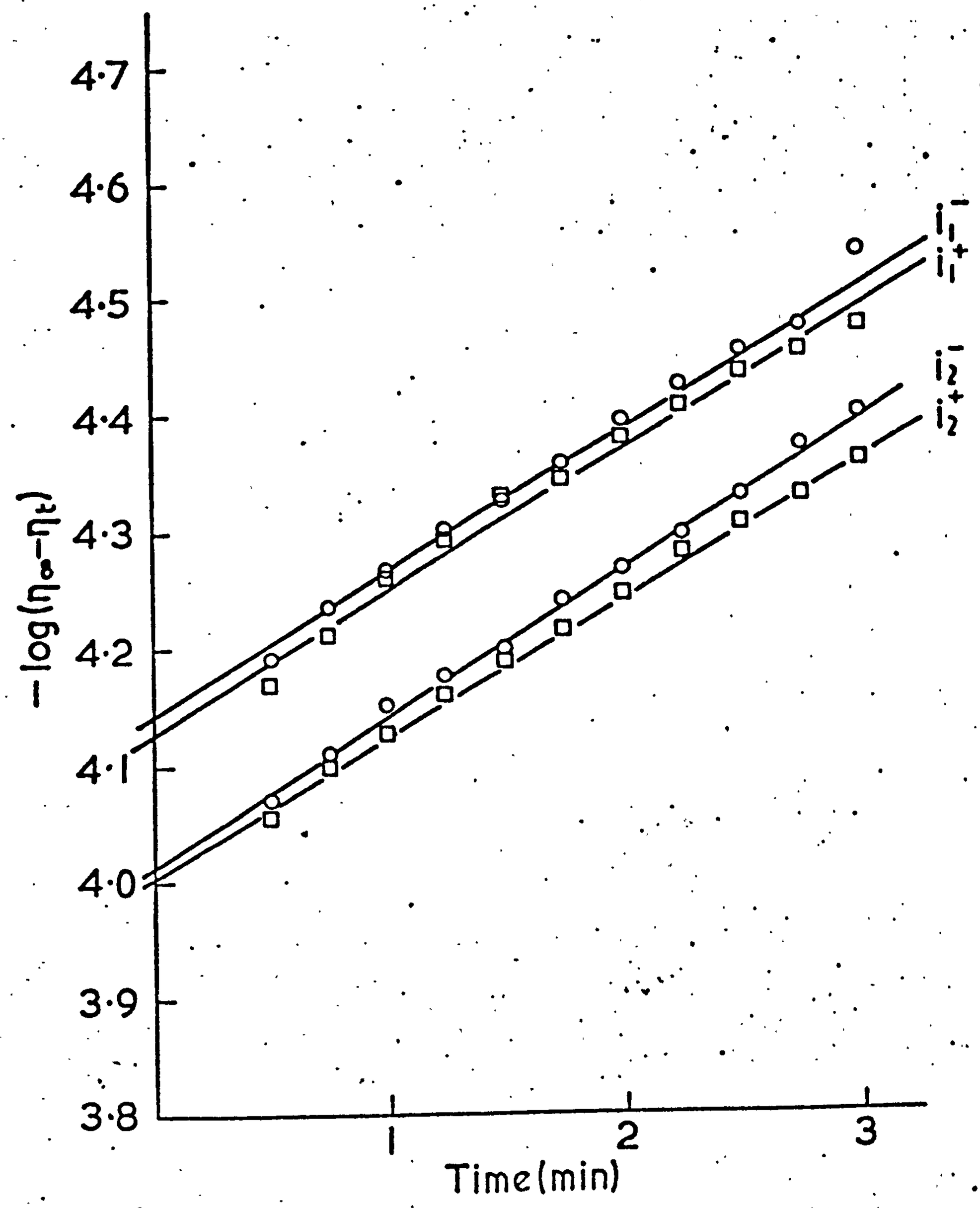

TABLE 14. Kinetic characteristics for the polarised silver-silver chloride electrode in (a) water, (b) NMP and (c) methanol.

(a) Water

	$10^6 i/A$	$10^3 k/s^{-1}$	-I		$10^6 i/A$	$10^3 k/s^{-1}$	-I
C=0.001 / mol dm^{-3}	0.100	6.7	4.24	C=0.003$_4$ / mol dm^{-3}	0.120	9.43	4.47
	-0.095	3.45	4.35		-0.120	8.69	4.62
	0.195	7.54	4.03		0.215	4.56	4.29
	-0.180	4.51	4.05		-0.205	5.13	4.24
	0.380	7.64	3.68		0.390	6.18	4.02
	-0.385	9.52	3.75		-0.400	4.87	4.0
	0.575	7.64	3.51		0.620	4.71$_5$	3.81
	-0.565	10.88	3.59		-0.617	5.13	3.78

Mean k = $7.23_5 \times 10^{-3}$ s^{-1}

Mean k = 6.09×10^{-3} s^{-1}

	$10^6 i/A$	$10^3 k/s^{-1}$	-I
C=0.006 / mol dm^{-3}	0.177	5.44	4.58
	-0.182	5.66	4.47
	0.372	5.76	4.19
	-0.375	5.66	4.23
	0.590	5.44	3.99
	-0.590	5.03	4.02
	0.790	5.24	3.93
	-0.790	5.61	3.91

Mean k = 5.48×10^{-3} s^{-1}

	$10^6 i/A$	$10^3 k/s^{-1}$	-I		$10^6 i/A$	$10^3 k/s^{-1}$	-I
C=0.01 / mol dm^{-3}	0.195	6.81	4.69	C=0.0157 / mol dm^{-3}	0.215	4.71$_5$	4.77
	-0.190	6.71	4.65		-0.220	4.87	4.67
	0.390	4.92	4.32		0.417	5.44	4.37
	-0.395	5.13	4.29		-0.425	4.45	4.44
	0.620	4.72	4.12		0.622	4.71$_5$	4.27
	-0.615	4.72	4.11		-0.625	4.98	4.24
	0.810	4.60	4.0		0.856	4.51	4.09
	-0.810	4.85	4.0		-0.865	4.51	4.11

Mean k = 5.31×10^{-3} s^{-1}

Mean k = 4.77×10^{-3} s^{-1}

TABLE 14 (Contd) (Water)

C=0.022$_4$ / mol dm^{-3}	10^6i/A	10^3k/s^{-1}	-I	C=0.045 / mol dm^{-3}	10^6i/A	10^3k/s^{-1}	-I
	0.315	4.92	4.65		0.630	5.76	4.51
	-0.310	4.98	4.62		-0.635	5.03	4.49
	0.460	5.35	4.47		0.902	4.71$_5$	4.35
	-0.452	5.08	4.50		-0.905	4.71$_5$	4.35
	0.612	4.87	4.35		1.285	4.08	4.17
	-0.605	4.98	4.38		-1.235	4.08	4.18
	0.810	4.82	4.21$_5$		1.735	4.19	4.05
	-0.812	4.71$_5$	4.21$_5$		-1.695	3.93	4.06
	Mean k = 4.96 x 10^{-3} s^{-1}				Mean k = 4.56 x 10^{-3} s^{-1}		

C=0.10 / mol dm^{-3}	10^6i/A	10^3k/s^{-1}	-I	C=0.20 / mol dm^{-3}	10^6i/A	10^3k/s^{-1}	-I
	0.735	5.44$_5$	4.65		0.85	6.34	4.91
	-0.745	5.13	4.62		-0.86	6.13	4.84
	1.170	4.61	4.48$_5$		1.17	7.23	4.81
	-1.145	4.51	4.49		-1.14	7. 38	4.79
	1.46	4.03	4.37		1.50	4.66	4.61
	-1.42	4.19	4.36$_5$		-1.46	5.97	4.61$_5$
	1.775	3.93	4.25$_5$		1.815	7.02	4.51
	-1.745	4.14	4.24$_5$		-1.76	8.12	4.57$_5$
	Mean k = 4.50 x 10^{-3} s^{-1}				Mean k = 6.60 x 10^{-3} s^{-1}		

TABLE 14 (Contd) (b) NMP.

	$10^6 i/A$	$10^3 k/s^{-1}$	-I		$10^6 i/A$	$10^3 k/s^{-1}$	-I
C=0.002 / mol dm^{-3}	0.155	4.94_5	3.86	C=0.005 / mol dm^{-3}	0.385	8.02	3.69
	-0.158	5.61	3.91		-0.350	7.69	3.71
	0.360	4.73	3.54		0.745	7.09	3.34
	-0.353	9.45	3.5		-0.740	7.15	3.36
	0.595	3.84_5	3.3		1.13	6.21	3.15
	-0.600	4.07	3.28		-1.14	5.93	3.13
	0.763	3.96	3.22		1.69	5.71	2.99
	Mean k = 5.23×10^{-3} s^{-1}				Mean k = 6.83×10^{-3} s^{-1}		

	$10^6 i/A$	$10^3 k/s^{-1}$	-I		$10^6 i/A$	$10^3 k/s^{-1}$	-I
C=0.008 / mol dm^{-3}	0.580	3.29	3.90	C=0.016 / mol dm^{-3}	0.530	4.56	3.74
	-0.560	3.36	3.86		-0.566	4.51	3.73
	1.33	3.63	3.58_5		0.880	4.83	3.56
	-1.40	3.13	3.61		-0.865	5.00	3.54
	1.81	3.69	3.44		1.70	4.62	3.35
	-1.735	3.56	3.45		-1.71	4.39_5	3.34_5
	Mean k = 3.44×10^{-3} s^{-1}				Mean k = 4.65×10^{-3} s^{-1}		

TABLE 14 (Contd) (NMP)

	$10^6 i/A$	$10^3 k/s^{-1}$	-I
C=0.03 / mol dm^{-3}	0.370	3.68	4.38
	-0.380	4.17	4.35
	0.935	4.67	3.99
	-0.930	4.14_5	3.97
	1.685	4.56	3.75
	-1.695	4.23	3.70

Mean k = 4.24×10^{-3} s^{-1}

	$10^6 i/A$	$10^3 k/s^{-1}$	-I
C=0.05 / mol dm^{-3}	0.920	3.52	4.08_5
	-1.05	3.29	4.07_5
	1.49	3.79	3.85
	-1.52	3.79	3.87
	2.49	3.84	3.62_5
	-2.52	3.82	3.63

Mean k = $3.67_5 \times 10^{-3}$ s^{-1}

	$10^6 i/A$	$10^3 k/S^{-1}$	-I
C=0.2 / mol dm^{-3}	1.20	3.84	4.29
	-1.25	4.94_5	4.25
	1.99	3.24	4.02
	-2.01	2.91_5	4.00
	2.68	3.96	3.93
	-2.71	4.07	3.94

Mean k = 3.83×10^{-3} s^{-1}

TABLE 14 (Contd) (c) Methanol

	$10^6 i/A$	$10^3 k/s^{-1}$	-I		$10^6 i/A$	$10^3 k/s^{-1}$	-I
C=0.001 / mol dm^{-3}	0.448	3.64	3.4	C=0.002$_5$ / mol dm^{-3}	0.458	3.58	3.52
	-0.449	3.73	3.38		-0.462	3.51$_5$	3.50$_5$
	0.839	3.03	3.11		0.865	3.10	3.22$_5$
	-0.831	2.92	3.1		-0.860	3.15	3.20$_5$
	1.80	2.85	2.8		1.32	2.92	3.06$_5$
					-1.37	2.85	3.07$_5$
	Mean k = 3.23 x 10^{-3} s^{-1}				Mean k = 3.19 x 10^{-3} s^{-1}		

	$10^6 i/A$	$10^3 k/s^{-1}$	-I		$10^6 i/A$	$10^3 k/s^{-1}$	-I
C=0.005 / mol dm^{-3}	0.530	3.42	3.51	C=0.007$_5$ / mol dm^{-3}	0.540	3.10	3.62
	-0.545	2.92	3.56		-0.540	2.84	3.66
	0.952	3.13$_5$	3.27		0.942	2.66	3.34$_5$
	-0.967	2.98	3.29		-0.955	2.80	3.33
	1.40	3.31$_5$	3.13		1.53	2.92	3.17
	-1.41	2.98	3.14		-1.50	2.76	3.17
	Mean k = 3.12$_5$ x 10^{-3} s^{-1}				Mean k = 2.85 x 10^{-3} s^{-1}		

TABLE 14 (Contd) (Methanol)

	$10^6 i/A$	$10^3 k/s^{-1}$	-I		$10^6 i/A$	$10^3 k/s^{-1}$	-I
C=0.028 / mol dm^{-3}	0.635	2.93_5	3.81_5	C=0.01 / mol dm^{-3}	0.600	3.32_5	3.65
	-0.610	3.73	3.83		-0.615	3.69_5	3.64
	1.24	2.74	3.5		1.10	3.22	3.38
	-1.20	2.86	3.5		-1.10	2.86	3.41
	1.77	2.86	3.36_5		1.72	2.86	3.18
	-1.73	2.78	3.37		-1.695	2.89	3.22
	Mean k = $2.98 \times 10^{-3} s^{-1}$				Mean k = $3.14 \times 10^{-3} s^{-1}$		

	$10^6 i/A$	$10^3 k/s^{-1}$	-I		$10^6 i/A$	$10^3 k/s^{-1}$	-I
C=0.067 / mol dm^{-3}	0.83	3.10	3.83_5	C=0.22 / mol dm^{-3}	1.33	3.0	3.61_5
	-0.81	2.92	3.9		-1.33	2.36_5	3.62_5
	1.70	2.18_5	3.45_5		2.60	2.88	3.40_5
	-1.69	2.24	3.48		-2.65	2.36_5	3.42
	Mean k = $2.61 \times 10^{-3} s^{-1}$				Mean k = $2.65 \times 10^{-3} s^{-1}$		

TABLE 15. Temperature dependence of i_o, C_{dl} and rate constants for the polarised silver-silver chloride electrode in aqueous hydrochloric acid (0.01 M).

T/°K	$10^6 i$/A	$10^5 i_o$/A	$10^2 C_{dl}$/F	$10^3 k/s^{-1}$	-I
	0.457			9.11	3.72
283.17	-0.462	4.14	7.9	9.06	3.73
	0.915			3.89	3.49
	0.441			10.03	3.82
288.21	-0.455	4.93	8.7	10.35	3.88
	0.914			4.12	3.56
	0.479			9.71	3.84
293.22	-0.480	5.83	11.0	9.59	3.89
	0.934			3.89	3.53
	0.395			8.44	3.88
	-0.410			8.97	3.93_5
298.60		7.80	11.8		
	0.874			4.71	3.60
	-0.872			3.31	3.60
	0.443			7.48	4.0
	-0.459			9.26	4.05
303.19		8.68	16.1		
	0.904			4.97	3.80
	-0.900			5.56	3.81
	0.405			8.88	4.12
308.18	-0.420	11.46	20.7	8.92	4.17
	0.868			4.21	3.94

Table 16. Characteristics of the polarised silver-silver chloride electrode aged one year.

C/mol dm^{-3}	$10^6 i/A$	$10^5 i_o/A$	C_{dl}/F	$10^4 k/s^{-1}$	-I
H_2O					
0.024_6	1.045	8.02	0.62_5	7.31_4 \ 7.31 / 7.31_4	3.65 / 3.62_5
	-1.00				
0.068	1.00	9.73	0.80	8.05 \ 8.16 / 8.28	3.73 / 3.68
	-1.015				
0.095	1.02	10.74	0.84	9.06_2 \ 9.13 / 9.20	3.78 / 3.75
	-1.00				
NMP					
0.075_5	0.625	3.0	0.09_5	19.16 \ 21.3 / 23.48	3.57_5 / 3.70
	-0.605				
0.155	0.622	6.37	0.20_5	15.57 \ 14.6 / 13.66	3.97_5 / 3.84
	-0.609				

the coverage and thickness of silver chloride layer. The dry electrode was weighed before coating, after silver was deposited, and after the final anodisation. The electrode was polarised after each anodisation, and the polarisation curves were analyzed.

The weight of the silver chloride layer after the final anodisation was calculated by two different methods (1) by weighing, and (2) from Faraday's Law. Method (1) gave 0.162 g and method (2) gave 0.118 g. (The difference must be attributed to weighing errors and/or variations in anodising current). Taking an average value (0.14 g) of the weight and using the initial weight of silver (0.241 g) with atomic weight of silver and silver chloride, simple calculation shows that there was ca.44% conversion of silver to silver chloride after the final anodisation. Furthermore, from the known density of AgCl $(5.56\ g/cc)^2$ and surface area of the electrode (1.54 cm^2), the thickness of the AgCl layer can be estimated (165 μm). This is of course calculated on the basis of the assumption that the AgCl layer is of even thickness, and does not allow for any roughness factor which may affect the real area available for anodisation. The results are illustrated in table 17.

Table 17. Values of the characteristics (i_o & C_{dl}) and the estimated thickness of silver chloride as a function of time for the Ag-AgCl electrode in aqueous HCl (0.01 M).

- Anodising current : 0.9 mA -

Anodisation-time/hr	% converted	AgCl thickness/μm	$10^5 i_o$/A	C_{dl}/F
0.25	0.5	1.8	1.08	0.17
1.58	3	11	1.84	0.30
3.58	7	26	1.70	0.25
22.75	44	165	1.80	0.29

(The AgCl - thickness is calculated from the Faraday's Law)

F. DEPENDENCE OF THE CHARACTERISTICS OF THE POLARISED SILVER-SILVER CHLORIDE ELECTRODE ON THE ELECTRODE-TYPE.

As for the type (a) of the silver-silver chloride electrode, which was polarised in water, NMP and methanol (results given in tables 8 and 12), the silver-silver chloride electrode of type (c) was polarised in aqueous hydrochloric acid solutions. The values of the exchange current density and the differential double layer capacitance as functions of concentration are presented in table 18. The results, for these two types of polarised silver-silver chloride electrode in aqueous hydrochloric solutions, will be discussed in section VI, together with the type (b).*

TABLE 18. Values of i_o and C_{dl} for the polarised silver-silver chloride electrode of type (c) in aqueous hydrochloric acid solutions.

$10^2 C$/mol dm^{-3}	$\sqrt{C}$/mol$^{1/2}$ dm$^{-3/2}$	$10^5 i_o$/A	$10^2 C_{dl}$/F
0.25	0.05	1.85±0.0	3.6±0.0
1.0	0.10	2.55±0.15	7.0±0.3
5.0	0.22	4.0 ±0.2	5.3±0.2

* The type (b) of electrode, however, has not been investigated as a function of concentration, but only as a function of time of anodisation (the concentration being kept constant). The values of i_o and C_{dl} for this type are given in table 17.

REFERENCES

1. P. Delahay, "New Instrumental Methods in Electrochemistry", Interscience, N.Y. and London, p. 181 (1954).

2. C. D. Hodgman, R. C. Weast and S. M. Selby, Handbook of Chemistry and Physics, Chemical Rubber Publishing Corp., Ohio, (1957).

SECTION VI

DISCUSSION

A. GENERAL ASPECTS.

The values of the exchange currents observed in the present work for aqueous HCl solutions (0.001 - 0.2 m) were in the range 5×10^{-5} - 1×10^{-3} A per electrode. These values refer to a rough electrode (type (a), section III) with a nominal area of 2.5 cm^2, but perhaps having a roughness factor as high as 100 (see later). It is of interest to compare these results with those of other workers, though work in this field is sparse. Meyer, Posey and Lantz[1] have studied the chronopotentiometry of the silver-silver chloride system. The value of the exchange current was 5×10^{-4} A cm^{-2} in 0.005 m NaCl. At the same concentration (0.005 m HCl), the value of the exchange current obtained from our results is 1×10^{-4} A per electrode. For thin film Ag/Ag I electrodes K. J. Peverelli[2] obtained exchange currents of 5×10^{-5} - 2×10^{-2} A cm^{-2} in the concentration range of 10^{-6} - 10^{-2} M. Values of i_o' for metal-metal ion systems usually cover the range 1×10^{-1} - 8×10^{-3} A cm^{-2} over the concentration range 0.01 - 0.2 M.

The values of the capacitances are much higher than those observed for the Ag^+/Ag or Cu^{2+}/Cu systems. The differential capacitances were in the range 3×10^{-2} - 1.5/F per electrode (at 0.01 - 0.2 M). For the Ag^+/Ag system, Bockris et al.[3] observed a capacitance equal to 5×10^{-4} $F cm^{-2}$, and Lorenz et al[4]. (Cu^{2+}/Cu) had capacitances of 20 - 35 μF cm^{-2} over the concentration range 0.05 -

0.5 mol l^{-1}. Peverelli[2] reported capacitances between 10 and 25 $\mu F\ cm^{-2}$ for the Ag-AgI/I^- system over the concentration range 10^{-7} - 10^{-3} M. Above 10^{-3} M, the capacitance increases very rapidly and may reach very high values, but no parallel can be drawn with the present work, because of the very low concentration range used. What could explain the differences between the capacitances observed in the present work and those of previous workers ? The reason is indicated by the results obtained for C_o, the equilibrium concentration of adsorbed anions. The calculation and detailed discussion of C_o values is deferred until later (section C), but we note that the values obtained are in the order of 8×10^{-7} moles per electrode or 3.2×10^{-7} moles cm^{-2} (using an electrode area = 2.5 cm^2). Bockris[3] found, for the Ag^+/Ag system, an average value of C_o equal to 8×10^{-10} moles cm^{-2}. The difference in C_o values obtained (and therefore in C_{dl} values) may be attributed to the fact that the Ag/AgCl system has a high adsorption, i.e. it is very rough and porous. Let us estimate the roughness factor by considering the number of silver atoms present in 1 cm^2 area of an AgCl surface layer, and the number of adions adsorbed from the average value of C_o, in our system. If one AgCl molecule is ~ 3.1 Å long ($Ag^+ \sim 1.3$ Å and $Cl^- \sim 1.8$ Å), then a square occupied by 2 molecules corresponding to 2 Ag, in the following arrangement, will be 9.6 $Å^2$:

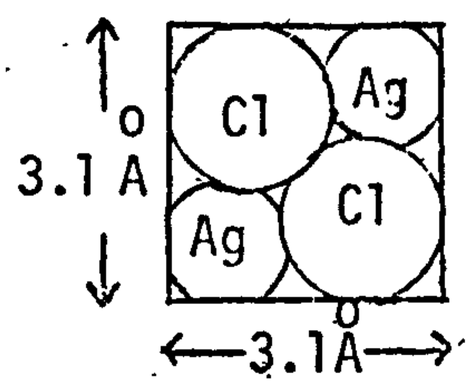

The area occupied by 1 Ag will, therefore, be 4.8 $\mathring{A}^2$. The number of Ag atoms contained in 1 cm^2 area is $\frac{1}{4.8\ 10^{-16}} = 2 \times 10^{15}$. If all the silver atoms in 1 cm^2 area are covered by Cl^- ions, (i.e. there is maximum coverage) there will be 2×10^{15} adions adsorbed/cm^2. The average value of C_o was found to be 3.2×10^{-7} moles cm^{-2} or $\sim 19.3 \times 10^{16}$ molecules cm^{-2}. Hence the minimum roughness factor (which is the excess of adions relative to sites) is $\frac{19.3 \times 10^{16}}{2 \times 10^{15}} \sim 100$. If the coverage of Ag sites by adions is less than complete, then the roughness factor may exceed 100. Consequently, the high values of the capacitances obtained may be explained by full coverage with adions and/or a high roughness factor.

We now turn our attention to the effects of variable time of anodisation (electrode of type (b)) evident in the results of table 17, (section V) which are plotted in fig. 17. The results show that with increasing anodising-time, both i_o' and C_{dl} increase very rapidly over about 3 hours. During this first period it was noticed that the colour of the electrode gradually changed first from white to a light brown after about half an hour (when the AgCl thickness is 1.8 μm), and then to a dark brown when the AgCl layer is about 26 μm thick. (The thickness is estimated according to table 17). After this period there was no further change. The coverage of silver by silver chloride was probably incomplete for the first 3 hours period, though some areas are likely to be well-covered and others not. Once the coverage was complete, the increase in the thickness of the silver chloride does not apparently further affect the electrodic characteristics since i_o' and C_{dl} reach a constant value at an anodising time

FIG. 17. Characteristics of the Ag/AgCl electrode as a function of the time of anodisation.

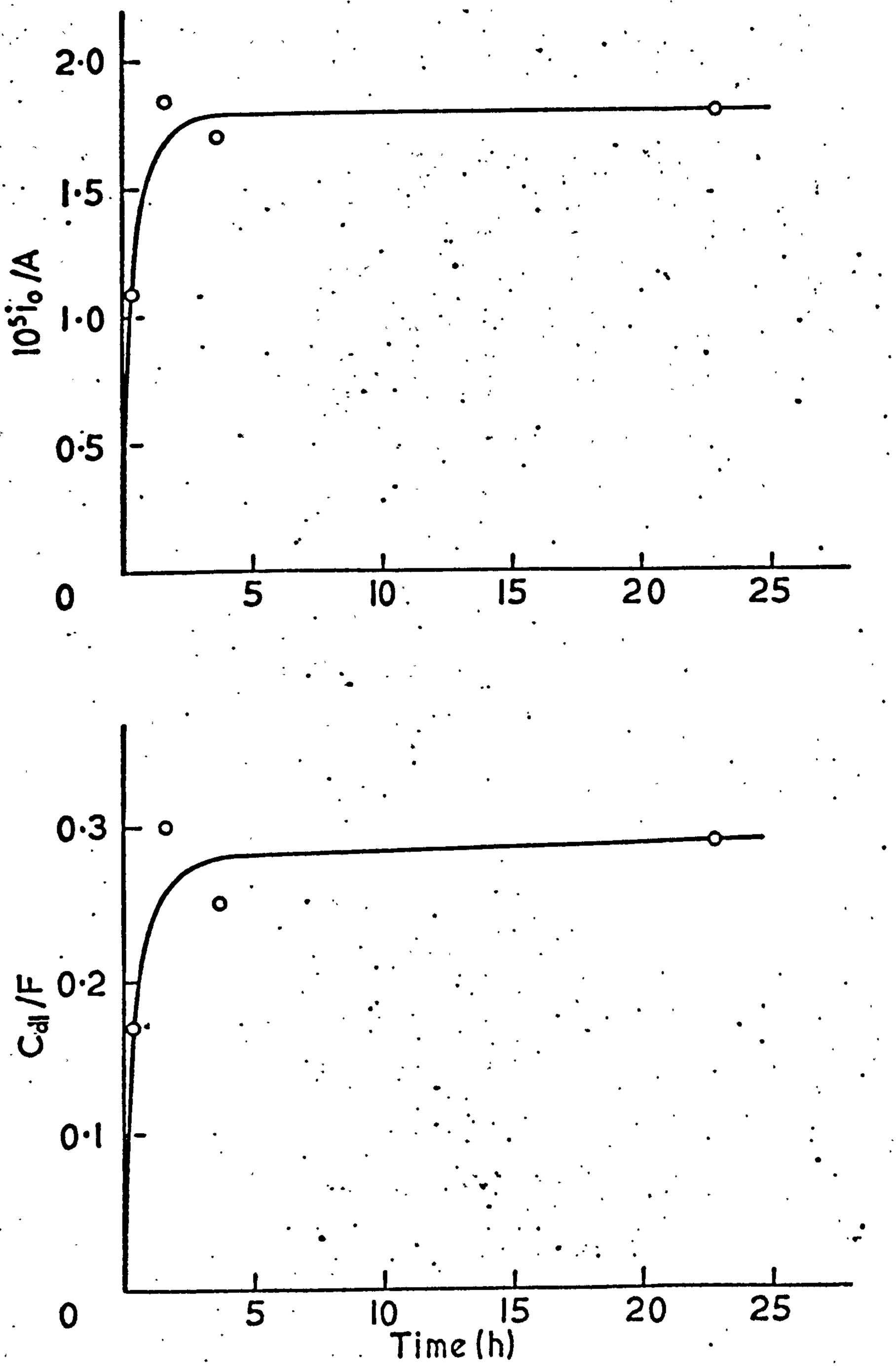

which corresponds to about 7% of silver converted to silver chloride (table 17). It may be conjectured that electrodes to be used for thermodynamic measurements should be anodized up to this degree of conversion, where they show good reversible characteristics (i.e. high i_o'). This finding is in essential agreement with the recommendations of Taniguchi and Janz[5] for the preparation of silver-silver chloride electrodes. Their suggested value (10% conversion), based upon the experience of trial and error, is given some explanation by the present results. Since both i_o' and C_{dl} increase in a parallel way and reach constant values, it is probable that the observed effect is indeed caused by an increase in the real surface of AgCl during the first part of the anodising procedure ($\ll$ 3 hr), and this implies that there is a high roughness factor resulting from the porous nature of the AgCl layer, as shown earlier. A further factor is that the roughness factor might increase with increasing thickness of the layer. Now the second part of the graphs, where i_o' and C_{dl} are constant with increasing time of anodisation, can be interpreted as follows. The roughness factor must have become relatively constant after a thick layer of AgCl has been deposited, so that the coverage must surely be complete. Further layers of AgCl do not appreciably increase the resistance of the electrode, which is low on account of the very imperfect nature of the AgCl lattice. A direct measurement of the resistance of the electrodes (all types) has given resistances $< 1\ \Omega$.

Another factor which can explain why values of exchange currents and capacitances may be different, even when different workers study the same system, is the time allowed for aging of electrodes. This matter will be examined now in more detail. The results obtained (tables 8 - 12 - 16) show a decrease in both i_o' and C_{dl}, over one year, of about 60% and 27% in H_2O respectively, and 80% and 60% in NMP respectively. This is in substantial agreement with the work of Peverelli[2] who found an 18% decrease for smooth electrodes (with an aging period of ~10 hrs). However, Peverelli did not study the same part of the surface before and after aging because the films (see review section) are destroyed by making the replicas. Engel[6], who studied AgI films grown on polished silver plates, suggested that this decrease is due to slow recrystallization during the aging process, which will clearly be more marked with rough electrodes. Peverelli[2] suggested that aging of the electrode simply results into a decrease of the surface roughness. He indicated that the roughness factor decreases with the same percentage as for the C_{dl} values (18%), and that aging, therefore, appears not to affect the kinetic parameters of the electrode, provided they are referred to the real surface area. Nevertheless, Engel[6] suggested that the roughness factor would increase upon aging. We can examine the problem in the light of our results from the values of C_o, for the non-aged and aged electrodes (of type (a))[calculated from tables 16 and 20]given on the next page :

Solvent	Age	$10^7 C_o$/moles area^{-1}	roughness factor(estimated from C_o as above)
H_2O	2-3 weeks	7.5 - 20	~ 165
(C=0.02-0.1 M)	1 year	14 - 17	~ 186
NMP	2-3 weeks	> 8(up to 15)	~ 145
(C=0.075-0.155 M)	1 year	2.5 - 9	~ 69

These results show that the roughness is little changed in H_2O, but the roughness factor decreases in NMP, perhaps confirming the conclusions of Peverelli[2]. Since the roughness factor is reduced, the real surface has decreased with aging; there are less 'holes' and less ions in open sites. One immediate consequence is the decrease in the kinetic rate constant k with aging.

B. CONCENTRATION DEPENDENCE OF THE EXCHANGE CURRENT AND THE DIFFERENTIAL CAPACITANCE.

The graphs presented earlier in section V (figs. 9 and 15) suggest a limiting linear dependence of i_o' and C_{dl} on the square root of concentration, confirming similar findings of previous work in this laboratory.

What justification can be given for plotting i_o' or C_{dl} against the square root of concentration in particular ? Let us recall the characteristic distance κ^{-1} in the Gouy-Chapman double-layer model, commonly known as the "Debye-length";

$$\kappa^{-1} = \left(\frac{\varepsilon_o \varepsilon_r kT}{2N_A e^2}\right)^{\frac{1}{2}} \frac{1}{\sqrt{c}}$$

From this equation, it may be seen that when $\sqrt{c}$ tends to zero, κ^{-1} is very large. The plots show that i_o' and C_{dl} tend to zero when $\sqrt{c}$ tends to zero. The picture suggested is that far from the electrode, in the bulk of a very dilute solution, there are almost no ions and hence no charges ($C_{dl \to 0}$), and no exchange of electrons. When $\sqrt{c}$ increases, κ^{-1} decreases and the density of charge in the diffuse cloud increases at all distances from the electrode. Consequently this has the effect of increasing the capacitance of the interface, and facilitating exchange of electrons to and from chloride ions near the interface (because of the greater number of exchange sites in the solution).

Both i_o' and C_{dl} are proportional to $\sqrt{c}$. Not surprisingly, they are proportional to each other, as shown from the values of tables 8 and 12 for H_2O, NMP and CH_3OH plotted in figs. 18(a), (b) and (c) respectively. This correlation between i_o' and C_{dl} was pointed out earlier by previous workers in this laboratory. One of the main tasks of the present studies was to re-check it and confirm it. The i_o' vs. C_{dl} plots seem to go to the origin, and the slopes computed with the aid of a least-squares programme, are given below:

Solvent	10^4 slope/V s^{-1}
H_2O	4.7 ± 0.3
NMP	7.0 ± 0.2
CH_3OH	3.9 ± 0.3

FIG. 18. Plot of i_o vs C_{dl} in the concentration range 0 - 0.2 molar - (a) water - (b) NMP - (c) methanol.

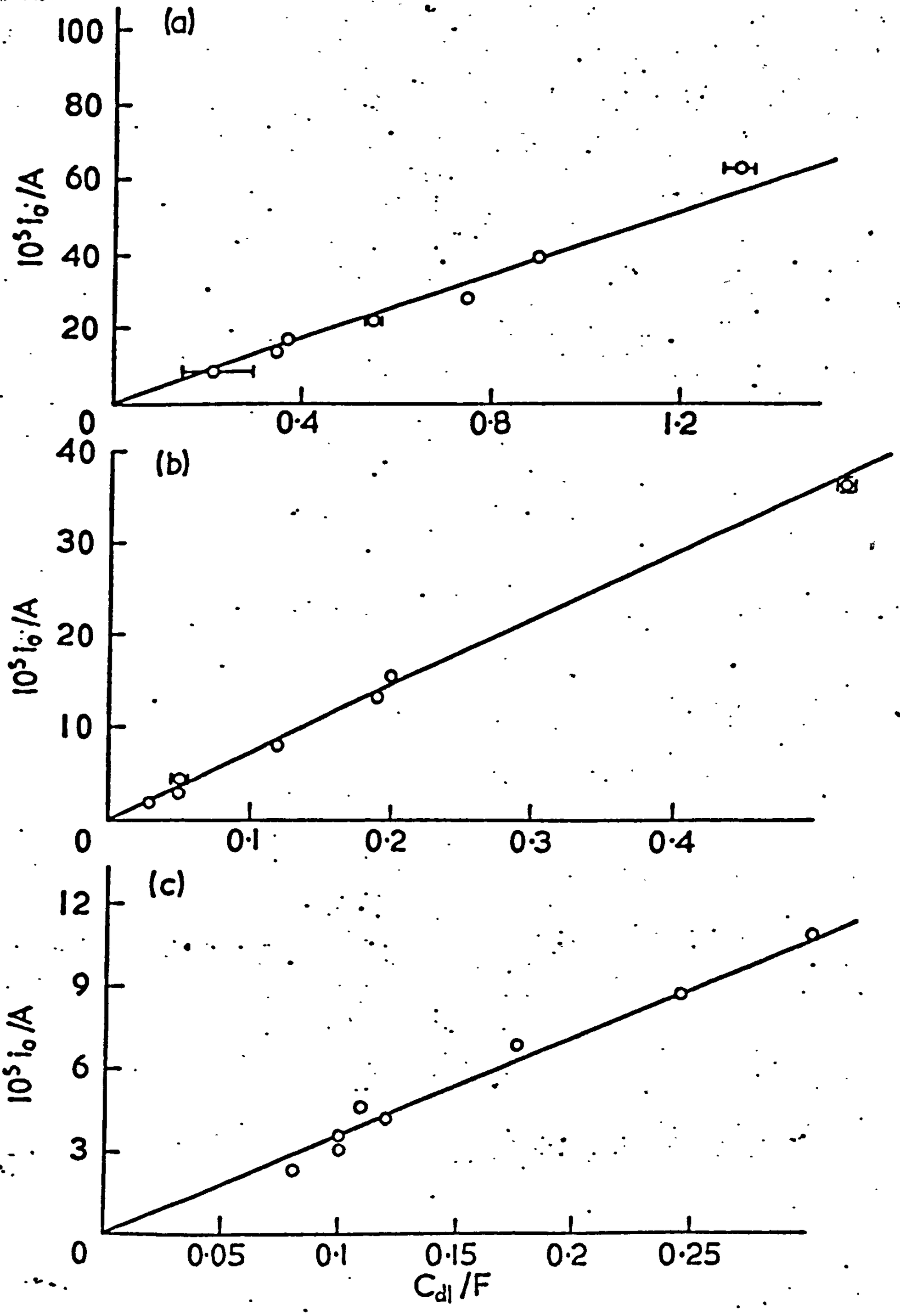

These slopes are thus constant for a given electrode in a given solvent, and appear to increase with the dielectric constant of the solvent,and the electrodic behaviour is completely defined. An interesting fact emerges with respect to the plots of i_o' against C_{dl}. The slope is not only solvent-dependent but also electrode-dependent. From the values of i_o' and C_{dl} given for type (a) and type (c) electrodes in tables 8 and 18 respectively, in the case of water, the values of the slopes are deduced

Electrode/type	10^4 slope/V s^{-1}
(a)	4.7
(c)	5.3

It appears that the slope, s, depends on the electrode-type used. As such a slope would be expected to be independent of the surface area, since both C_{dl} and i_o' would be expected to be dependent on a common area, then the observed difference in these slopes arises from the roughness factor, which is different for each electrode. Let us consider the value of C_o for electrode (a) polarised at 25^oC in aqueous hydrochloric acid (c=0.01) given in table 20 which is 4.17×10^{-7} mole $area^{-1}$ or 1.668×10^{-7} mole cm^{-2} (area = 2.5 cm^2). From table 15, the calculation of C_o for the same experimental conditions of electrode (c) [c = 0.01, 25^oC, HCl in H_2O] gives an average value for C_o of 1.44×10^{-7} mole $area^{-1}$ or 1.84×10^{-7} mole cm^{-2} (area = 0.785 cm^2). The estimation of the roughness factor, r, as made earlier (section A of this chapter)

gives for electrodes (a) and (c), r(a) = 50 and r(c) = 55 respectively. The roughness factor between electrodes (a) and (c) being different, this may explain the difference obtained in the slopes of i_o' vs. C_{dl} plots for these electrodes. It may be relevant to notice that the ratio $(\frac{\text{slope}}{r})$ is about the same for these two types of electrodes $(\frac{4.7 \times 10^{-4}}{50} \sim \frac{5.3 \times 10^{-4}}{55})$. It may be concluded that the smoother the electrode, the lower is the value of the slope. Using the values of i_o' and C_{dl} given in table 17 for the type (b) electrode, the value of the slope for the plot of i_o' vs. C_{dl} is 0.646×10^{-4} V s^{-1}. If the ratio $\frac{s}{r}$ is the same for any type of the silver-silver chloride electrode, we may deduce a roughness factor for the electrode (b) by writing

$$\frac{S(a)}{r(a)} = \frac{S(b)}{r(b)}$$

or
$$r(b) = \frac{S(b)r(a)}{S(a)} = 7.$$

(There is perhaps a limit for the roughness factor of 1.5 - 2, judging from Peverelli's results[2]).

A more conventional treatment of concentration dependence of i_o' is in terms of the transmission coefficient β. Substitution for $\Delta\Phi_e$ in eq. (25) using the Nernst equation leads[7] to the following equation for i_o' :

$$i_o' = nFk_s[R]^{\beta}\,[OX]^{(1-\beta)}$$

where k_s is the heterogenous rate constant of the reaction, [OX] the reductant concentration which is maintained constant, and [R] the variable concentration of chloride ions $[Cl^-]$ in our system. From

the above, we may derive

$$\log i_o' = \beta \log [C] + \log [\text{const}].$$

Hence the slope of the plot of log i_o' against log c gives the value of the transmission coefficient (or symmetry factor) β. Using the data given in table 8, these plots are presented for water, NMP and methanol in fig. 19, and the data yield the following values for β:

Solvent	β
H_2O	0.61
NMP	0.72
CH_3OH	0.33

Bockris et al.[3] gave a symmetry factor of about 0.5 for the Ag^+/Ag system in water, and Peverelli[2] found a transmission coefficient for the Ag/AgI system in water of ~0.6. It is relevant to say that the transmission coefficient β varies greatly with the solvent, and appears to be related to the dielectric constant (increasing, with increasing ε_r). Regardless of the view taken concerning the concentration dependences, one main conclusion arises : the solvent markedly affects the charge transfer kinetics of the reaction. Since there is uncertainty about the precise meaning of the transmission coefficient[8], we will not discuss it further here.

C. ELECTRODEPOSITION KINETICS.

1. Examination of a one-step model. According to the simple model outlined in section II, when an electrode is polarised, the

FIG. 19.

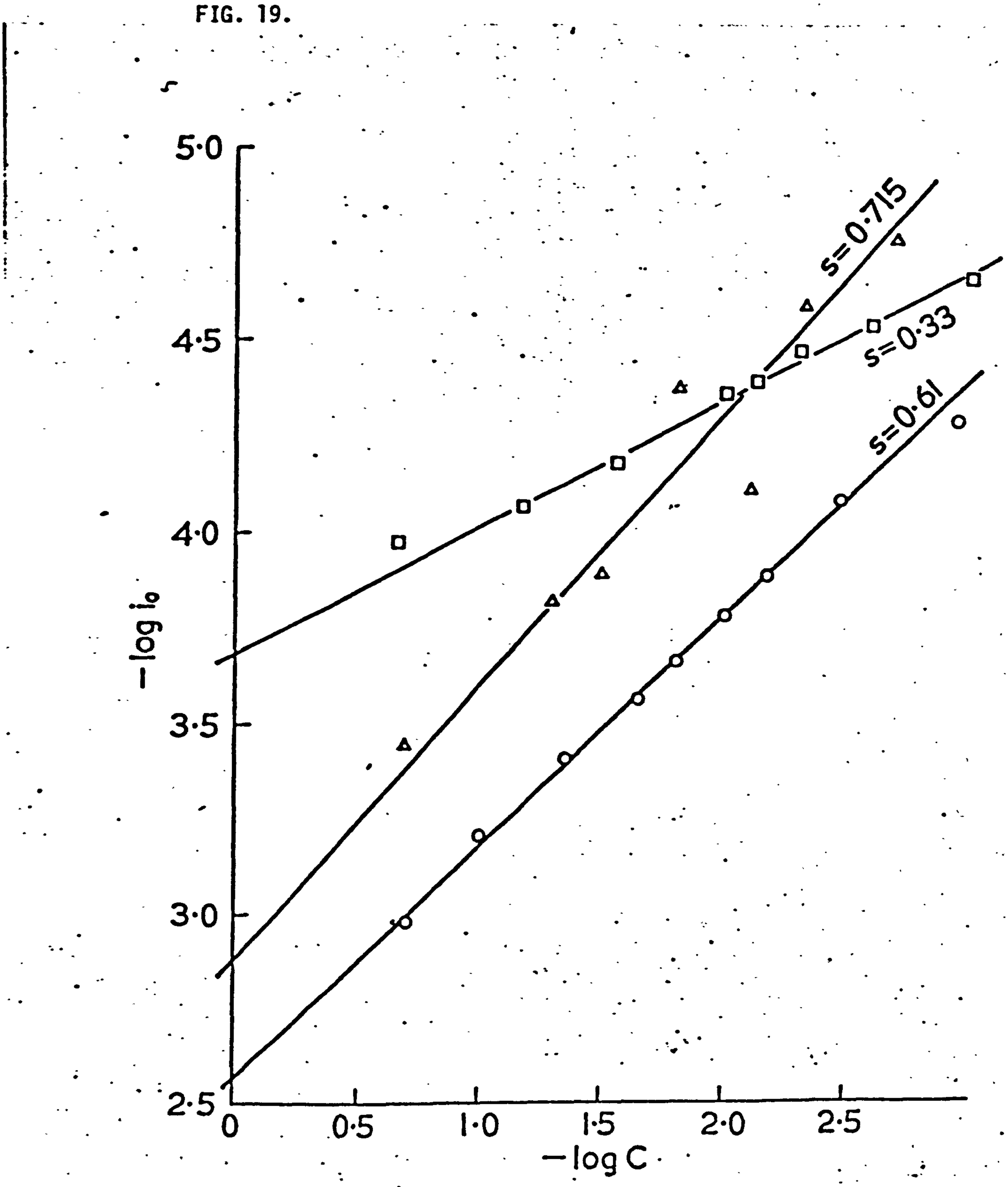

FIG. 19. Determination of the transmission coefficient β for the Ag-AgCl electrode in H_2O(○), NMP(△) and CH_3OH(□).

change of the potential difference from the equilibrium value after a certain time τ_{ct} (the charge transfer relaxation time equal to $\frac{RTC_{dl}}{Fi'_o}$) should be 63% of the total overpotential n. This provides a test for the silver-silver chloride electrode, using the values of the exchange current and the differential capacitance given in tables 8 and 12, to calculate the relaxation time, τ_{calc}. This value is the same as that which would be expected if the electrode polarisation was exactly analogous to the charging of a condenser, and the corresponding overpotential value n_t would be 63% of the steady-state overpotential n_∞. The relaxations observed, τ_{obs}, were not, however, pure exponentials, as is seen from the values of n_t obtained in practice. In table 19, the values of the relaxation time calculated ($\tau_{calc} = \frac{RTC_{dl}}{F\, i'_o}$) are compared with the time τ_{obs} taken to reach 63% of n_∞, and read off from the representative experimental plots of V_t(or n_t) vs. t, given earlier (section V). The results show that the observed build-up of the overpotential, τ_{obs}, is slower than that predicted (τ_{calc}) on the basis of a single charge-transfer step by an average factor of about 2.5 . (These results agree substantially with Bockris et al.'s findings[3]. However, these workers indicated that the observed overpotentials were ten times slower than those predicted by the above model in the case of silver electrodes.) This discrepancy between the predicted values and the experiments implies, therefore, a more complex mechanism, which may be interpreted in terms of the build-up of an adsorption layer of adions, as shown in the next section.

TABLE 19. Test of the one-step mechanism for the Ag-AgCl electrode (comparison of τ_{calc} with τ_{obs}).

Solvent	C/mol dm^{-3}	10^6 i/A	τ_{calc}/s	τ_{obs}/s
Water	0.010	0.810 -0.810 > 57		138 138 > 138
NMP	0.016	1.70 -1.71 > 29		56 59 > 57.5
Methanol	0.005	1.40 -1.41 > 73		184 221 > 202.5

2. Examination of a two-step model. According to Bockris et al[3,9] the electrodeposition process may consist of a charge-transfer step followed by a surface-diffusion step. In the first stage the reacting ion moves from the bulk solution onto the electrode surface, where it exists as a partly solvated anion ("adion"). In the second stage the adion moves along a surface concentration gradient until it can be accommodated in a suitable site in the lattice. Now consider the interface at equilibrium. If there is no net current flowing across the interface, the rate (or number) of adions landing on the plane is virtually equal to the rate of adions leaving the plane. This means that the concentration of adions at equilibrium, C_o, is constant everywhere on the surface planes. With a net current flowing from the electrode to the solution, the number of adions increases on the plane and the average adion concentration at a time t is $\bar{C}_t$. A concentration gradient develops and the perturbation in the adion concentration due to the current is $(\bar{C}_t - C_o)$. It is this quantity which is responsible for the motion and surface-diffusion of ions. Now it is clear that if $(\bar{C}_t - C_o)$ is set at zero, there is no surface-diffusion step, but only a charge-transfer process, and if $(\bar{C}_t - C_o)$ is not zero, the reaction is a two-step process. For the Ag-AgCl electrode, the relative contributions to the charge-transfer and surface-diffusion processes can be calculated from our results. Table 20 gives the values of C_o and i_{SD} $(=FkC_o)$ for hydrochloric acid solutions in water, NMP and methanol, calculated from eqn. (51) (section II) using the values of the rate constants k and intercepts I presented in table 14. The

Table 20. Values of C_o and $i_{SD}(FkC_o)$ for the polarised silver-silver chloride electrode in hydrochloric acid solutions in water, NMP and methanol.*

a. Water.

$10^6 i/A$	$10^8 C_o$/mol.	$10^5 i_{SD}/A$	$10^6 i/A$	$10^8 C_o$/mol.	$10^5 i_{SD}/A$
$C = 0.001/mol.dm^{-3}$			$C = 0.003_4/mol.dm^{-3}$		
0.100	6.8	4.41	0,120	9.8	8.99
-0.095	16.2	5.40	-0.120	15.1	12.69
0.195	7.3	5.31	0.215	24.2	10.65
-0.180	11.8	5.13	-0.205	18.2	9.05
0.380	6.2	4.63	0.390	17.4	10.38
-0.385	5.9	5.49	-0.400	21.6	10.17
0.575	6.4	4.74	0.620	22.3	10.18
-0.565	5.3.	5.59	-0.617	19.1	9.46
Mean $i_{SD} = 5.09\ 10^{-5}$ A			Mean $i_{SD} = 10.20\ 10^{-5}$ A		

	$10^6 i/A$	$10^8 C_o$/mol.	$10^5 i_{SD}/A$
$C = 0.006_7/mol.dm^{-3}$	0.177	32.5	17.10
	-0.182	24.9	13.63
	0.372	26.3	14.63
	-0.375	29.6	16.19
	0.590	27.9	14.66
	-0.590	32.3	15.71
	0.790	33.8	17.10
	-0.790	30.1	16.32
	Mean $i_{SD} = 15.67\ 10^{-5}$ A		

$10^6 i/A$	$10^8 C_o$/mol.	$10^5 i_{SD}/A$	$10^6 i/A$	$10^8 C_o$/mol.	$10^5 i_{SD}/A$
$C = 0.01/mol.dm^{-3}$			$C = 0.015_7/mol.dm^{-3}$		
0.195	36.9	24.25	0.215	70.5	32.11
-0.190	33.2	21.54	-0.220	55.5	26.12
0.390	43.6	20.70	0.417	47.3	24.85
-0.395	39.5	19.57	-0.425	69.2	29.75
0.620	45.6	20.78	0.622	64.6	29.43
-0.615	44.2	20.14	-0.625	57.4	27.59
0.810	46.4	20.60	0.856	61.5	26.77
-0.810	44.0	20.60	-0.865	65.1	28.33
Mean $i_{SD} = 21.02\ 10^{-5}$ A			Mean $i_{SD} = 28.12\ 10^{-5}$ A		

* Values of C_o are given per electrode in table 20.

TABLE 20. (Contd.) (Water).

$10^6 i$/A	$10^8 C_o$/mol.	$10^5 i_{SD}$/A	$10^6 i$/A	$10^8 C_o$/mol.	$10^5 i_{SD}$/A
	$C = 0.022_4$/mol.dm^{-3}			$C = 0.045$/mol.dm^{-3}	
0.315	75.2	35.71	0.630	93.1	51.8
-0.310	68.2	32.77	-0.635	102.6	49.8
0.460	66.7	34.47	0.902	112.6	51.3
-0.452	74.0	36.29	-0.905	113.0	51.4
0.612	74.0	34.78	1.285	122.7	48.3
-0.605	76.7	36.89	-1.235	120.6	47.5
0.810	72.6	33.77	1.735	122.5	49.5
-0.812	74.4	33.85	-1.695	130.4	49.5
	Mean $i_{SD} = 34.82\ 10^{-5}$ A			Mean $i_{SD} = 49.88\ 10^{-5}$ A	

$10^6 i$/A	$10^8 C_o$/mol.	$10^5 i_{SD}$/A	$10^6 i$/A	$10^8 C_o$/mol.	$10^5 i_{SD}$/A
	$C = 0.10$/mol.dm^{-3}			$C = 0.20$/mol.dm^{-3}	
0.735	158.6	83.32	0.85	286.4	175.3
-0.745	159.1	78.76	-0.86	255.1	150.9
1.170	204.1	90.81	1.17	274.7	191.7
-1.145	206.7	89.95	-1.14	250.4	178.4
1.46	223.5	86.94	1.50	345.0	155.1
-1.42	206.7	83.59	-1.46	265.1	152.7
1.775	213.9	81.14	1.815	220.1	149.1
-1.745	195.1	77.96	-1.76	214.3	167.9
	Mean $i_{SD} = 84.06\ 10^{-5}$ A			Mean $i_{SD} = 165.1\ 10^{-5}$ A	

TABLE 20 (Contd.) b. NMP

$10^6 i$ /A	$10^8 C_o$ /mol.	$10^5 i_{SD}$ /A	$10^6 i$ /A	$10^8 C_o$ /mol.	$10^5 i_{SD}$ /A
	$C = 0.002$ /mol.dm^{-3}			$C = 0.005$ /mol.dm^{-3}	
0.155	5.99	2.86	0.385	6.20	4.80
-0.158	6.03	3.26	-0.350	6.16	4.57
0.360	6.95	3.18	0.745	6.07	4.15
-0.353	3.12	2.84	-0.740	6.26	4.32
0.595	8.14	3.02	1.13	6.79	4.07
-0.600	7.40	2.91	-1.14	6.85	3.92
0.763	8.44	3.22	1.69	7.64	4.21
	Mean $i_{SD} = 3.04\ 10^{-5}$A			Mean $i_{SD} = 4.29\ 10^{-5}$ A	

$10^6 i$ /A	$10^8 C_o$ /mol.	$10^5 i_{SD}$ /A	$10^6 i$ /A	$10^8 C_o$ /mol.	$10^5 i_{SD}$ /A
	$C = 0.008$ /mol.dm^{-3}			$C = 0.016$ /mol.dm^{-3}	
0.580	36.9	11.71	0.530	16.85	6.08
-0.560	31.83	10.32	-0.566	17.77	7.73
1.33	37.18	13.02	0.880	17.45	8.13
-1.40	48.06	14.51	-0.865	15.83	7.64
1.81	35.65	12.69	1.70	21.74	9.69
-1.735	36.25	12.45	-1.71	22.73	9.64
	Mean $i_{SD} = 12.45\ 10^{-5}$ A			Mean $i_{SD} = 8.15\ 10^{-5}$ A	

TABLE 20 (Contd) (NMP)

$10^6 i$ /A	$10^8 C_o$ /mol.	$10^5 i_{SD}$ /A	$10^6 i$ /A	$10^8 C_o$ /mol.	$10^5 i_{SD}$ /A
C = 0.03 /mol.dm^{-3}			C = 0.05 /mol.dm^{-3}		
0.370	63.43	22.52	0.920	83.74	28.44
-0.380	53.68	21.60	-1.05	99.96	31.73
0.935	51.55	23.23	1.49	73.35	26.82
-0.930	55.18	22.07	-1.52	78.37	28.66
1.685	54.78	24.10	2.49	72.12	26.72
-1.695	52.96	21.62	-2.52	74.24	27.36
Mean i_{SD} = 22.52 10^{-5} A			Mean i_{SD} = 28.29 10^{-5} A		

	$10^6 i$ /A	$10^8 C_o$ /mol.	$10^5 i_{SD}$ /A
C = 0.2 /mol.dm^{-3}	1.20	160.4	59.44
	-1.25	118.3	56.49
	1.99	169.4	52.98
	-2.01	181.7	51.12
	2.68	151.8	58.0
	-2.71	152.8	60.02

Mean i_{SD} = 56.34 10^{-5} A

TABLE 20 (Contd)

c - Methanol.

$10^6 i$ /A	$10^8 C_o$ /mol.	$10^5 i_{SD}$ /A	$10^6 i$ /A	$10^8 C_o$ /mol.	$10^5 i_{SD}$ /A
C = 0.001 /mol.dm^{-3}			C = 0.002$_5$ /mol.dm^{-3}		
0.448	8.16	2.87	0.458	11.18	3.86
-0.449	7.62	2.74	-0.462	11.09	3.76
0.839	9.42	2.75	0.865	12.37	3.70
-0.831	9.46	2.67	-0.860	11.56	3.51
1.80	10.53	2.89	1.32	13.87	3.91
			-1.37	15.09	4.15
Mean i_{SD} = 2.78 10^{-5} A			Mean i_{SD} = 3.82 10^{-5} A		

$10^6 i$ /A	$10^8 C_o$ /mol.	$10^5 i_{SD}$ /A	$10^6 i$ /A	$10^8 C_o$ /mol.	$10^5 i_{SD}$ /A
C = 0.005 /mol.dm^{-3}			C = 0.007$_5$ /mol.dm^{-3}		
0.530	13.23	4.37	0.540	19.16	5.73
-0.545	17.88	5.04	-0.540	22.92	6.28
0.952	14.93	4.52	0.942	20.69	5.31
-0.967	16.70	4.80	-0.955	19.25	5.20
1.40	15.05	4.81	1.53	20.47	5.77
-1.41	17.25	4.96	-1.50	21.23	5.65
Mean i_{SD} = 4.75 10^{-5} A			Mean i_{SD} = 5.66 10^{-5} A		

TABLE 20 (Contd.) (Methanol)

$10^6 i$ /A	$10^8 C_o$ /mol.	$10^5 i_{SD}$ /A	$10^6 i$ /A	$10^8 C_o$ /mol..	$10^5 i_{SD}$ /A
C = 0.01 /mol.dm^{-3}			C = 0.028 /mol.dm^{-3}		
0.600	21.26	6.82	0.635	37.26	10.55
-0.615	19.16	6.83	-0.610	29.14	10.49
1.10	21.63	6.72	1.24	37.76	9.98
-1.10	26.09	7.20	-1.20	35.01	9.66
1.72	24.04	6.63	1.77	37.85	10.44
-1.695	25.70	7.17	-1.73	38.50	10.33
Mean i_{SD} = 6.90 10^{-5} A			Mean i_{SD} =10.24 10^{-5} A		

$10^6 i$ /A	$10^8 C_o$ /mol.	$10^5 i_{SD}$ /A	$10^6 i$ /A	$10^8 C_o$ /mol.	$10^5 i_{SD}$ /A
C = 0.067 /mol.dm^{-3}			C = 0.22 /mol.dm^{-3}		
0.83	48.26	14.43	1.33	48.20	13.95
-0.81	58.06	16.36	-1.33	62.54	14.27
1.70	58.53	12.34	2.60	60.54	16.82
-1.69	60.12	13.0	-2.65	77.77	17.75
Mean i_{SD} = 14.03 10^{-5} A			Mean i_{SD} = 15.70 10^{-5} A		

values of the exchange current controlled by activation polarisation, $i_o(\frac{i'_o\ i_{SD}}{i_{SD} - i'_o})$ (as defined in section II - eqn (54)), are tabulated in table 21. The plots of $i_o(=i_{CT})$ and i_{SD} vs. $\sqrt{c}$ for H_2O, NMP and CH_3OH are illustrated in fig. 20. As for i'_o vs. $\sqrt{c}$ plots, they seem to present a linear limiting law going through zero. Table 21 shows that $i_o >> i_{SD}$. This would indicate that surface-diffusion is rate determining (i.e. the resistance R_{SD} is greater than the resistance R_{CT}*) and R_{SD} is mostly responsible for total overpotential. The model proposed by Bockris et al.[3,9], which implies resistances "in series", is confirmed by our results. Table 21 indicates that the total observed exchange current i'_o is smaller than either contribution (i_{SD} or $i_o = i_{CT}$). This means that the total observed reistance R_{Tot} (inversely proportional to the exchange current) is greater than either contribution. What is now the situation in terms of capacitances ?

According to Bockris et al.[3,9] it was established that

$$\eta_{\infty Tot} = \eta_{CT} + \eta_{SD}$$

where $\eta_{SD} = \frac{RTi}{F^2kC_o}$. It is apparent that $\frac{nk}{i}(= \frac{RT}{F^2C_o})$ has the dimensions of V x coulombs^{-1}, i.e. (capacitance)$^{-1}$. Thus the quantity $(\frac{F^2C_o}{RT})$ might be considered as a "surface-adsorption capacitance", or in the terms of Conway[10] a "pseudo capacitance".

---

* the term $R_{CT}(= \frac{RT}{Fi_o})$ contains the exchange current controlled by activation polarisation i_o which could have been also written as i_{CT}.

TABLE 21. Values of the surface-diffusion and calculated exchange currents for the polarised silver-silver chloride electrode in hydrochloric acid solutions in water, NMP and methanol.

	$10^2 C/mol\ dm^{-3}$	$\sqrt{C}/mol^{\frac{1}{2}}\ dm^{-\frac{3}{2}}$	$10^5 i'_o/A$	$10^5 i_{SD}/A$	$10^5 i_o/A$
H_2O	0.112	0.033_5	5.36	5.09	—
	0.336	0.058	8.55	10.20	16.53
	0.672	0.082	13.55	15.67	100.1
	1.008	0.100	16.76	21.02	82.70
	1.568	0.125	22.27	28.12	107.1
	2.24	0.150	28.25	34.82	149.7
	4.48	0.212	39.85	49.88	198.2
	10.08	0.318	63.01	84.06	251.6
	20.16	0.45	107.7	165.1	309.5
NMP	0.204	0.045	1.78_5	3.04	4.32
	0.490	0.070	2.69	4.29	7.21
	0.801	0.089	7.92	12.45	21.77
	1.603	0.127	4.38	8.15	9.47
	3.24	0.180	12.99	22.52	30.70
	5.11	0.226	15.38	28.29	33.70
	20.44	0.452	36.41	56.34	102.9
CH_3OH	0.100	0.032	2.26	2.78	12.08
	0.250	0.050	3.00	3.82	13.98
	0.500	0.071	3.50	4.75	13.30
	0.750	0.087	4.13	5.66	15.28
	1.00	0.10	4.48_5	6.90	12.81
	2.78	0.167	6.74	10.24	19.72
	6.72	0.26	8.65	14.03	22.56
	22.0	0.47	10.80	15.70	34.60

FIG. 20. Plots of the surface-diffusion and charge transfer exchange currents vs. $\sqrt{c}$ - Ag/AgCl electrode in HCl and (a) H_2O - (b) NMP - (c) CH_3OH^-

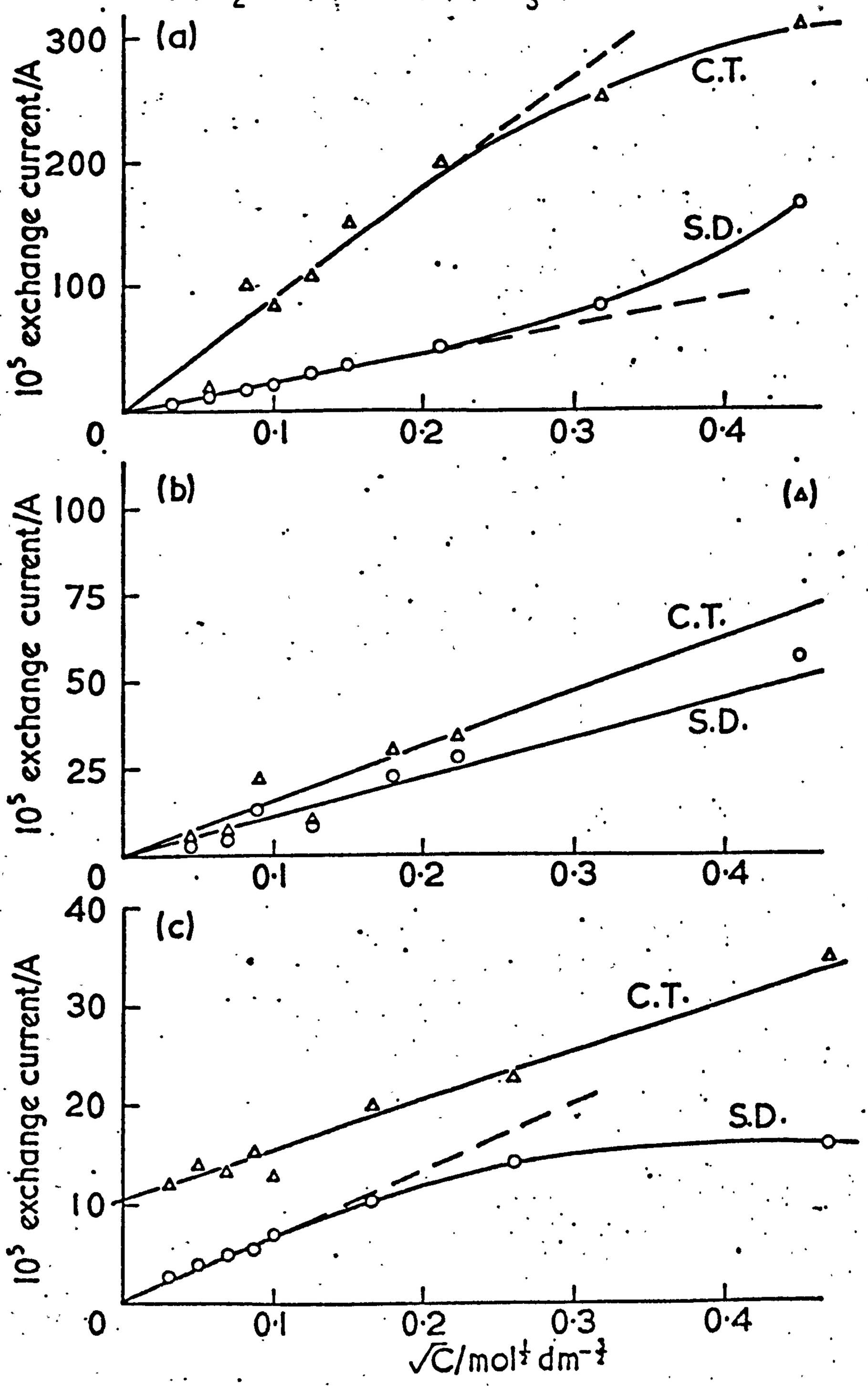

The equation for the "charging" of the adsorption capacitance could be written as $i = C_{SD} \cdot \frac{d\eta_{SD}}{dt} = (\frac{F^2 C_o}{RT})\, \eta_{SD} . k$. This affords us a method of separating the observed capacitances into two components, as follows. Let us consider first capacitances "in series" (an equivalent path to that followed for exchange currents is used here). We may write :

$$\frac{1}{C_{tot}} = \frac{1}{C_{SD}} + \frac{1}{C_{CT}}$$

C_{tot} being the total observed capacitance obtained from the initial linear rise of the polarisation curves, $C_{SD} (= \frac{F^2 C_o}{RT})$ is the "pseudo capacitance" defined above, and C_{CT} the capacitance associated with the charge-transfer step. From the above equation, C_{CT} can be deduced :

$$C_{CT} = \frac{C_{tot}\, C_{SD}}{C_{SD} - C_{tot}}$$

Using the mean values of C_o from table 20, the values of C_{SD} and those of C_{CT} calculated from this equation, are given as a function of concentration in table 22. The plots of C_{SD} and C_{CT} against the square root of concentration are illustrated in fig. 21. They show a linear dependence of these capacitances on $\sqrt{c}$, going to the origin in a sensible manner. It appears that the charge-transfer and surface-diffusion capacitances obey the "in series" model. An "in parallel" scheme, which would imply that $C_{tot} = C_{SD} + C_{CT}$, requires that the values of C_{CT} $(= C_{tot} - C_{SD})$ are negative, and is therefore incompatible with the present results. As previously

TABLE 22. Values of the surface-diffusion and charge-transfer capacitances as functions of concentration for the Ag-AgCl electrode in hydrochloric acid solutions, in water, NMP and methanol.

	$\sqrt{c}$ /mol$^{\frac{1}{2}}$ dm$^{-\frac{3}{2}}$	C_{SD} /F	C_{CT} /F
H_2O	0.033_5	0.31	-
	0.058	0.69_5	0.311
	0.082	1.12	0.509
	0.100	1.57	0.484
	0.125	2.31	0.722
	0.150	2.73	1.03
	0.212	4.31	1.14
	0.317	7.36	1.61
	0.450	9.91	1.70
NMP	0.045	0.25	0.003
	0.070	0.25	0.062
	0.089	1.41	0.131
	0.127	0.70	0.053
	0.180	2.07_5	0.209
	0.226	3.01_5	0.214
	0.452	5.85	0.571
CH_3OH	0.032	0.34	0.105
	0.050	0.47	0.127
	0.071	0.59_5	0.120
	0.087	0.77	0.142
	0.100	0.86	0.126
	0.167	1.35	0.202
	0.260	2.11	0.277
	0.470	2.34	0.344

FIG. 21. Plots of the surface diffusion and charge-transfer capacitances vs. $\sqrt{c}$ - Ag/AgCl electrode in HCl and (a) water - (b) NMP - (c) methanol.

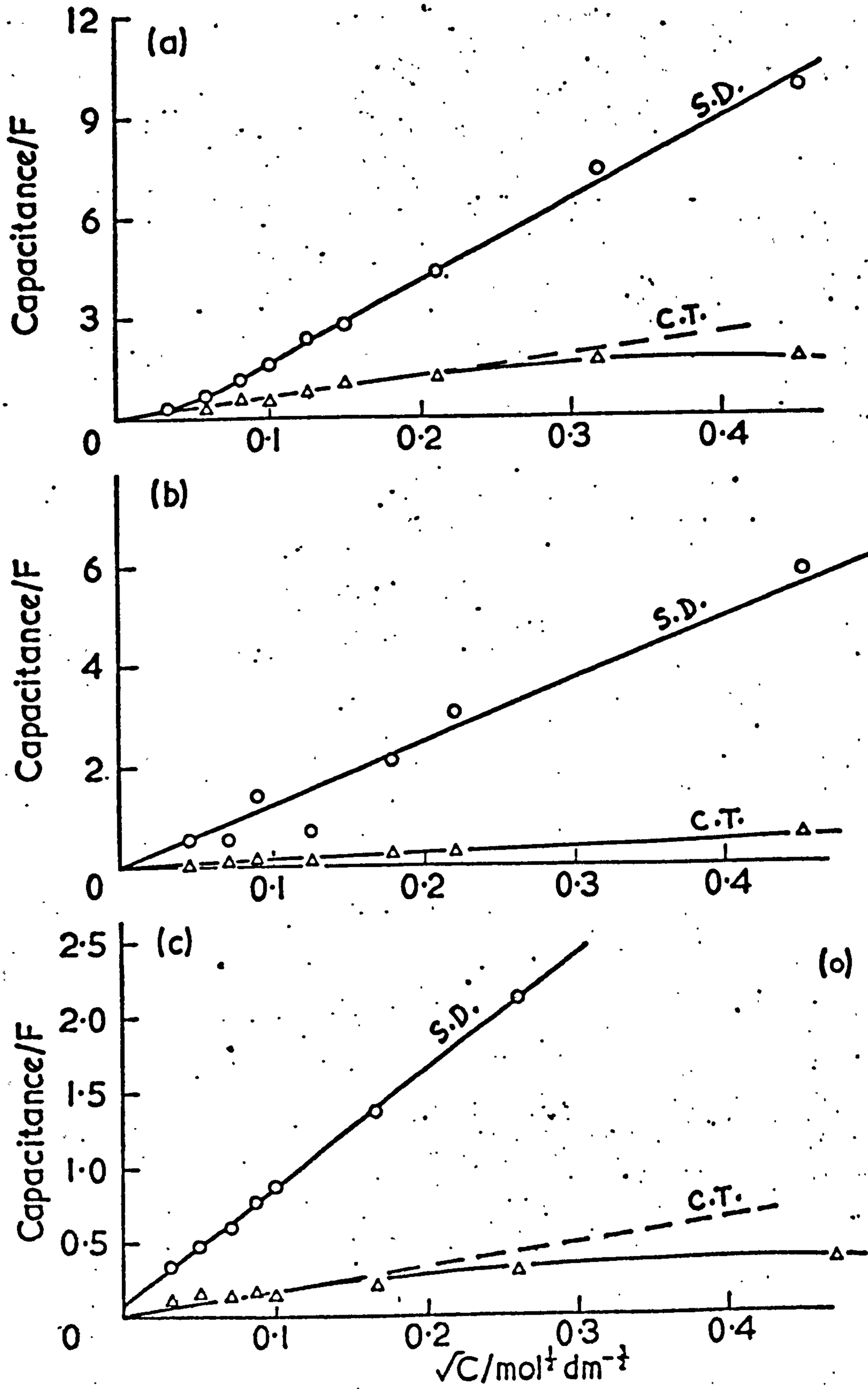

shown for the observed exchange current i'_o and the differential capacitance C_{dl}, there are correlations between i_o(or i_{CT}) and C_{CT}, and between i_{SD} and C_{SD}. The plots of $i_o(=i_{CT})$ against C_{CT} and i_{SD} against C_{SD} are represented in figs. 22 and 23 respectively, for water, NMP and methanol. These correlations suggest that the separation into C_{CT} and C_{SD} is valid, or at least reasonable. The separation has been made on the basis of an "in series" model, since the evidence from i_o data supports this. We may note that an analysis given by Brockris et al. assumes a parallel model[3], such as :

$$i_g - i_{CT} - i_{SD} = i_{DL} + i_{Ai},$$

where i_g is the total constant current, i_{DL} the current used in the non-Faradaic storage of charge by the double layer, and i_{Ai} is that used similarly as storage of adsorbed ionic charges. If the total observed capacitance is C_{obs}, then

$$i_g - i_{CT} - i_{SD} = C_{obs} \frac{d\Delta\Phi}{dt}$$

Now C_{obs} clearly contains contributions from that part of the double layer not associated with adsorbed species (i.e. solvent dipoles, Gouy-Chapman diffuse layer) and from the adsorbed layer itself (the so-called "pseudo capacitance"). Separation of these two quantities is to some extent arbitrary and model-dependent, and for a given system, should be examined in the light of experimental results. Thus there is no firm basis for writing (c.f. Bockris and Reddy)

$$C_{obs} = C_{DL} + C_{Ai}$$

FIG. 22. Plots of i_{CT} vs. C_{CT} in (a) H_2O - (b) NMP - (c) methanol.

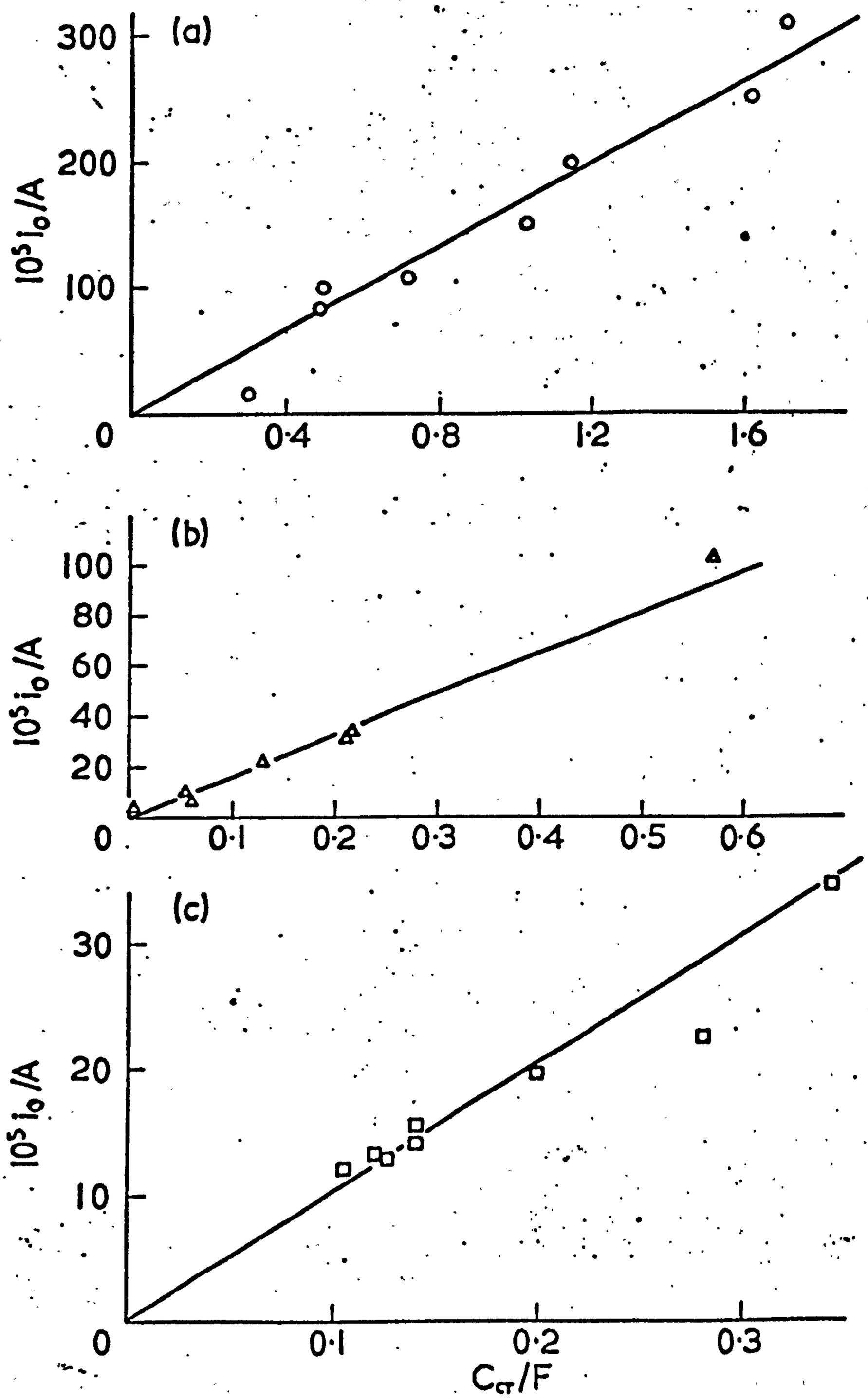

FIG. 23.

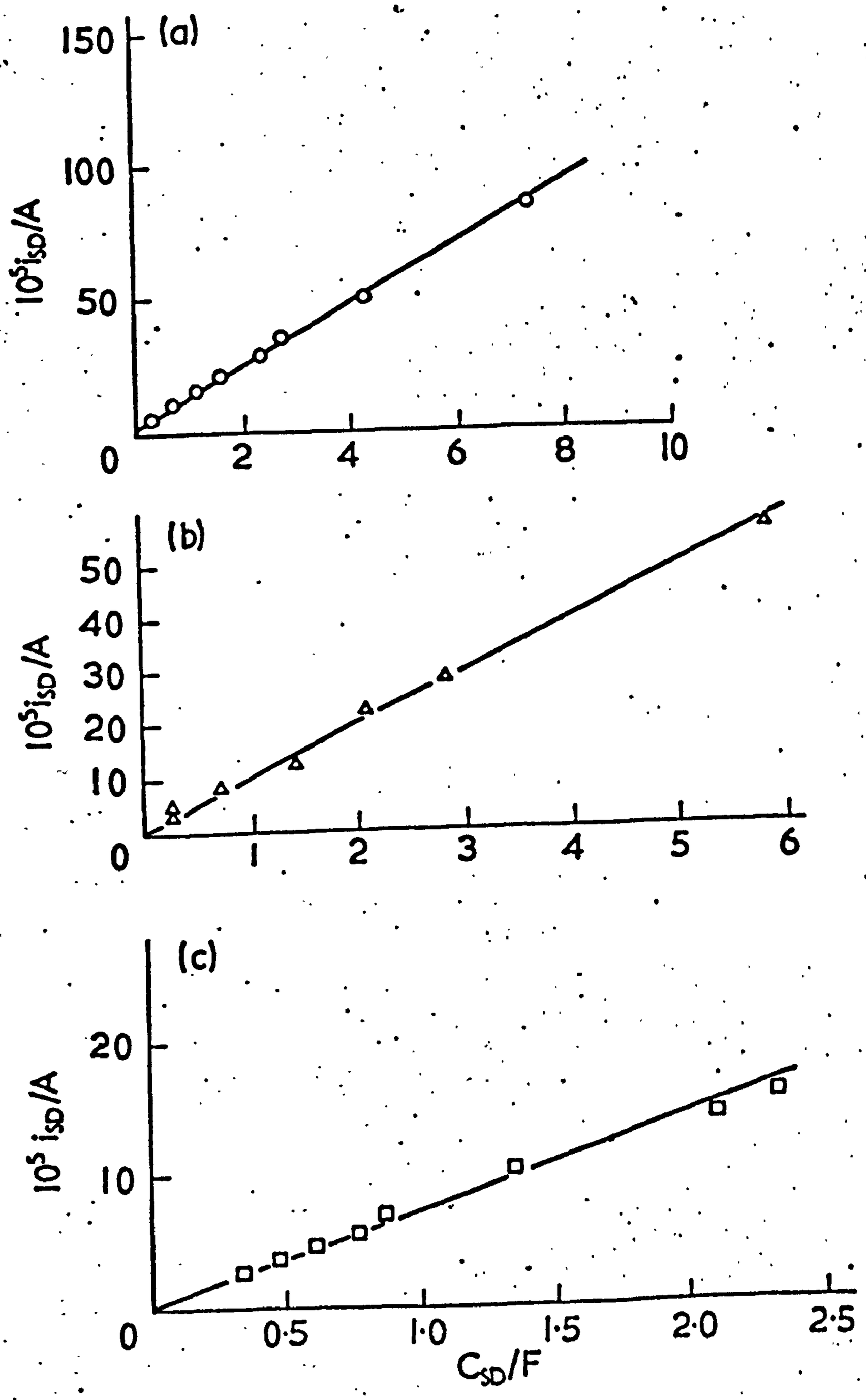

FIG. 23. Plots of i_{SD} vs. C_{SD} in (a) water - (b) NMP - (c) methanol.

where C_{DL} is equivalent to C_{CT}, and C_{Ai} to C_{SD} used here. This relation implies that the charging processes for C_{DL} and C_{Ai} are in parallel. The alternative "in series" model, as above, gives

$$C_{obs} = \left(\frac{C_{DL}\ C_{Ai}}{C_{DL} + C_{Ai}}\right).$$

Since the "in series" model is in accord with our results and is consistent with the analysis of i_o data, it is to be preferred. Thus a possible model for the electrode-solution interface can be represented electrically as follows :

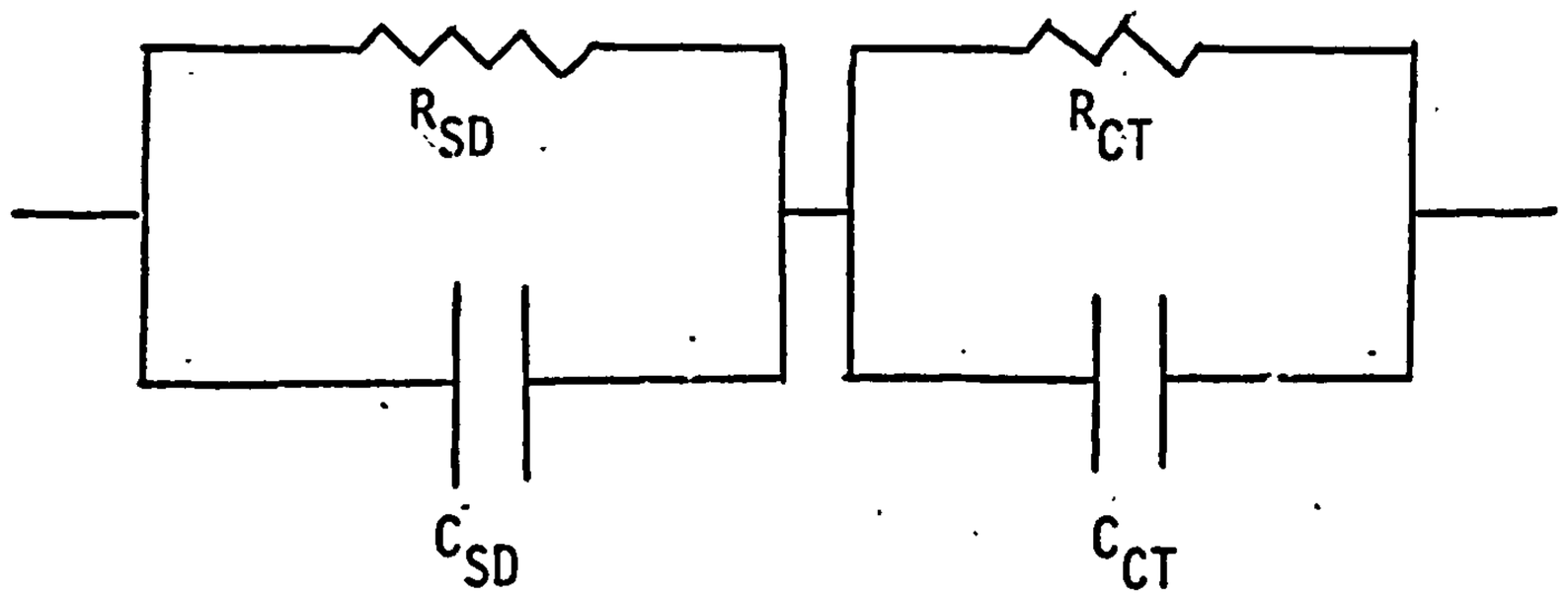

From the equation above, all consistent with our results, when $C_{SD} >> C_{CT}$, the observed capacitance, C_{obs}, tends to C_{CT}. It means that the initial rise is mostly dependent on C_{CT}, whereas the end of the charging process is mostly concerned with C_{SD}. Several other facts emerge from our analysis. Firstly, it is clear that the relaxation times of both components of the double-layer τ_{ct} and τ_{sd} (given by $\frac{RTCCT}{Fi_o}$ and $\frac{RT\ C_{SD}}{F\ i_{SD}}$ respectively) are independent of concentration, since the current-capacitance plots are linear (figs. 22 and 23), but they are depending on the solvent as these figs. show. Also it is of interest that the ratios of the slopes of these plots, and thus the ratios of the relaxation times, are

$\sim$ 15 for all three solvents, i.e. the "split" is the same in all solvents. Below are the values of τ_{sd} and τ_{ct} calculated for water, NMP and methanol

Solvent	τ_{ct}/s	τ_{sd}/s
H_2O	15	218
NMP	16	257
CH_3OH	25	368

It might be noted that the exact point of the sequence when the charge transfer occurs is rather arbitrarily decided in the Bockris model, where it is assumed that the charge transfer step occurs before the adion "surface-diffuses". An alternative scheme should be considered in which the main de-solvation step accompanies charge transfer and inclusion of an ion into the AgCl lattice. This process then induces movement of solvated ions along the inner Helmholtz layer adjacent to the electrode. This variation of the mechanism is not at variance with the "in series" picture given above. The processes occuring on the basis of the model are as follows:

(i) On charging, the diffuse double-layer rapidly adjusts, as the ions in the bulk immediately and instantly move towards the electrode, to increase the charge density near the electrode by a very small amount. There is a change in potential across the interface which influences the transfer of charge, and so we link the charging of the diffuse double-layer with the transfer process, and call it

C_{CT}. (This association is arbitrary, but is suggested by the results, though Bockris[3] indicated that C_{CT} has reached a maximum in the first stages of the polarisation process). At this stage there is also oxidation of a silver atom at the Ag/AgCl interface

$$Ag \rightleftharpoons Ag^{+} + e$$

This is fast[2] and starts as soon as the current is switched on.

(ii) Under the influence of a change in surface potential, the "leakage" of charges (represented by $i_o = i_{CT}$) occurs via the charge-transfer resistance R_{CT}. This probably involves complete de-solvation of the ion as it falls into a suitable site in the lattice.

(iii) The loss of ions from the adsorbed layer sets up a concentration gradient of adions as they surface-diffuse towards an appropriate site.

(iv) The surface-diffusion current, i_{SD}, is set up through the surface-diffusion resistance R_{SD}, and changes slightly the "pseudo-capacitance", C_{SD}, which becomes fully charged.

D. TEMPERATURE DEPENDENCE OF THE EXCHANGE CURRENT.

Since i_o' is effectively a rate, it would not be surprising if the temperature coefficient were to obey some relation such as the Arrhenius law. Indeed such an equation has been derived[11] and takes the form

$$\frac{d(\ln i_o')}{d(1/T)} = - \frac{\Delta H i_o'}{R} + \text{const.}$$

where i_o' is the apparent exchange current, T the absolute temperature, $\Delta H i_o'$ the "apparent activation enthalpy" and R the gas constant. Using

the values of i'_o given as a function of temperature in table 15, the plot of log i'_o against 1/T is illustrated in fig. 24. From table 15, the values of C_o, $i_{SD}(=FkC_o)$, $i_o(=i_{CT})$, C_{SD} and C_{CT} have been determined in the usual manner for each temperature. The general pattern of the temperature dependences is indicated by the results given below :

Temperature/^oC	$10^7 C_o$/mol.elec	$10^5 i_{SD}$/A	$10^5 i_o$/A	$C_{SD/F}$	$C_{CT/F}$
10.02	1.24	6.2	12.7	0.49	0.094
35.03	3.27	16.8	43.0	1.19	0.25

Very surprisingly the rate coefficient k is found to be invariant with temperature (table 15), within experimental error. We notice that $i_{SD}(=FkC_o)$ increases with increasing temperature, but only because C_o increases. Values of ΔH were computed for the above quantities, and are presented below (values in $kJ\,mol^{-1}$) :

$\Delta H(i'_o)$	$\Delta H(i_{SD})$	$\Delta H(i_{CT})$	$\Delta H(C_o)$	$\Delta H(C_{SD})$	$\Delta H(C_{CT})$
27.8±4.0	27.5±1.7	33.6±4.2	23.6±3.2	19.6±3.1	19.9±1.6

An enthalpy of activation ofabout 28 $kJ\,mol^{-1}$ (within the experimental error) seems to be a common factor for the first four quantities. This value is close to that for ionic conduction in silver chloride, where it was found that E_a = 28.6 $kJ\,mol^{-1}$ [12]. It is tempting to think that the ionic conduction represented by the

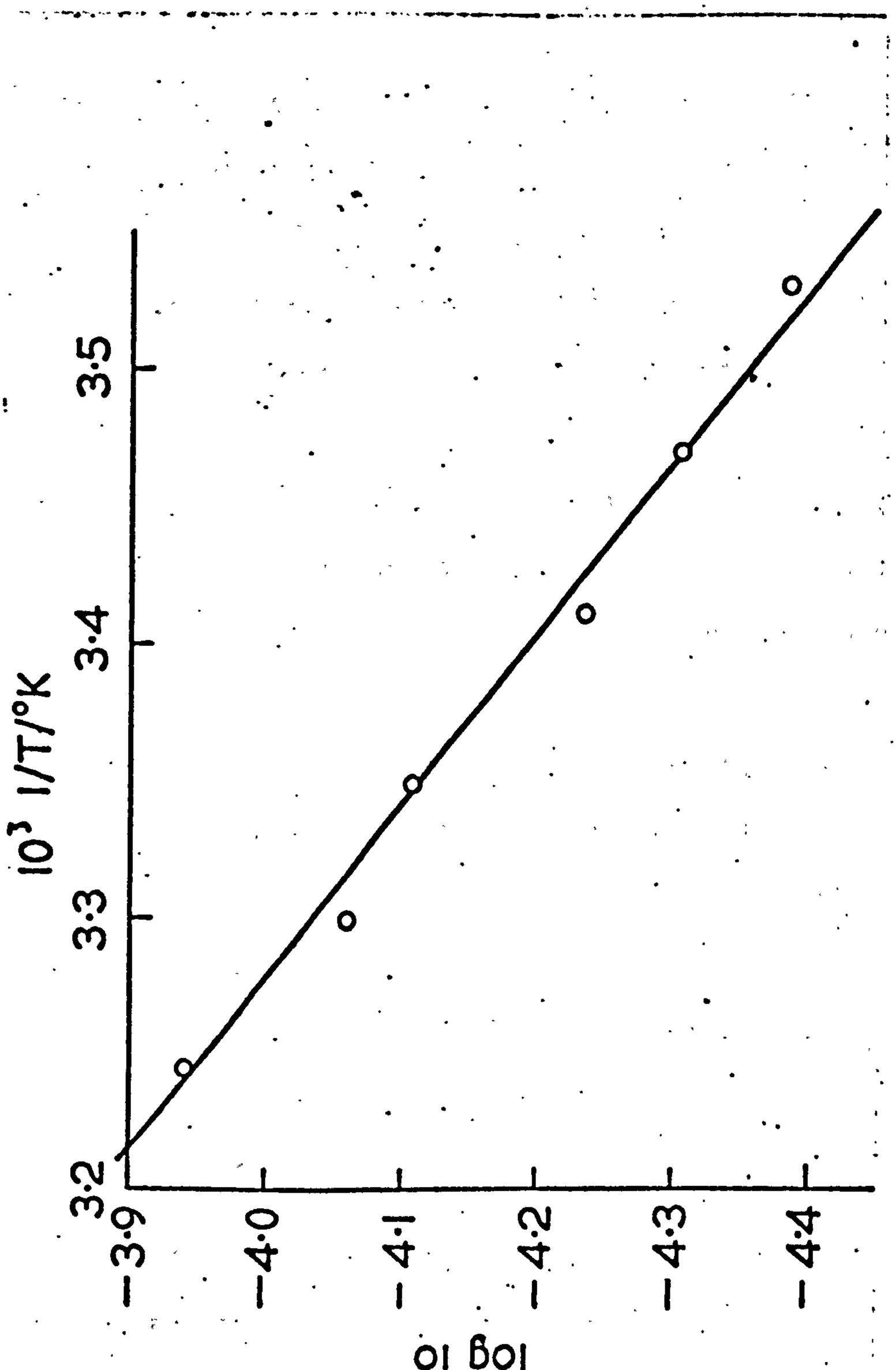

FIG. 24. Plot of log i_o vs. (1/T) for the Ag/AgCl system (- HCl in H_2O -)

FIG. 24.

equation

$$Ag^{+} + Ag^{*}Cl \rightleftharpoons Ag^{*+} + AgCl,$$

controls i_o', since the two values are very close to each other. It is possible, however, that the ionic conduction only controls the amount of space-charge in the silver chloride layer. If the conduction process were rate-determining, we might expect similar i_o' values in all solvents. It would, therefore, be interesting to measure ΔH values for other media than aqueous solutions. It may be also noted that when the temperature of the system is raised, the Ag/Ag^{+} reaction (at the Ag/AgCl interface) also becomes faster, so that the measured ΔH values may include contributions from this reaction.

For the temperature variation experiments, as for the earlier ones, we find that i_o' correlates linearly with C_{dl}, and the plot extrapolates to the origin. This gives weight to the statement made earlier (section A) that the ratio i_o/C_{dl} only depends on the solvent and the electrode used, and not on the temperature.

E. MAIN CONCLUSIONS.

1) The results presented in this work confirm the low-field approximation of the Butler-Volmer theory. The overpotential/current plots are linear, independently of the sign of the current, and all go through the origin. Despite of the very imperfect nature of the silver chloride layer and the complications caused by "coverage" and aging effects, the silver-silver chloride electrode, near its

equilibrium potential, behaves as a reversible system with stable potentials and fairly reproducible kinetics.

2) The fundamental quantities, i_o' and C_{dl}, can be measured from the potential/time, and overpotential/current curves with good accuracy. The values are given "per electrode", which points to a limitation of work with this type of electrode; the real surface area is not known. Both i_o' and C_{dl} are dependent on concentration and solvent, but depend also on both the type of preparation, the surface area, and the aging period of the electrode. A linear correlation between log i_o' and log c is found, the slope of which gives the transmission coefficient β. The transmission coefficient β varies widely with the solvent. An alternative approach to the concentration dependence has been explored : evidence is presented which suggests that i_o' and C_{dl} depend linearly on the square root of concentration in dilute solutions.

3) A linear correlation between i_o' and C_{dl} is also observed. The slope of such a correlation (ratio i_o'/C_{dl}), and hence the relaxation time, are constant for a given electrode in a given solvent, regardless of concentration (at least in dilute solutions). The slope of the plots of i_o' vs. C_{dl} appears to increase with increasing dielectric constant . It would be of relevance to study a bigger range of solvents and so test this hypothesis.

4) A two-step model consisting of a charge-transfer and surface-diffusion steps is proposed for the electrodic reaction of the $Ag/AgCl/Cl^-$ system. Surface-diffusion is the rate-determining step.

5) The total observed resistance and capacitance could be split tentatively into charge-transfer and surface diffusion resistances and capacitances. These are assumed to obey an "in-series" model.

6) In aqueous solutions, the quantities i_o' and C_{dl} increase with increasing temperature, but the ratio (i_o'/C_{dl}) is independent of the temperature.

7) An enthalpy of activation of $\sim$28 kJ mol^{-1} seems to be a common factor for the various quantities measured in aqueous solution within the experimental error, (except for the charge-transfer and surface-diffusion capacitances).

8) There are many aspects of the work which hold promise for future investigations. Further studies would be made easier by computer-assisted processing of results.

REFERENCES.

1. R. E. Meyer, F. A. Posey, P. M. Lantz, J.Electroanalyt.Chem. and Interfa Electrochem., 19, 99, (1968).
2. K. J. Peverelli, Ph. D. Thesis, Netherlands, (1979).
3. W. Mehl and J. O'M. Bockris, Can.J.Chem., 37, 190, (1959).
4. Q. J. M. Slaiman and W. J. Lorenz, Electrochim.Acta, 19, 791, (1974).
5. H. Taniguchi and J. G. Janz, Anal.Chem., 28, 287, (1956).
6. D. J. C. Engel, Ph.D. Thesis, Utrecht, (1968).
7. I. Fried, "The Chemistry of Electrode Processes", Academic Press, London and New York, (1973).
8. J. P. Brenet and K. Traore, "Transfer Coefficients in Electro-chemical Kinetics", Academic Press, London & New York, (1971).
9. H. Gerischer and R. P. Tischer, Z. Elektrochem., 61, 1159, (1957).
10. B. E. Conway, Trans.Far.Soc., 47, 756, (1951).
11. J. O'M. Bockris and S. U. M. Khan, "Quantum Electrochemistry", Plenum Press, New York and London, (1979).
12. R. P. Buck, J. Electroanalyt.Chem. and Interfacial Electrochem., 80, 245, (1977).